GRIMBEEK, JACOMINA CAROLINA

THE EFFECT OF THE VAALKOP REPLACEMENT PEGMATOID ON THE SULPHIDE MINERALOGY AT WESTERN PLATINUM MINE IN THE MOOINOOI DISTRICT

MSc UP 1995

The effect of the Vaalkop replacement pegmatoid on the sulphide mineralogy at Western Platinum mine in the Mooinooi district.

by

Jacomina Carolina Grimbeek

Submitted in partial fulfillment of the
requirements for the degree of
Magister Scientiae
in the Faculty of Science
of the
University of Pretoria
Pretoria

November 1995

ABSTRACT

Western Platinum mine is situated 30 km due east of Rustenburg in the Western Bushveld Complex. Replacement pegmatoid areas occur sporadically at the mine and range in diameter from a few metres to approximately 250 m.

The effect of the replacement pegmatoid was investigated in six profiles through the chromitite. The replacement pegmatoid footwall consists predominantly of amphibole with minor pyroxene, talc, clay-minerals, serpentine, olivine, and magnetite. A characteristic feature of the alteration in the UG-2 chromitite by replacement pegmatoid is the sintering of the bottom 5-10 cm. The sintered area consists of magnetite and Fe-Ti-oxides. Footwalls of "unaltered" UG-2 chromitite are anorthosite or pyroxenite.

Pentlandite is the major sulphide in altered UG-2 chromitite. Chalcopyrite, chalcocite-group minerals, bornite, violarite, mackinawite, haezlewoodite, cubanite and pyrrhotite are minor constituents in altered UG-2. Trace amounts of sphalerite and millerite occur. The base metals sulphides in a reference profile of unaltered UG-2 consist primarily of pentlandite with minor chalcopyrite, pyrrhotite, and pyrite.

The platinum group mineral assemblage of the altered UG-2 chromitite contains a considerable amount (36%-55%) of alloys, Bi-containing, As-containing and Te-containing platinum group minerals. The amount of arsenides increases with increasing alteration and is 2% (reference profile), 28% (average of altered UG-2 profiles 1, 3, 5, and 2) and 64% for the most intensely altered UG-2 chromitite (profile 8) respectively. The proportion of platinum group sulphides decreases from 96% to 18% with increasing alteration. Platinum group element association with sulphides decreases gradually from 87% for the reference profile to 20% for the most intensely altered UG-2 chromitite.

The sulphide mineral assemblages, platinum group element assemblages, and the presence of hydrous silicates in the profiles of altered UG-2 chromitite is an indication of the presence of a late-stage hydrothermal fluid modifying a primary magmatic assemblage. This is further supported by the sintering of the oxides, the presence of Co-rich pentlandite in the sintered area, and the textural and chemical overprinting of the chromites.

SAMEVATTING

Western Platinum myn is 30 km oos van Rustenburg in die westelike Bosveldkompleks geleë. Veranderingspegmatoïedareas kom sporadies in die myn voor en varieer vanaf 'n paar meter tot ongeveer 250 m in grootte.

Die effek van die veranderingspegmatoïed was ondersoek op ses profiele deur die UG-2 chromitiet. Die veranderingspegmatoïedvoetwal bestaan hoofsaaklik uit amfibool met pirokseen, talk, klei-minerale, serpentyn, olivien, en magnetiet as bykomstige minerale. 'n Tipiese verskynsel van die verandering in die UG-2 chromitiet deur die veranderingspegmatoïed is sintering van die onderste 5-10 cm. Die gesinterde area bestaan uit magnetiet en Fe-Ti-oksiede. Die voetwal van "onveranderde" UG-2 chromitiet is anortosiet en pirokseniet.

Die hoofsulfied in die profiele met veranderde UG-2 chromitiet is pentlandiet, met chalkopiriet, chalkosiet-groep minerale, borniet, violariet, makinawiet, haezlewoodiet, kubaniet, en pirrotiet as bykomstige sulfiede. Sfaleriet en milleriet kom voor in spoorhoeveelhede. Die sulfiedes in die verwysingsprofiel van "onveranderde" UG-2 chromitiet, is hoofsaaklik pentlandiet, met chalkopiriet, pirrotiet, en piriet as bykomstige minerale.

Die profiele bestaande uit veranderde UG-2 bevat 36-55% Bi-, As-, en Te-bevattende platinum-groep minerale en platinum-groep allooie. Die hoeveelheid arseniedes neem toe met toenemende verandering en is 2% (verwysingsprofiel), 28% (gemiddeld van profiele 1, 3, 5, en 2) tot 64% vir die mees veranderde UG-2 chromitiet (profiel 8). Die verhouding van platinum-groep sulfiedes neem af van 96% tot 18% met toenemende verandering. In die verwysingsprofiel kom 87% van die platinum-groep minerale voor as insluitsels in sulfiedes in vergelyking met net 20% platinum-groep minerale wat geassosieer is met sulfiedes vir die mees veranderde profiel.

Die tipes sulfiedminerale, platinum-groep minerale, en die teenwoordigheid van waterhoudende silikate in die profiele van veranderde UG-2 chromitiet dui op 'n laat-fase hidrotermale vloeistof wat die primêre magmatiese gesteente verander het. Dit word verder ondersteun deur die sintering van die chromitiet, Co-ryk pentlandiet en die teksturele en chemiese oorskrywing van die chromiete.

Table of Contents

LIST OF ABBREVIATIONS

ACE	- acid soluble element
born	- bornite
BMS	- base metal sulphides
ccgm	- chalcocite-group minerals
chr	- chromite
chr g.b.	- chromite grain boundary
cobalt	- cobaltite
cov	- covellite
cp	- chalcopyrite
FW	- footwall
gersd	- gersdorffite
haezl	- haezlewoodite
HW	- hanging wall
lld	- lower limit of detection
LOI	- loss on ignition
mack	- mackinawite
mauch	- maucherite
max	- maximum
mill	- millerite
min	- minimum
N	- number of grains
N%	- number percentage
n.a.	- not available
nicc	- niccolite
pent	- pentlandite
PGM	- platinum group mineral
PGE	- platinum group element
po	- pyrrhotite
Pt\Pd-comp	- all remaining Pt and\or Pd compounds
Ref	- reference
s	- standard deviation
sil	- silicates
sphal	- sphalerite
sulph	- sulphides
sulphars	- sulpharsenides
V%	- volume percentage
viol	- violarite

1. INTRODUCTION AND AIM OF INVESTIGATION

1.1 General

The Bushveld Complex is a major geological feature and extends over hundreds of kilometres. It is divided into a lower zone (bronzitite), critical zone (pyroxenite, norite-anorthosite), main zone (gabbronorite), and an upper zone (gabbro, diorite) (Von Gruenewaldt et al., 1985). The critical zone contains the Merensky Reef and the UG-2 chromitite which are mined for their platinum-group mineral (PGM) content.

Western Platinum mine is situated approximately 30 km due east of Rustenburg in the Western Bushveld Complex (Figure 1). The mine is engaged in the mining of platinum from the Merensky Reef and the UG-2 chromitite.

Replacement pegmatoid areas occur sporadically at the mine and range in size from a few metres to approximately 250 m. The Vaalkop replacement area is one of four such areas, as shown in Figure 1. At the surface the pegmatoid consists of an iron-rich pyroxenite where the Vaalkop forms a koppie-like structure (Figure 2) of approximately 30 metres high and 250 metres in diameter.

The average dip of the UG-2 reef is approximately 10°N and increases to 20°N in some of the replacement areas. A strike change can be observed over the Vaalkop replacement area which forms a pothole-type structure approximately 400 m in length.

A geochemical and mineralogical study of the UG-2 layer and its immediate hanging and/or footwall in the replacement area underneath the koppie was undertaken.

The aim of the investigation of the Vaalkop replacement pegmatoid is to determine the type of mineralogical and chemical alteration of the UG-2 chromitite and associated hanging-wall and footwall. The aim is also to determine the effect of the mineralogical and chemical alteration on the beneficiation of the platinum-group minerals, as modification of the base-metal sulphide or platinum-group mineral assemblage or sintering of the oxide minerals can be detrimental to flotation.

1.2 Previous work

Different examples of 'alteration' in the Bushveld Complex which lead to changes in the chromite chemistry and PGM assemblage are known. The following reports are available on the influence of replacement pegmatoids on UG-2, UG-1, and Merensky Reef.

McLaren and de Villiers (1982) investigated borehole cores from the eastern and western Bushveld Complex. The borehole cores include areas at Marikana which were relatively "unaltered" and a borehole core close to Maandagshoek which has indications of alteration in the form of the predominance of bornite and the presence of intermetallic PGM's of the compositions Pt-Fe, Pd-Cu, Pd-Pb, and Pd-Te. In all the borehole cores individual PGE's and Au, Cu, and Ni in the UG-2 chromitite were determined. McLaren (1980) also presents qualitative analyses of 6000 grains of PGM's.

Close to the Marikana area in the Brits graben, pegmatoidal pockets in the UG-2 layer were investigated by Winkels-Herding et al. (1991). They found unusual textures of chromitite and a distinctive difference in the frequency and distribution of base-metal sulphides and PGM's compared with normally textured areas.

The severe influence of the Onverwacht, Mooihoek, and Driekop pipes on the UG-2 were investigated by Stumpfl and Rucklidge (1982), and Peyerl (1982). The former indicate that microprobe analyses of chrome spinels from the pipe do not fall within the field of stratiform deposit-type spinels as defined by the chromitite layers of the Bushveld Complex, because they are characterized by lower Cr, Fe, and Mg and higher Ti-contents. PGM's in the area around the Driekop dunite pipe indicate a progressive change from a Pt-Fe alloy and Pt-Pd-As-Sb-type, to a Rustenburg-Merensky Reef Pt-Pd-sulphide type away from the pipe as described by Vermaak and Hendriks (1976) and Kinloch (1982a).

Papers on alteration of Merensky Reef and UG-1 chromitite have also been published. Kinloch and Peyerl (1990) give a rather detailed description of the various types of Merensky Reef and their characteristic PGM assemblage. The Merensky Reef types include normal and anomalous assemblages which include wide, pothole, contact, rolling, lens, regional pothole, pegmatoid-replaced, and dunite-affected. Different suites of PGM's, typical for the different types of normal and anomalous Merensky Reef, were recognized and a model for their genesis was proposed which invoked various kinds and periods of volatile activity.

The PGE assemblage in UG-1 chromitite in the Eastern Bushveld in the vicinity of a magnetite pipe shows some resemblance to that of the UG-2 in the area of the Driekop pipe as described by Peyerl (1982). Merkle (1987) investigated UG-1 samples which indicated that close to the pipe Pt-Fe alloys become more abundant and Pt-Rh-Fe and Pt-Pd-Fe-alloys were observed, while the bulk PGE content remained constant. The samples also show an increase in Fe, Ti, V, and Mn, and a decrease in Mg, Al, and Cr in spinel.

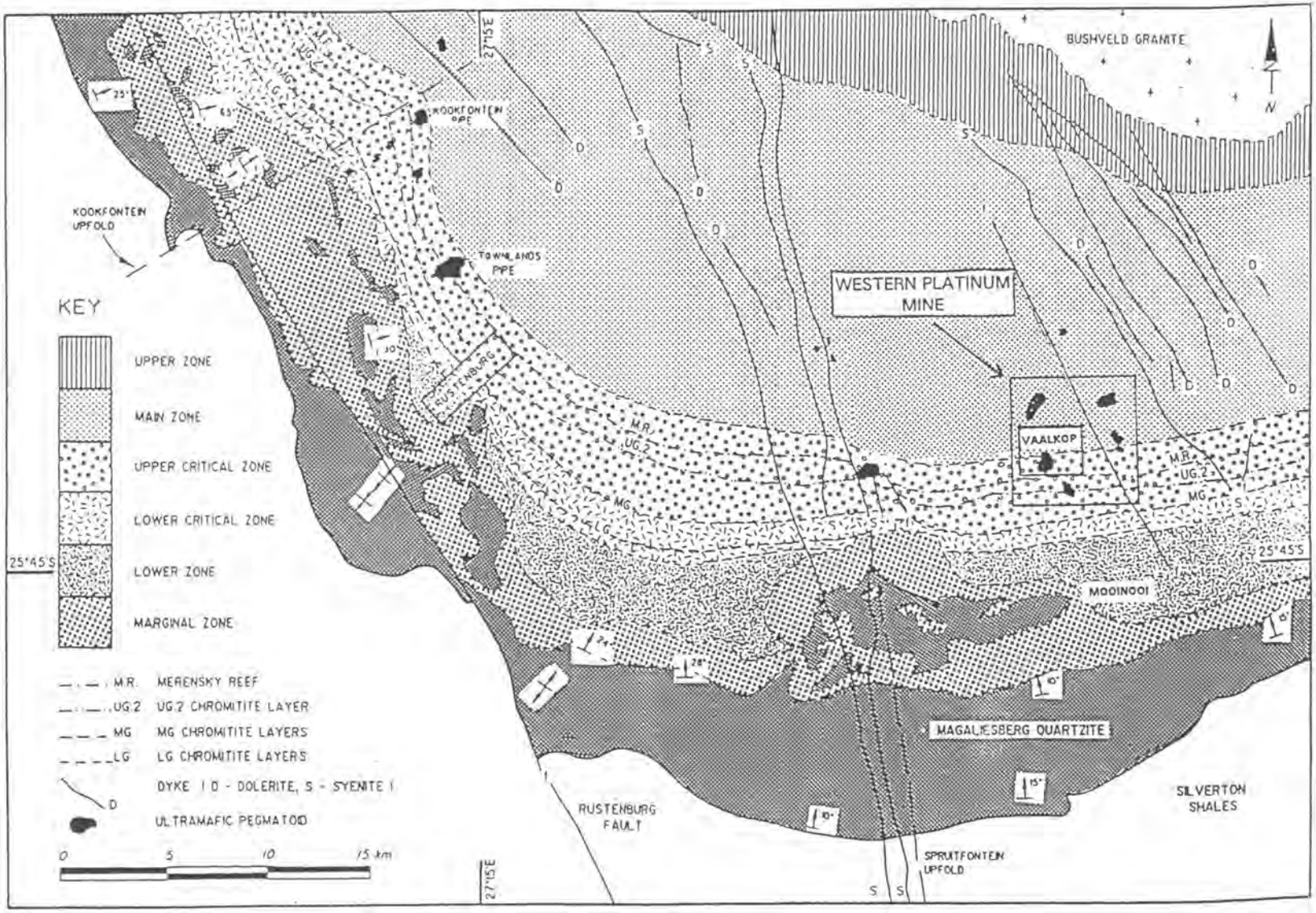

Figure 1. The setting of the Vaalkop replacement area in the Western Bushveld Complex. (Adapted after Davey 1992).

Figure 2. The Vaalkop replacement area on surface.

2. SAMPLING

The UG-2 and its hanging- and/or footwall were sampled underground as continuous profiles. Figure 3 shows the position of the profiles sampled in 9E5 raise. The 9E5 raise cuts through the Vaalkop pipe from east to west in the centre of the pipe. An attempt was made to sample the pegmatoid in such a way that varying degrees of alteration could be studied. Unfortunately, this was not always possible because of the irregular shape of the pegmatoid. The profiles were taken of altered UG-2 chromitite in 9E5 raise, because it contained the largest replacement pegmatoid area exposed underground at the time of sampling.

A reference profile was obtained from an underground borehole at level 11 in a relatively unaltered zone, approximately 1 km north-east of the altered profiles.

Profile 6 was obtained from an underground borehole in the 9E5 crosscut and its position is shown in Figure 3. Profile 13, which is not shown in Figure 3, is from a borehole drilled on level 10.

The remainder of the profiles, (1, 2, 3, 5, and 8) represent face samples. The profiles were taken of the chromitite and accessible hanging- and footwall by first marking the location with a grid pattern and numbering each block. After the individual chunks of rock were removed, they were reassembled in the laboratory to obtain a continuous profile.

The profiles were subdivided vertically into subsections for:
- thin sections
- polished sections
- chemical analyses
- X-ray diffraction analyses
- flotation tests
- a reference

The subsections all contained the whole thickness of the UG-2 chromitite and varying thickness of the hanging-wall and/or footwall, where possible.

For the chemical analyses the subsections were subdivided into 10 cm samples which were individually analyzed. The 0-20 cm of hanging-wall and footwall were also subdivided and analyzed in the same way.

3. GENERAL CHARACTERISTICS OF THE REPLACEMENT PEGMATOID

3.1 Petrography

Figure 3 shows the lithological characteristics of every profile. The average thickness of the UG-2 in the profiles is 1 m and ranges from 0.7 to 1.2 m. The reference profile consists of a leopard-skin type chromitite caused by areas with a varying chromite/(pyroxenite + feldspar) ratio. Sharp contacts exist between the chromitite and the anorthositic footwall (consisting of appoximately 80% plagioclase and approximately 20% pyroxene) and a pyroxenitic hanging-wall. The pyroxenite consists of fine-grained (<1 mm) orthopyroxene with interstitial feldspar.

All the profiles of altered UG-2 have a pegmatitic footwall consisting predominantly of metamorphic minerals (Moorhouse, 1959) and are therefore replacement pegmatoidal. The footwalls range from a dark-green pegmatoid consisting essentially of amphibole with minor pyroxene, chlorite, talc, clay-minerals, serpentine, and magnetite to a bluish-green pegmatoid consisting also of amphibole with smaller amounts of the minor minerals, but with additional olivine. A maximum grain size is approximately 3 cm. Amphibole is mainly a Fe-rich variety (actinolite) which replaces pyroxene and forms elongated, unorientated fibres with the original grain boundary of the pyroxene sometimes still present. Hornblende replaces the pyroxene to a lesser extent than actinolite. The hornblende contains exsolutions of small (10 μm) magnetite grains. Serpentine and chlorite occur as alteration products of pyroxene mainly in the area just below the contact of the replacement pegmatoid footwall and chromitite.

Fine-grained talc in the footwall occurs as an alteration product of feldspar and can replace it completely. Veins of varying width (maximum 2 mm) cut through the replacement pegmatoid footwall parallel to the strike and dip of the chromitite. The veins contain calcite as the major phase and are lined by talc, hornblende, and magnetite.

Profiles 1, 5, 6, and 8 have a replacement pegmatoid hanging-wall as well, which contains the same mineral assemblage as the footwall, except for olivine. The maximum grain size of 5 cm was measured just above the hanging-wall contact with chromitite. In most cases pyroxene is only partially altered to fine-grained amphibole, but feldspar has been pervasively replaced by talc. Magnetite occurs throughout the hanging-wall as fine exsolutions in orthopyroxene. Fine veins (1 mm wide) consisting of amphibole, magnetite, and minor calcite occur parallel to the strike and dip of the chromitite.

Silicate minerals in profiles of the altered UG-2 chromitite are microscopically small (approximately 10 μm) and include amphibole, clay-minerals and talc, occurring interstitially with respect to chromite grains. Thin veins, which are parallel to the layering (as shown in Figure 3) are common in the altered UG-2 and are filled with unorientated amphibole mixed with clay and calcite. Olivine occurs interstitially to chromite and is partially altered to chlorite containing magnetite exsolutions.

Graphite occurs predominantly in the profiles of altered UG-2 as small (approximately 10 μm), isolated grains at silicate grain boundaries. In Profile 8, graphite occurs as rims around silicate, chromite or BMS and also as isolated grains of maximum 50 μm.

A characteristic feature of alteration in the chromitite is sintering of the bottom 5-10 cm. In profiles 1, 2, 5 and 8 (Figure 3), the bottom of the chromitite is sintered to such an extent that grain boundaries of oxide phases are not distinguishable in handspecimen and a solid mass of magnetite and Fe-Ti-oxides is formed which is highly magnetic (Figure 4). The bottom contact of the chromitite with the replacement pegmatoid is normally sharp, but undulating. To the top of the sintered area the amount of silicates increases and the grain shapes become visible.

Sintering decreases gradually and the rock grades into a normal UG-2 chromitite. Figure 3 also shows varying amounts of thin quartz/calcite veins parallel to the strike at several levels in the chromitite.

The profiles in order of increasing macroscopically visible alteration are: Reference, 3, 1, 6, 5, 2, 8, based on:
- the degree of alteration of the hanging-wall
- the size of the sintered zone at the bottom of the chromitite
- the thickness and colour of the replacement pegmatoid footwall (as observed)
- the presence of quartz-calcite veins in the footwall of UG-2 chromitite.

3.2 Major and trace element geochemistry

Bulk chemical analyses for major and trace elements were performed on all the complete UG-2 chromitite profiles. The chromitite was divided into 10 cm samples, starting from the bottom contact with the footwall. (Figure 3.)

Figure 4. The bottom contact of the Reference Profile and the highly altered Profile 8 (left).

Representative powder samples were taken from the individual samples by using the rotary sample splitter. The samples were crushed in a chrome steel container for approximately 3 minutes and issued for chemical analysis.

Estimation for the reproducibility of analyses (Appendix 1) was obtained by calculating the standard deviation from duplicate analyses with the formula given by Kaiser and Specker (1956).

3.2.1 Major element analyses

Major element analyses for SiO_2, TiO_2, Al_2O_3, Fe_2O_3, MnO, MgO, CaO, Na_2O, K_2O, P_2O_5, Cr_2O_3, NiO and V_2O_5 were performed on the chromitite, as well as the footwall where possible. (Figure 3). The analyses were done by X-ray fluoresence spectrometry at the University of Pretoria.

The results of the major element analyses are shown in Appendix 2. In the case of Profile 6, only the TiO_2, Cr_2O_3 and Fe_2O_3 determinations were carried out, because of a limited amount of sample material. Tables 1 to 4 give the arithmetic means, standard deviations, maximum-, and minimum-values of the Reference Profile and Profiles 1, 5, and 8, which are arranged in order of increasing macroscopic alteration. Values lower than the detection limits were taken as zero in calculating the averages or standard deviations.

The chemical composition of the Reference Profile is relatively constant over the thickness of the chromitite and is reflected in the low standard deviations calculated for all the elements.

The mean values of Profile 1 show a decrease in the average Al_2O_3, SiO_2 and CaO values in the footwall when compared to the Reference Profile. The average TiO_2-, Cr_2O_3-, and Fe_2O_3-values in the chromitite of the altered profiles show a relative increase (by 50%, 86%, and 75% respectively) in comparison to the Reference Profile. These deviations are caused mainly by the bottom 10 cm of the chromitite.

The variations in TiO_2 in particular, but Cr_2O_3 and Fe_2O_3 as well, are even more pronounced in Profiles 5 and 8. The highest TiO_2 contents encountered are increased eleven-fold in the bottom 10 cm, compared to the Reference Profile. Figure 5 shows the compositional variation in the various profiles over the thickness of the chromitite.

Table 1. Average whole-rock compositions of the Reference Profile.

Ele-	Mean		s		min		max	
ment	Chr	FW	Chr	FW	Chr	FW	Chr	FW
SiO_2	16.54	47.92	0.77	1.26	15.50	43.24	17.50	50.13
TiO_2	0.58	n.a.	0.05	n.a.	0.53	n.a.	0.66	n.a.
Al_2O_3	19.34	32.66	0.56	1.24	18.46	31.03	19.96	34.38
Fe_2O_3	20.96	0.62	0.52	0.62	20.34	0.38	21.96	0.92
MnO	0.28	n.a.	0.03	n.a.	0.25	n.a.	0.31	n.a.
MgO	9.75	1.46	0.41	1.46	9.23	0.93	10.55	2.22
CaO	2.69	14.97	0.18	0.49	2.46	14.96	3.13	15.79
Na_2O	0.64	n.a.	0.10	n.a.	0.57	n.a.	0.80	n.a.
K_2O	0.21	n.a.	0.08	n.a.	0.10	n.a.	0.35	n.a.
P_2O_5	0.06	n.a.	0.03	n.a.	0.01	n.a.	0.11	n.a.
V_2O_5	0.28	n.a.	0.00	n.a.	0.17	n.a.	0.40	n.a.
Cr_2O_3	29.37	<lld	0.99	<lld	27.58	<lld	30.89	<lld
L.O.I.	1.15	0.18	0.40	<lld	<lld	0.17	1.45	0.20

(s-standard deviation, min-minimum, max-maximum, L.O.I.-loss on ignition, n.a.- not available, lld-lower limit of detection; 10 chromitite (Chr) and 5 footwall (FW) samples were analyzed.)

Table 2. Average whole-rock compositions of Profile 1.

Ele-	Mean		s		min		max	
ment	Chr	FW	Chr	FW	Chr	FW	Chr	FW
SiO_2	7.25	44.69	1.70	2.80	4.19	39.66	8.96	46.59
TiO_2	1.15	0.32	0.64	0.20	0.80	0.19	2.57	0.66
Al_2O_3	15.70	1.50	1.20	0.30	13.35	1.00	1.70	1.78
Fe_2O_3	27.98	2.73	3.93	0.66	25.21	2.11	36.63	3.82
MnO	0.35	0.33	0.02	0.07	0.32	0.29	0.40	0.44
MgO	9.03	20.08	1.29	1.20	6.30	18.22	9.89	21.13
CaO	1.71	10.19	0.61	2.00	0.81	7.25	2.69	12.77
Na_2O	0.05	n.a.	0.03	n.a.	0.01	n.a.	0.10	n.a.
K_2O	0.04	n.a.	0.03	n.a.	0.01	n.a.	0.08	n.a.
P_2O_5	0.02	n.a.	0.02	n.a.	<lld	n.a.	0.05	n.a.
V_2O_5	0.38	n.a.	0.28	n.a.	0.27	n.a.	0.48	n.a.
Cr_2O_3	33.98	0.23	1.20	0.14	32.05	0.12	35.25	0.47
L.O.I.	0.21	0.62	0.33	2.40	<lld	-0.89	0.99	0.00

(s-standard deviation, min-minimum, max-maximum, L.O.I.-loss on ignition, n.a.-not available, lld-lower limit of detection; 7 chromitite (Chr) and 5 footwall (FW) samples were analyzed.)

Table 3. Average whole-rock compositions of Profile 5.

Ele-	Mean		s		min		max	
ment	Chr	FW	Chr	FW	Chr	FW	Chr	FW
SiO_2	9.12	42.07	3.18	3.70	2.52	36.53	13.27	44.29
TiO_2	1.11	0.66	0.42	0.95	0.87	0.20	2.30	2.09
Al_2O_3	17.18	1.17	0.64	0.08	15.50	1.07	17.76	1.25
Fe_2O_3	25.49	2.88	2.76	0.52	23.98	2.62	32.75	3.65
MnO	0.24	0.31	0.09	0.31	0.22	0.28	0.31	0.33
MgO	9.94	22.30	0.85	2.97	7.67	17.91	10.72	24.25
CaO	1.88	9.28	0.82	1.13	0.37	7.61	2.71	10.01
Na_2O	0.16	n.a.	0.14	n.a.	<lld	n.a.	0.26	n.a.
K_2O	0.04	n.a.	0.07	n.a.	<lld	n.a.	0.20	n.a.
P_2O_5	0.04	n.a.	0.02	n.a.	<lld	n.a.	0.06	n.a.
V_2O_5	0.37	n.a.	0.04	n.a.	0.33	n.a.	0.45	n.a.
Cr_2O_3	32.41	0.28	1.70	0.12	29.68	0.21	35.01	0.45
L.O.I.	<lld	1.42	<lld	2.14	<lld	-1.00	<lld	3.53

(s-standard deviation, min-minimum, max-maximum, L.O.I.-loss on ignition, n.a.-not available, lld-lower limit of detection; 10 chromitite (Chr) and 4 footwall (FW) samples were analyzed.)

Table 4. Average whole-rock compositions of Profile 8.

Ele-	Mean		s		min		max	
ment	Chr	FW	Chr	FW	Chr	FW	Chr	FW
SiO_2	6.20	40.45	2.53	8.89	3.19	26.51	9.88	57.85
TiO_2	2.05	1.33	3.46	1.88	0.74	0.11	11.88	5.91
Al_2O_3	15.95	2.61	2.12	3.73	10.49	<0.30	17.29	11.66
Fe_2O_3	27.80	29.82	4.23	12.23	23.99	8.89	38.73	48.70
MnO	0.33	0.40	0.04	0.15	0.24	0.16	0.42	0.65
MgO	8.82	16.26	0.85	1.34	6.63	13.52	9.57	18.15
CaO	1.61	6.30	0.55	0.29	0.67	2.22	2.28	8.31
Na_2O	0.06	n.a.	0.06	n.a.	<lld	n.a.	0.14	n.a.
K_2O	0.04	n.a.	0.08	n.a.	<lld	n.a.	0.22	n.a.
P_2O_5	0.02	n.a.	0.02	n.a.	<lld	n.a.	0.07	n.a.
V2O5	0.52	n.a.	0.12	n.a.	0.42	n.a.	0.80	n.a.
Cr_2O_3	34.48	<0.30	4.52	<0.30	22.63	<0.30	35.96	<0.30
L.O.I.	n.a.	1.48	n.a.	1.27	n.a.	-0.78	n.a.	2.80

(s-standard deviation, min-minimum, max-maximum, L.O.I.-loss on ignition, n.a.-not available, lld-lower limit of detection; 10 chromitite (Chr) and 8 footwall (FW) samples were analyzed.)

The relationship of the certain major elements with one another is presented in Figure 6. The isocon diagram is based on the assumption of constant mass during 'alteration'. C^O is the concentrations of the major elements in the unaltered profile and C^A the concentrations of the major elements in the altered profiles. Fe_2O_3 and Cr_2O_3 are enriched relative to the other elements. MgO, SiO_2, and Al2O3 are depleted in comparison to the other elements, except for Profile 3 which is enriched in MgO. In almost all the cases, Profile 8 has the maximum change in chemical composition compared to the Reference Profile.

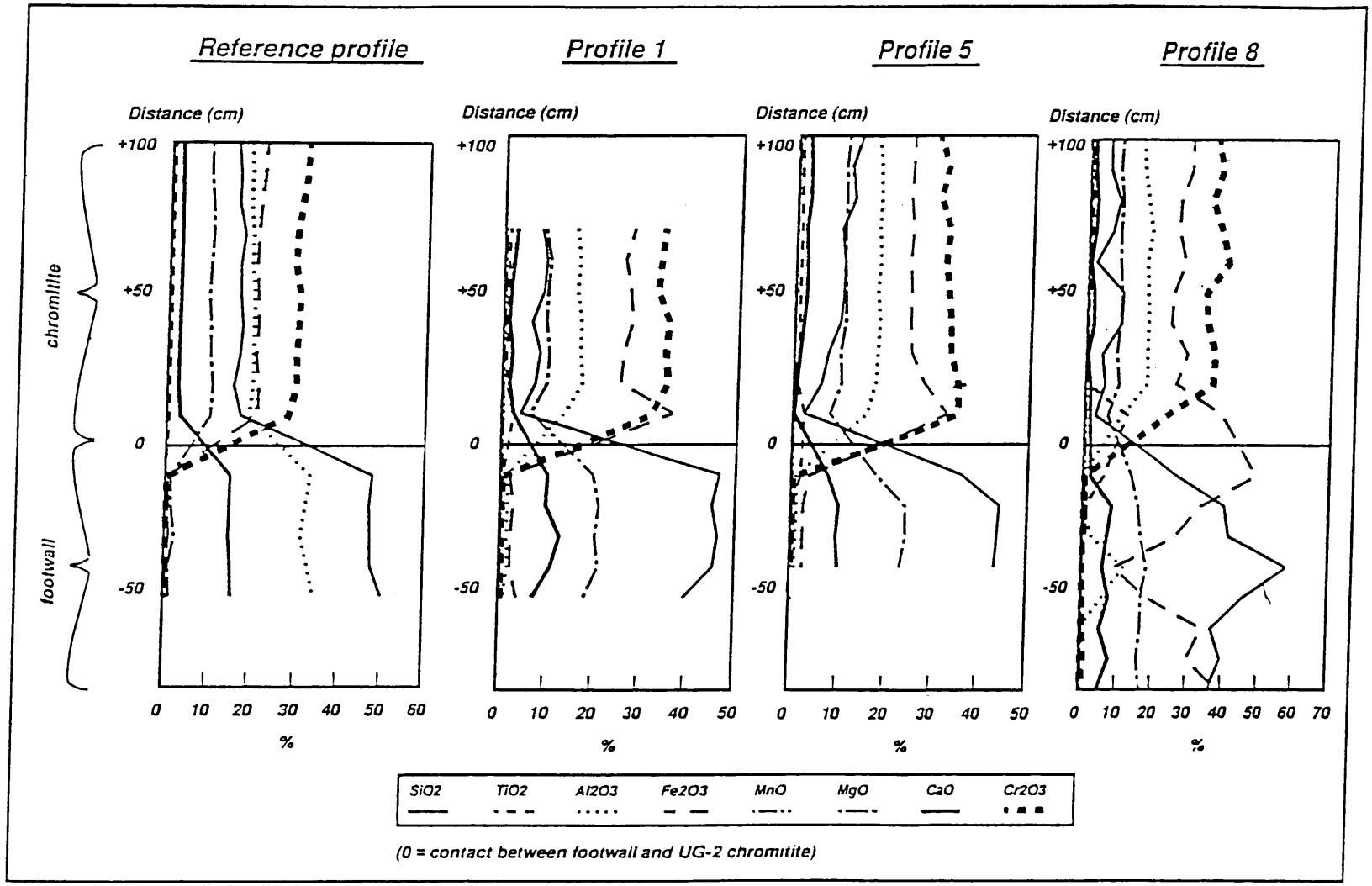

Figure 5. Compositional variation in major element analyses in the various profiles.

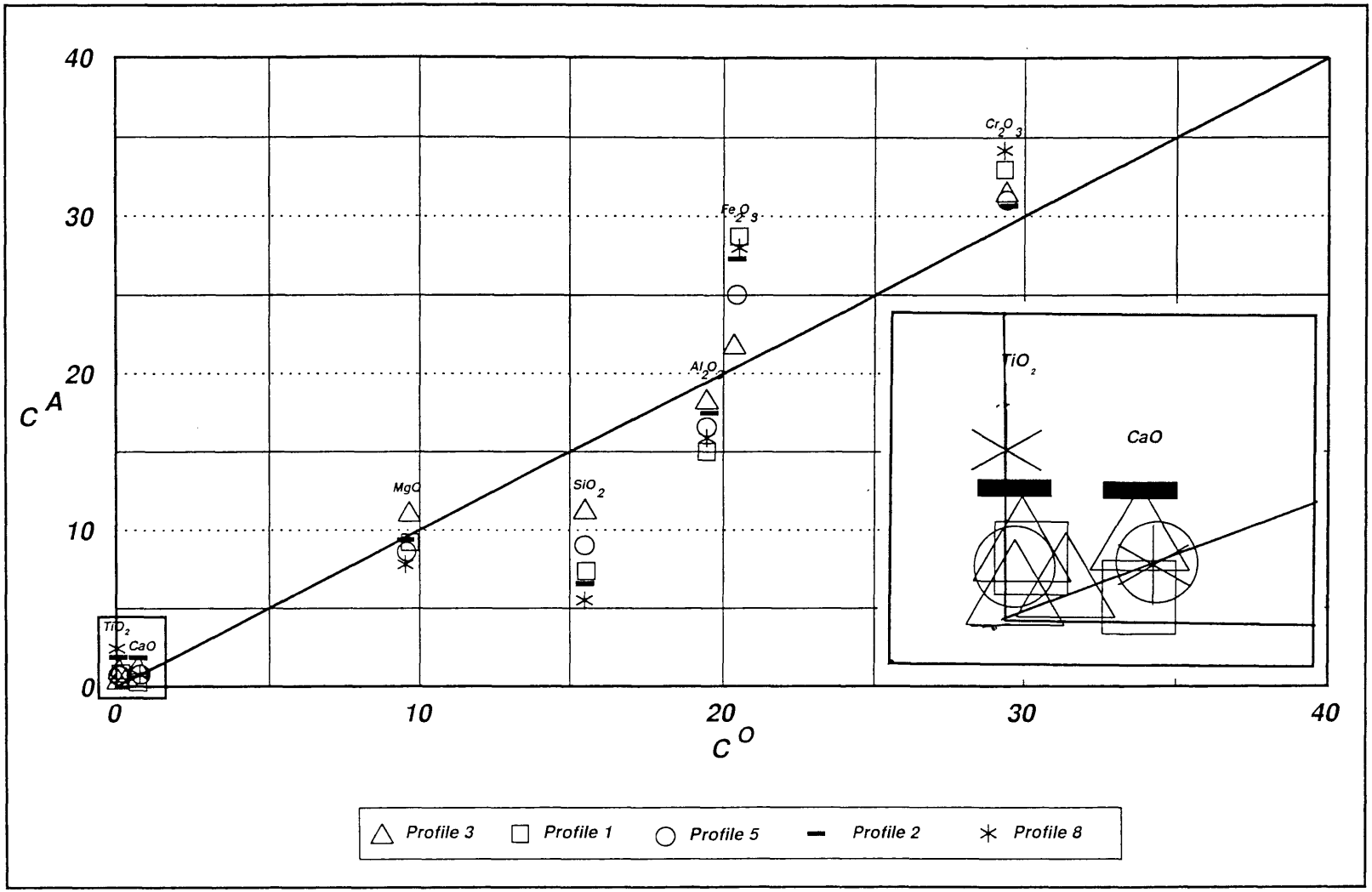

Figure 6. Isocon diagram of profiles 1, 2, 3, 5, and 8.

(C^O = Reference Profile, C^A = Profiles of altered UG-2)

3.2.2 Trace element analyses

Trace element analyses for Zn, Cu, Ni, Co, Ga, Mo, Nb, Zr, Y, Sr, Rb, U, Th, Pb, V, Ba, Sc, As, S, and Cr were performed on the Reference Profile, and Profiles 1, 2, 3, 5, and 8. The trace elements U, Th, Pb and As were only determined on the chromitite and Cr analyses only on the silicate sections. The analyses were done by X-ray fluoresence spectrometry at the Geology Department of the University of Pretoria. The trace element values are given in Appendix 3.

The average trace element contents of the Reference Profile, as well as Profiles 1 (minor macroscopic alteration) and 8 (intense macroscopic alteration) are shown in Tables 5 to 7.

The results of the trace element analyses indicate an increase in the elements Zn, Cu, and Ni in the chromitite of the altered profiles from the Reference Profile to Profile 8. The elements increase by a factor of 1.7, 1.4 and 1.1 for Zn, Cu, and Ni respectively. Other elements, which show a variation in the average value when compared to the Reference Profile, are Sr decreasing with a factor of 0.39, and V and S increasing by a factor of 1.95 and 1.5 respectively.

Figure 7 shows the distribution of the trace elements over the thickness of the chromitite and footwall in the Reference Profile, and in Profiles 1 and 8. Cu, Ni, Co and S vary sympathetically in the Reference Profile and Profile 1. In Profile 8 these elements all have peaks in varying distances from the bottom contact. The footwall of Profiles 1 and 8 is enriched in the elements Zn, Cu, Ni, Co, V, and S compared to the Reference Profile.

Table 5. Average trace element content of the Reference Profile.

Ele-	Mean		s		min		max	
ment	Chr	FW	Chr	FW	Chr	FW	Chr	FW
Zn	479	9	65	1.4	466	8	633	11
Cu	96	12	63	2.5	49	10	273	15
Ni	1218	24	236	8	1102	14	1890	35
Co	299	5	21	1	263	<lld	328	6
Ga	47	17	2	1.2	43	16	50	19
Mo	<lld	<lld	<lld	<lld	<lld	<lld	<lld	<lld
Nb	3	<lld	2.4	<lld	<lld	<lld	5	<lld
Zr	17	5	6	1.9	8	<lld	26	8
Y	7	<lld	3	<lld	<lld	<lld	13	<lld
Sr	98	439	13	11.1	63	426	108	454
Rb	2	<lld	3.4	<lld	<lld	<lld	8	<lld
U	1	<lld	2.2	<lld	<lld	<lld	6	<lld
Th	1	<lld	1.6	<lld	<lld	<lld	5	<lld
Pb	6	4	16.6	2.3	<lld	<lld	14	7
V	1312	12	262	7.4	1030	<lld	1900	23
Ba	104	21	19	15	79	<lld	145	49
Sc	11	<lld	2	<lld	8	<lld	13	<lld
As	<lld	n.a.	<7	n.a.	<lld	n.a	<lld	n.a.
S	352	n.a.	335	n.a.	156	n.a	1327	n.a.
Cr	n.a.	510	n.a.	47.2	n.a.	459	n.a.	573

(s - standard deviation, min - minimum, max - maximum, lld - lower limit of detection, n.a. - not available; 11 chromitite (chr) and 5 footwall (FW) analyses)

Table 6. Average trace element content of Profile 1.

Ele-	Mean		s		min		max	
ment	Chr	FW	Chr	FW	Chr	FW	Chr	FW
Zn	753	85	144	35	583	91	975	112
Cu	136	19	97	6	43	20	334	28
Ni	1713	531	392	39	1281	476	2384	569
Co	282	192	46	53	233	202	375	244
Ga	46	1	4	1.8	40	<lld	50	5
Mo	0.6	0	1.5	0	<lld	<lld	4	<lld
Nb	2.4	10	2.3	3	<lld	10	5	14
Zr	11	9	2.5	2	<lld	5	6	11
Y	34	13	3	12	<lld	5	7	34
Sr	31	1.1	9	1	14	<lld	47	3
Rb	1	0.4	2	0.8	<lld	<lld	4	2
U	3	0.6	4	0.9	<lld	<lld	9	1.9
Th	<lld	n.a.	<lld	n.a.	<lld	n.a.	<lld	n.a.
Pb	13	n.a.	5	n.a.	6	n.a.	19	n.a.
V	1778	691	289	75	1446	598	2073	793
Ba	69	<lld	19	<lld	42	<lld	164	<lld
Sc	10	71	2	18	7	45	14	80
As	5	0.1	11	0.1	<lld	0.1	29	0.2
S	584	599	382	141	145	410	1301	752
Cr	n.a.	1318	n.a.	613	n.a.	866	n.a.	1162

s - standard deviation, min - minimum, max - maximum, lld - lower limit of detection, n.a. - not available; 7 chromitite (chr) and 5 footwall (FW) analyses)

Table 7. Average trace element content of Profile 8.

Ele-	Mean		s		min		max	
ment	Chr	FW	Chr	FW	Chr	FW	Chr	FW
Zn	871	142	273	48	734	52	187	187
Cu	140	44	214	26	32	22	101	101
Ni	1337	476	131	67	1064	395	517	613
Co	286	264	28	123	258	64	420	420
Ga	53	6	7	2.8	40	<lld	10	10
Mo	1	1	2.4	1.3	<lld	<lld	6	4
Nb	4	3	4.2	3.4	<lld	<lld	13	10
Zr	3	10	7.2	4	<lld	6	23	18
Y	3	7	3.1	4.1	<lld	<lld	7	10
Sr	38	47	24	38	5	7	66	168
Rb	1	<lld	1.3	1.3	<lld	<lld	9	4
U	<lld	3	<lld	3.5	<lld	<lld	<lld	10
Th	2	3	3.3	3.5	<lld	<lld	9	10
Pb	7	5	5.7	4.1	<lld	<lld	18	13
V	2560	740	909	373	1905	102	5067	1437
Ba	139	4	227	9	38	<lld	777	29
Sc	11	33	5	10	6	19	23	43
As	2	n.a.	6.3	n.a.	<lld	n.a.	20	n.a.
S	529	n.a.	462	n.a.	189	n.a.	1633	n.a.
Cr	n.a.	2054	n.a.	978	n.a.	849	n.a.	2956

s - standard deviation, min - minimum, max - maximum, lld - lower limit of detection, n.a. - not available; 10 chromitite (chr) and 8 footwall (FW) analyses)

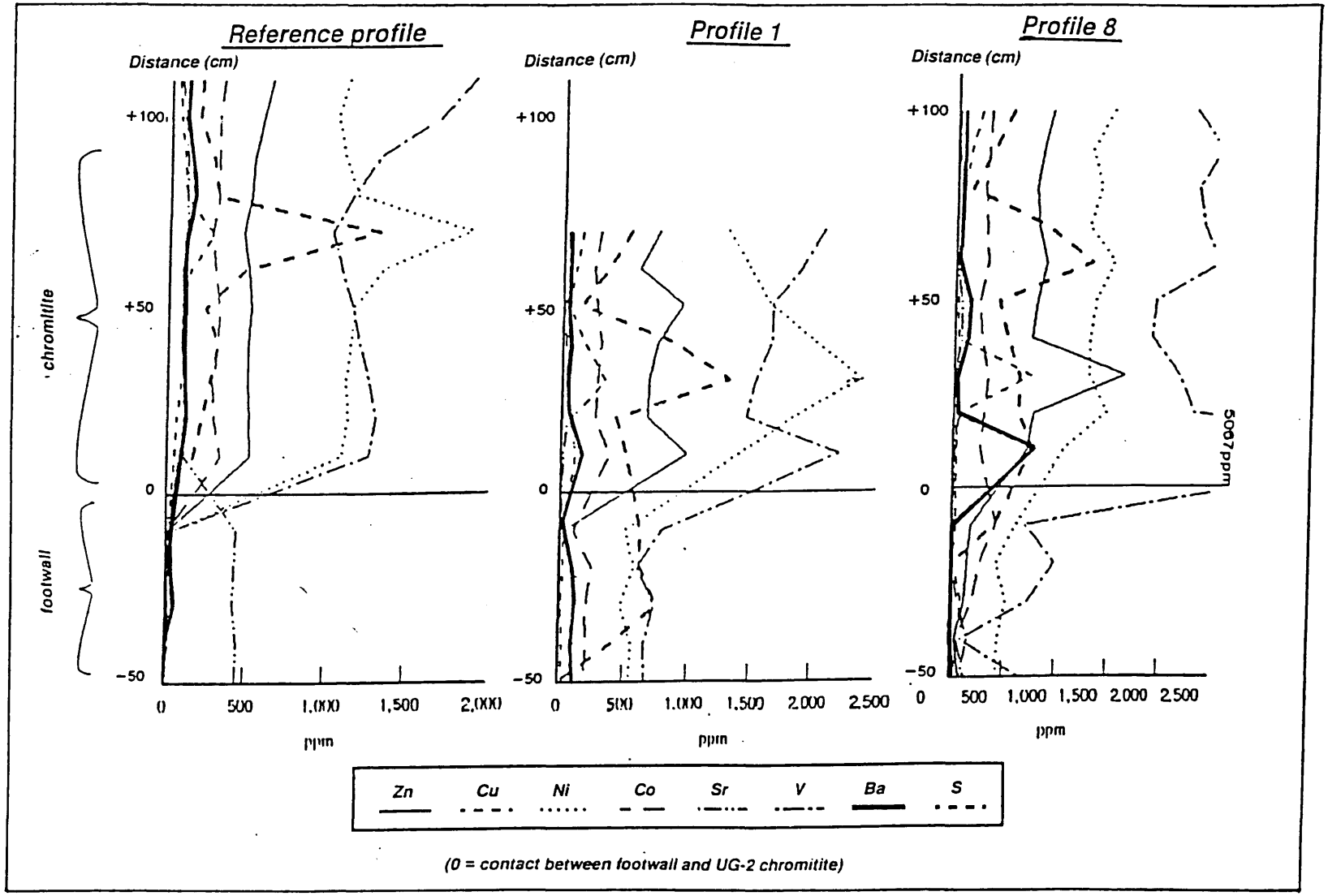

Figure 7. Trace element distribution in the Reference Profile and Profiles 1 and 8.

4. OXIDE MINERALS

The predominant oxide phase in the chromitite of the Reference Profile is chromite. Rutile is a common constituent of the chromitite and occurs as elongated inclusions in chromite or at chromite grain boundaries. The second most common oxide, after chromite, is magnetite which is present as fine inclusions in hydrous silicates and as veins of up to 30 μm in width, perpendicular to the strike of the UG-2 chromitite.

Various oxide phases occur in the altered UG-2 chromitite profiles, especially overprinted chromites with differing chemistry and optical properties similar to those described by Stumpfl and Rucklidge (1982).

4.1 Chemical analyses

Table 8 shows the chemical analyses of chromite and overprinted chromite at the Vaalkop replacement area. The electron microprobe analyses were performed by the Mineralogy Division at Mintek. A chromite grain from the UG-2 at Marikana analyzed by McLaren (unpub. thesis) is included in Table 8. Chromite was calculated ussuming stoichiometry.

Figure 12e shows overprinted chromites (Table 8) which reveal a decrease in the reflectivity of the chromite. The alteration has been described in the sulphide section as it evolves simultaneously with incorporation of adjacent sulphides.

Analyses 2 and 3 are alteration zones in chromite with a lower reflectivity than "normal" chromite. The analyses show a marked increase in Al, and a decrease in Cr and Fe. Analysis 3, which is a low-reflectivity oxide with inclusions of sulphides, also has a higher Al content and lower Fe content than the reference chromite. The phases 2, 3, 4 and 5 fall into the spinel-hercynite continuous series.

Figure 8 shows overprinted chromite which contains wustite inclusions. The wustite also occasionally occur as rims around the chromite grains. In table 8 the analysis of the chromite containing the wustite inclusion are given.

Table 8. Chemical analyses of overprinted chromites.

Oxides	1	2	3	4	5
SiO_2	n.d.	1.27	<lld	<lld	<lld
TiO_2	0.83	0.02	0.46	0.78	0.81
Al_2O_3	14.79	43.75	22.31	19.57	19.24
Cr_2O_3	43.89	22.07	43.14	44.29	44.26
FeO	31.79	18.09	25.92	27.02	28.35
MnO	0.35	0.15	0.28	0.28	0.33
MgO	8.07	14.64	7.83	8.05	7.46
CaO	n.d.	0.02	0.07	0.01	0.01
Number of cations per 32 oxygens					
Si	n.d.	0.28	<lld	<lld	<lld
Al	5.65	11.53	6.74	6.00	4.45
Cr	8.73	3.90	8.73	9.09	9.13
Ti	0.18	<lld	0.09	0.16	0.16
Fe^{3+}	4.63	0.29	0.44	0.76	2.27
Fe^{2+}	1.26	3.09	5.11	5.11	3.92
Mn	0.07	0.03	0.06	0.06	0.08
Mg	3.43	4.88	2.98	3.12	2.91

(n.d.=not determined, lld=lower limit of detection)

1. Chromite from Marikana analyzed by McLaren (unpub. thesis).
2. Zone at triple point of sintered chromite showing lower reflectivity (Figure 12e).
3. Alteration of chromite at rim, incorporating sulphides, with low reflectivity (Figure 12e).
4. The unaltered remainder of the chromite particle containing the zone of low reflectivity (Figure 12e).
5. Chromite containing inclusions of wustite (Figure 8).

Figure 8.

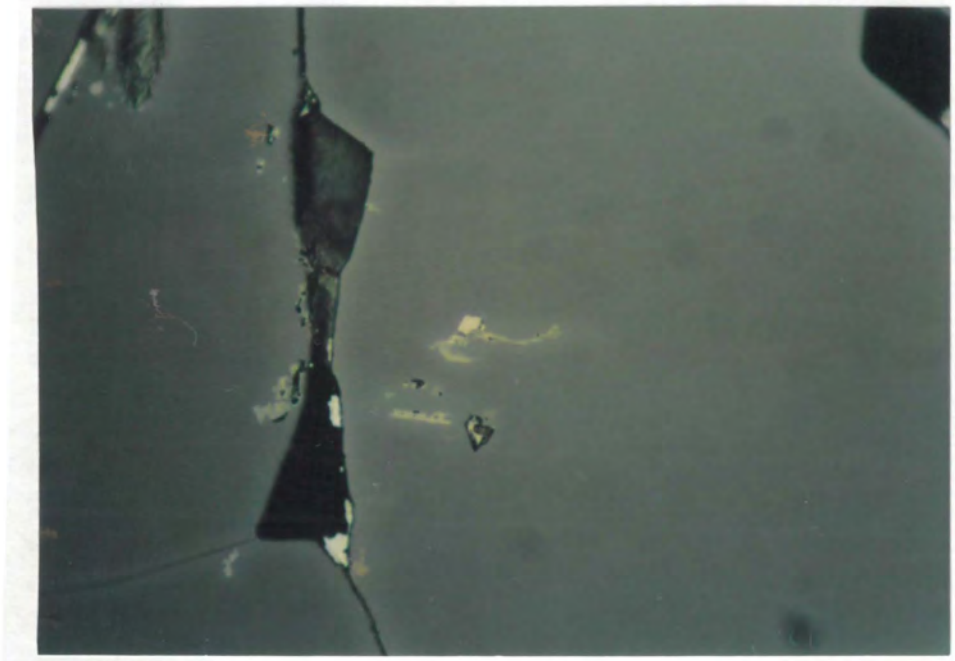

Figure 8

Overprinted chromite with wustite inclusions. Uncrossed nicols, oil immersion. Width of photomicrograph 150 μm. (For analysis see Table 8.)

The bottom 5-10cm of the chromitite shows intense sintering and alteration. The various stages of sintering are shown in Figures 9a to 9d. Figure 9a shows subhedral chromite grains surrounded by silicate. In Figure 9b certain of the chromite grains are still subhedral and the volume of the silicate material are decreasing. In Figure 9c, the original grain boundaries and the shape of the chromite grains are no longer visible. In Figure 9d the amount of the silicate material are mostly limited to veins.

4.2 Grain size distribution

Quantitative size distribution analyses were performed on chromite and sulphide grains in Profiles 2, 5, 6, 8 and the Reference Profile. Measurements were carried out in the Mineralogy Division of Mintek with a Leitz textural image analysis system. Seven polished sections were used for each profile to cover the entire chromitite layer. Forty fields were measured on every polished section with a 16X magnification consisting of 60% to 90% of chromite area. The sulphides were measured with a 20X magnification and 200 fields were measured per polished section.

The microscopic size distributions quoted refer to diameter measurements carried out on sectioned particles as they appear in polished sections and are therefore not 'true' size distributions (Underwood, 1968). They are related to the true size distribution (King, 1978) and can be used to compare the size distributions of different samples. The diameter measured is the size of the largest hexagon that fits into the chromite or BMS grain (Figure 10).

The maximum size of the altered profiles is significantly larger than the Reference Profile as shown in Table 9. The median values of the altered profiles furthermore emphasise the increase in chromite grain size with alteration.

Figures 11a-11e show the chromite size distribution determined for Profiles 2, 5, 6, 8, and the Reference Profile.

Figure 9.

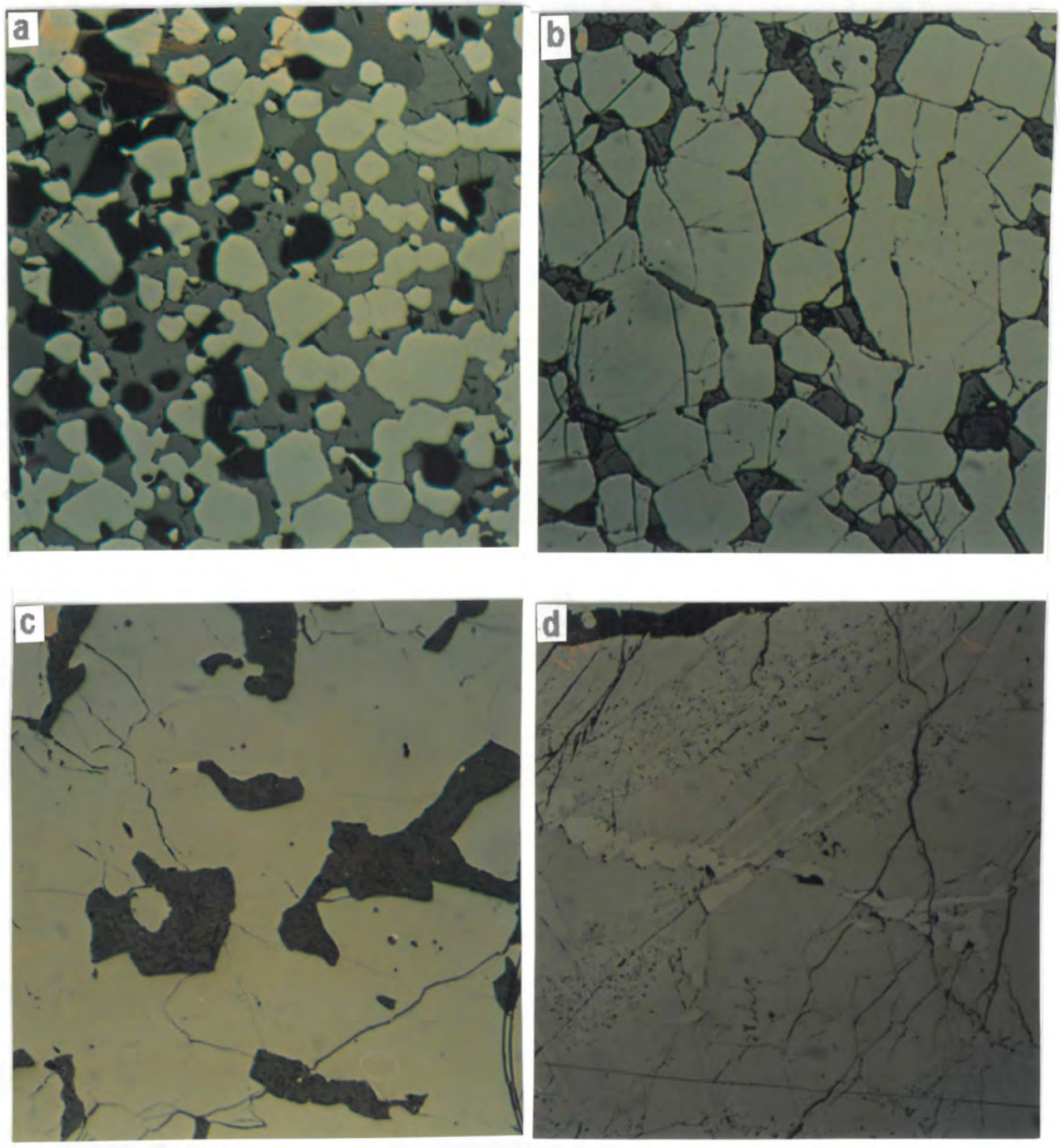

Figure 9.
(increasing amount of sintering)

9a. Chromitite from the Reference Profile. Oil immersion, uncrossed nicols. Width of photomicrograph 580 μm.

9b. Volume of silicate material decreasing. Original grain boundaries visible. Oil immersion, uncrossed nicols. Width of photomicrograph 580 μm.

9c. Original grain boundaries and shape of chromite no longer visible. Oil immersion, uncrossed nicols. Width of photomicrograph 580 μm.

9d. The amount of silicate material are mostly limited to veins. Oil immersion, uncrossed nicols. Width of photomicrograph 580 μm.

Table 9. Chromite size distributions

Profile	Maximum size (μm)	Median (μm)
Reference	400	75 - 125
6	300	100 - 140
5	500	100 - 250
2*	370	120 - 220
8*	600	150 - 200

(* - Bottom 10 cm of chromitite sintered - not included.)

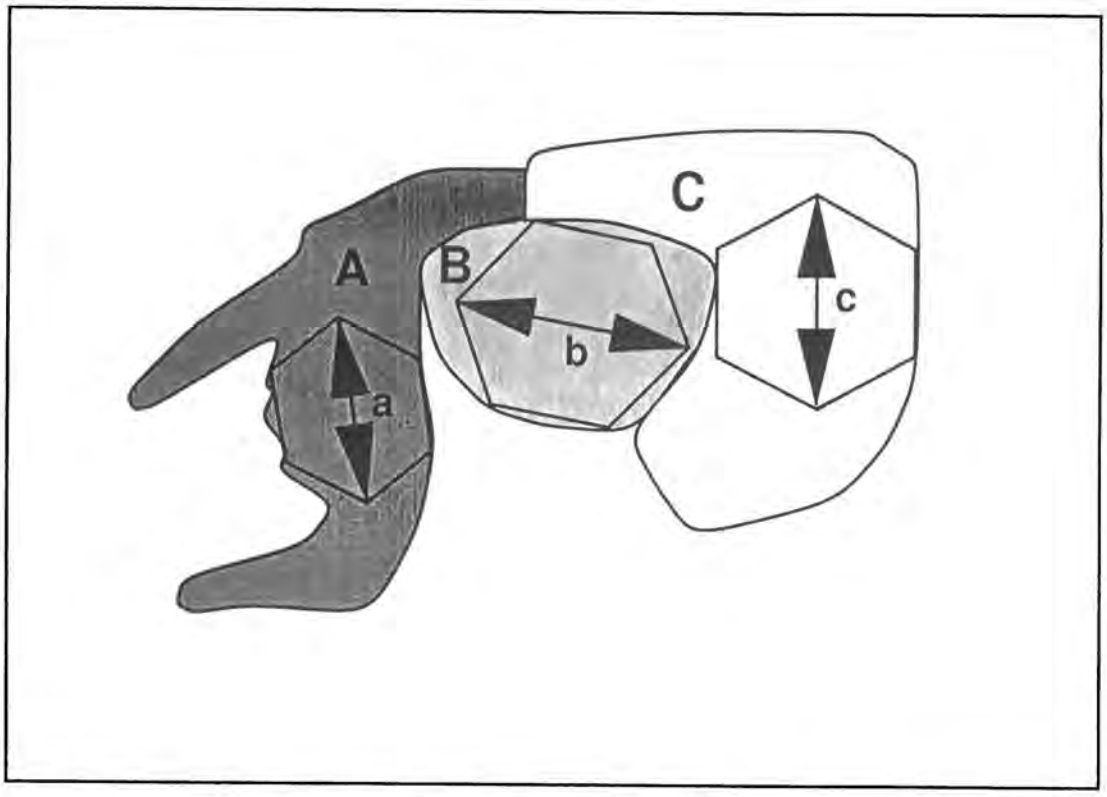

Figure 10. Grains A, B, and C have diameters a, b, and c which are the diameters of the largest hexagons that fit into the grains.

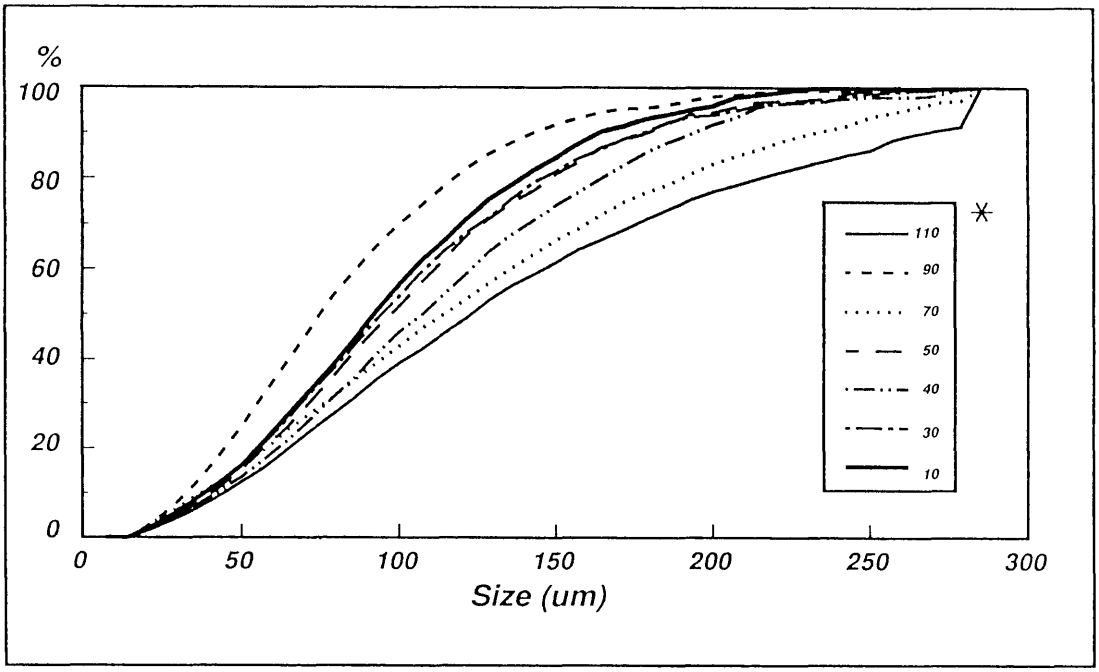

Figure 11a. Cumulative chromite size distribution of the reference profile.

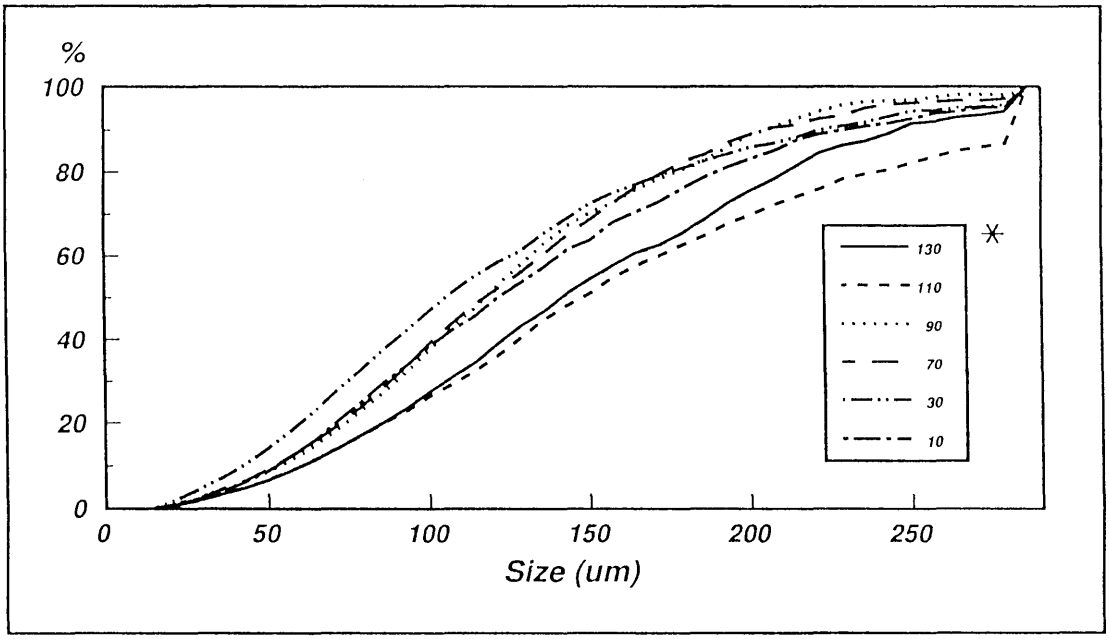

Figure 11b. Cumulative chromite size distribution of profile 6

✳ *approximate distance from footwall contact (cm)*

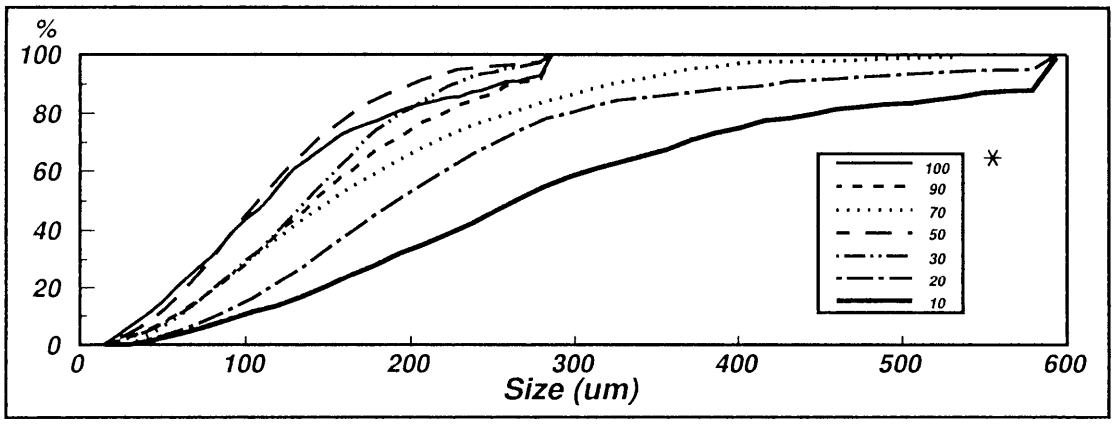

Figure 11c. Cumulative chromite size distribution of Profile 5.

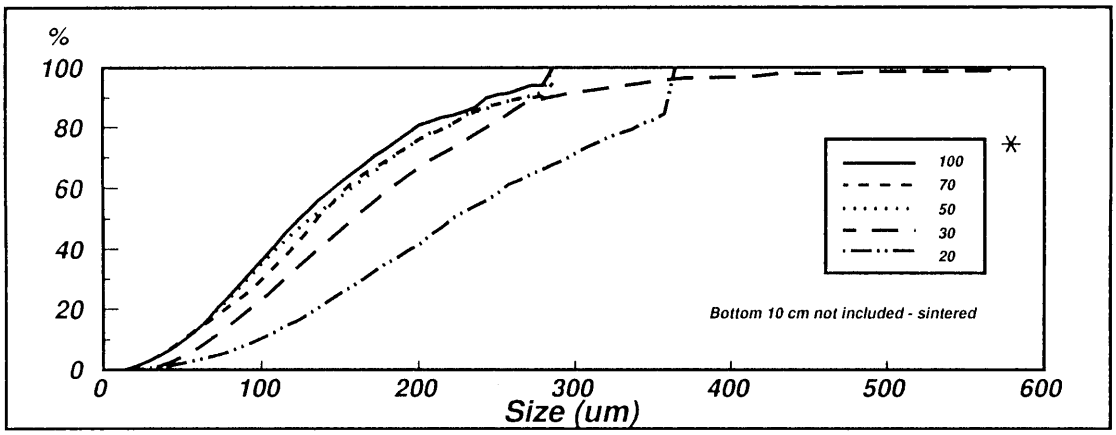

Figure 11d. Cumulative chromite size distribution of Profile 2.

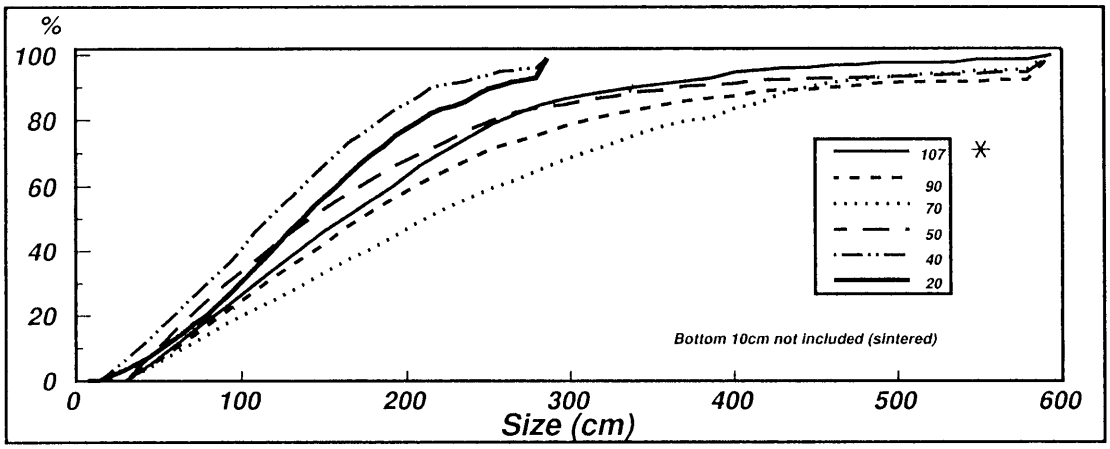

Figure 11e. Cumulative chromite size distribution of Profile 8.

✳ *approximate distance from footwall contact (cm)*

5. BASE METAL SULPHIDES

One-hundred and fifty polished sections were made of the chromitite from Profiles 1, 2, 3, 5, 8, and the Reference Profile and seven of the footwall of Profile 5. The polished sections were scanned with a 32x oil immersion objective for location of the sulphide minerals. Minerals that could not be identified were marked with a diamond marker and were qualitatively analyzed on the electron microprobe.

5.1 Microscopical mode of occurrence

Table 10 shows the base-metal sulphide assemblage in the various profiles. The profiles are arranged in order of increasing macroscopic alteration.

5.1.1 The Reference Profile

The sulphide minerals in the Reference sample consist mainly of pentlandite as anhedral grains with minor chalcopyrite and pyrrhotite. (Ramdohr (1980) was used for the identification of the ore minerals.) The type of occurrence is very similar to the description by Liebenberg (1970). Pyrite occurs as small, rounded grains as inclusions in pentlandite (Figure 12a). Thin veins consisting of sulphides also follow cracks in chromite grains.

5.1.2 Profile 3

Pentlandite is present throughout the UG-2 chromitite as the major sulphide phase. The monomineralic grains are mostly subhedral to anhedral, typically approximately 30 μm in diameter and occur at chromite grain boundaries. Pentlandite and chalcopyrite also form small (15 μm) inclusions in hydroxyl - bearing silicates as shown in Figure 12b.

Chalcopyrite occurs over the whole thickness of the chromitite layer as a minor phase. In Profile 3, chalcopyrite is mostly altered to bornite, covellite and Cu-S[1]. Bornite occurs as replacement bodies and lamellae in the chalcopyrite (Figure 12c and 12d). In some cases bornite completely replaces chalcopyrite and occurs with pentlandite in composite grains. Chalcopyrite also sporadically forms thin veins between chromite grains.

---

1 Note: Small intergrowths consisting of Cu and S are apparently chalcocite, but were not closer specified (see also Mumm et Al, 1988: Goble, 1980) and will be referred to as chalcocite - group minerals (ccgm).

Table 10. Sulphide assemblage in the profiles.

Profile nr.	Ref	3	1	5	2	8
Major constitu-ents	Pent	Pent	Pent	Pent	Pent	Pent
Minor constitu-ents	Cp Po	Cp Ccgm Cov Born Po	Cp Cov Ccgm Born Viol Po Cub	Cp Cov Ccgm Born Viol Mack Haezl Po Cub	Cp Cov Ccgm Born Viol Haezl	Cp Viol Po Haezl
Trace constitu-ents	Pyrite	Sphal Haezl	Mack	Gersd Nicc Mauch Cobalt Mill Galena	Sphal Po Mill Cub Mack	Born Mack Mill Mauch

Abbreviations: Pent - pentlandite, Cp - chalcopyrite, Po - pyrrhotite, Cov - covellite, Ccgm - chalcocite-group minerals, Born - bornite, Sphal - sphalerite, Haezl - haezlewoodite, Viol - violarite, Cub - cubanite, Mack - mackinawite, Gersd - gersdorffite, Nicc - niccolite, Mauch - maucherite, Cobalt - cobaltite, Mill - millerite.

Figure 12

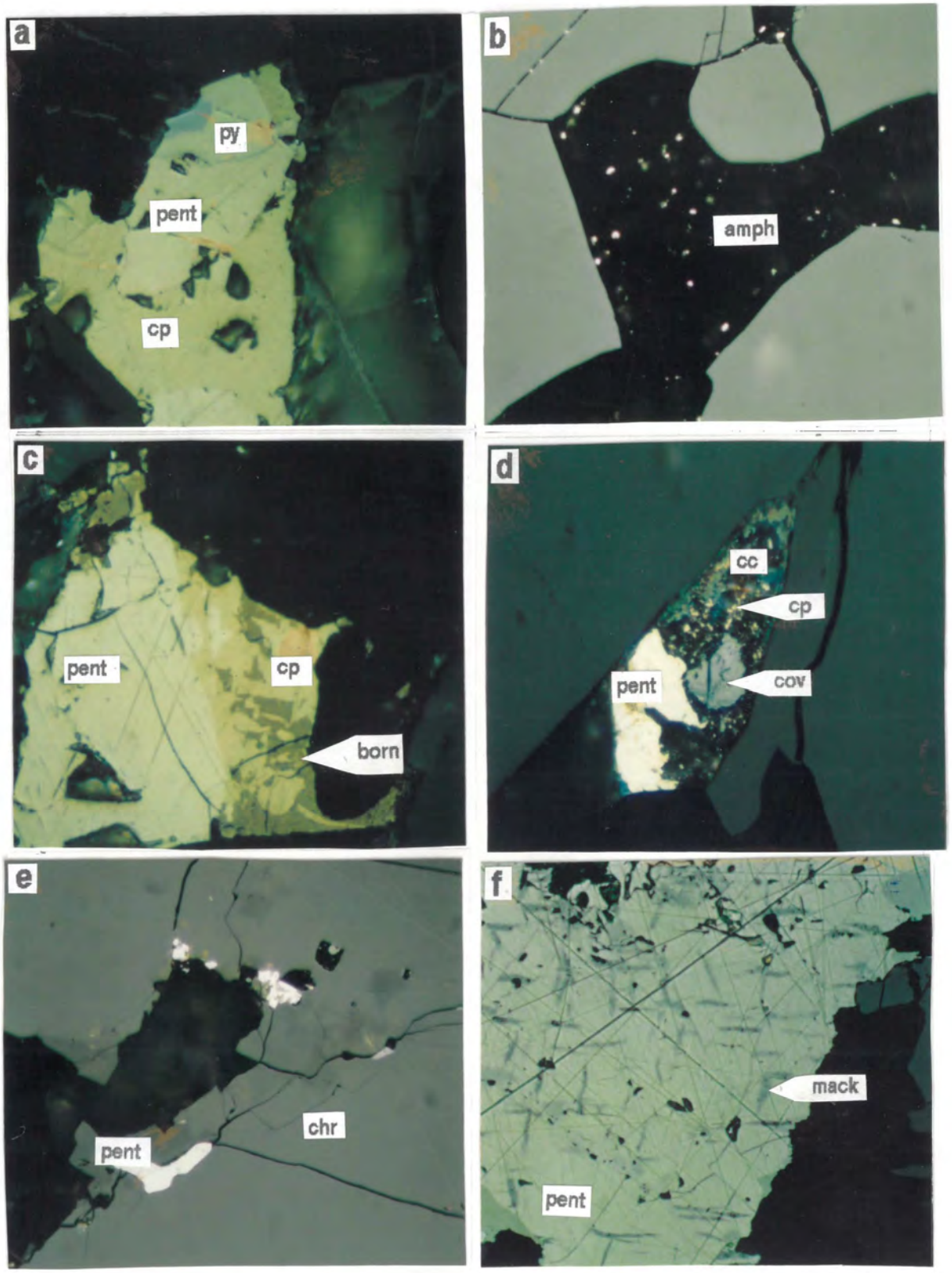

Figure 12.

a. Sulphide assemblage consisting of chalcopyrite (cp), pentlandite (pent), and pyrite (py). Pyrite contains an inclusion of laurite. Uncrossed nicols; oil immersion; width of photomicrograph 90 μm.

b. Inclusions of pentlandite and chalcopyrite in amphibole (amph). Uncrossed nicols; oil immersion; width of photomicrograph 140 μm.

c. Composite sulphide grain consisting of pentlandite (pent), and chalcopyrite (cp) partly altered to bornite (born). Uncrossed nicols; oil immersion; width of photomicrograph 90 μm.

d. Composite grain of pentlandite (pent), chalcocite - group minerals (cc), and covellite (cov), with remains of chalcopyrite (cp). Uncrossed nicols; oil immersion; width of photomicrograph 36 μm.

e. Pentlandite (pent) enclosed by chromite (chr) edges. Uncrossed nicols; oil immersion; width of photomicrograph 90 μm.

f. Mackinawite (mack) inclusions in pentlandite (pent). Uncrossed nicols; oil immersion; width of photomicrograph 36 μm.

Sphalerite occurs in composite sulphide grains as small (20 μm) particles, sometimes with chalcopyrite inclusions.

Haezlewoodite was noted in a few cases as isolated, anhedral, porous grains in silicate.

Sporadically, pentlandite and chalcopyrite are enclosed by chromite rims as shown in Figure 12e. In these growth zones, the chromite shows a decrease in reflectivity and sometimes red or yellow internal reflections.

5.1.3 Profile 1

The bottom 5 cm of the chromitite is sintered and therefore only small (15 μm) sulphide grains are present in the Fe-Ti-oxides. These sulphides are mainly pyrrhotite, pentlandite, mackinawite and violarite. The pyrrhotite and pentlandite form composite sulphide grains, with pentlandite partially or completely replaced by violarite. Mackinawite forms small (5 μm), worm-like exsolutions in pentlandite, often following pentlandite crystal planes (Figure 12f).

In the unsintered portion of the chromitite of Profile 1, pentlandite is the major phase, also associated with mackinawite and violarite.

5.1.4 Profile 5

In Profile 5, the 20 cm of the footwall directly below the chromitite was included in the study. The sulphides in this area consist mainly of pyrrhotite and cubanite as shown in Figure 13a. These two minerals form large (up to 2 mm) composite sulphide grains with millerite, chalcopyrite and pentlandite as minor phases. Pentlandite is intergrown with small, worm-like exsolutions of mackinawite. Most of the composite sulphide grains are rimmed by approximately 10 μm magnetite. Magnetite lenses also occur in some of the millerite grains.

In the footwall directly below the chromitite (within 1 mm), arsenic-rich phases were detected in the large composite grains. Anhedral niccolite (NiAs) and a more Ni-rich arsenide, possibly maucherite (Ni_3As_2) or orcelite (Ni_5As_2) (Lorand, et al, 1984), occur with cubanite at the rims of the sulphide grains. Cobaltite (CoAsS) is also present as euhedral to anhedral grains in cubanite at the rims of the sulphide grains (Figure 13b). The cobaltite is weakly anisotropic. Gersdorffite (NiAsS) was detected with the microprobe as a rarity.

Figure 13.

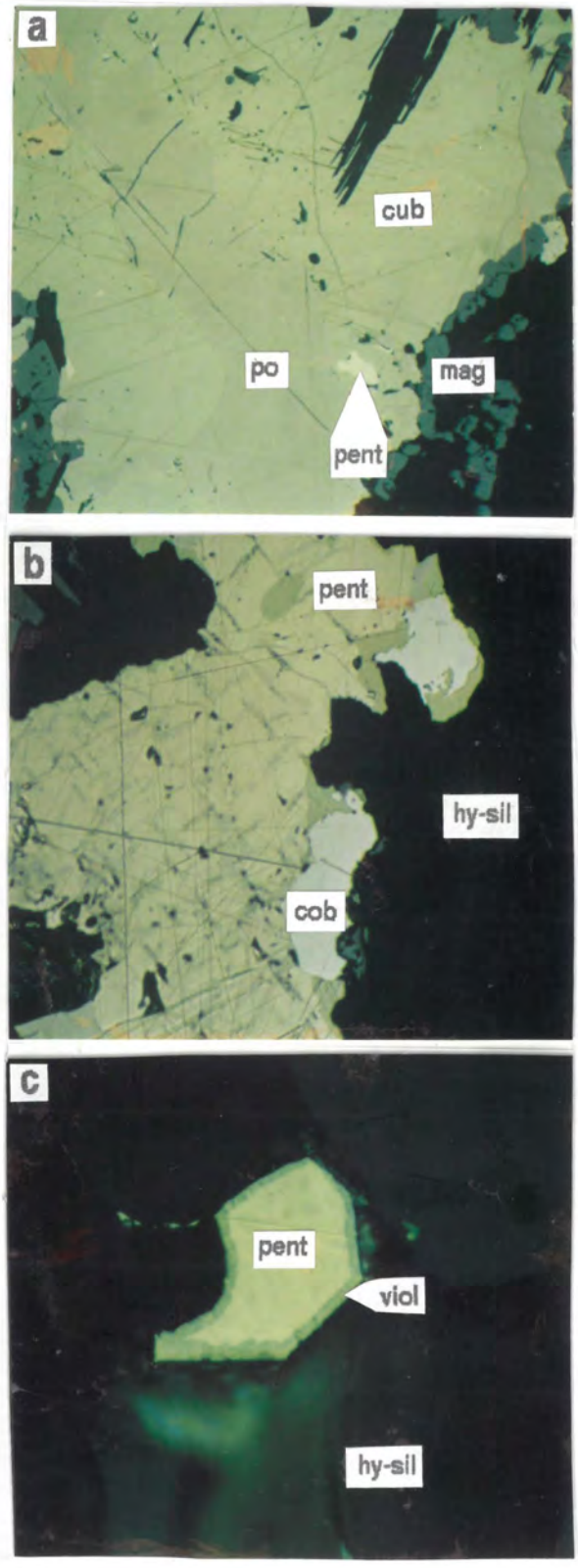

Figure 13.

a. Composite grain of pyrrhotite (po) containing inclusion of pentlandite (pent), and cubanite (cub). The BMS has a rim of magnetite (mag). Uncrossed nicols; oil immersion; width of photomicrograph 420 μm.

b. Cobaltite (cob) inclusions in cubanite surrounding pentlandite (pent) surrounded by hydrous silicates (hy-sil). Uncrossed nicols; oil immersion; width of photomicrograph equals 420 μm.

c. Pentlandite (pent) with a rim of violarite (viol) in hydrous silicates (hy-sil). Uncrossed nicols; oil immersion; width of photomicrograph equals 36 μm.

The bottom 2 cm of the chromitite, which is sintered to a solid intergrowth of magnetite and Fe-Ti-oxides (ilmenite and ulvospinel), contains small (30 μm) sulphide grains in the sintered oxide phase, originally at chromite grain boundaries. The main sulphide in this area is pyrrhotite with minor pentlandite, chalcopyrite, cubanite and mackinawite.

5.1.5 Profile 2

The mode of occurrence of sulphides in Profile 2 is similar to that in Profile 1 and will therefore only be discussed briefly.

Profile 2 is also sintered at the bottom of the chromitite with the result that sulphides such as pentlandite, covellite, bornite and chalcopyrite occur as small (20 μm), rounded grains enclosed in the magnetite.

In the unsintered chromitite, pentlandite is the major sulphide phase and occurs unaltered, rimmed by, or completely altered to violarite. Mackinawite is a trace constituent and only rarely occurs as worm-like exsolutions in pentlandite.

Chalcopyrite is a minor phase and occurs either with bornite or is completely altered to mixtures of bornite and/or chalcocite-group minerals, with a simultaneous decrease in volume. Cubanite lamellae in chalcopyrite occur only sporadically.

In the unsintered portion of the chromitite, sulphide minerals such as pentlandite, covellite and chalcopyrite are incorporated into edges of chromite grains in the same manner as described for Profile 5.

5.1.6 Profile 8

The sulphide mineral assemblage of Profile 8 is slightly different from the previously described profiles in that Cu-rich sulphide phases are relatively rare, with only minor amounts of chalcopyrite with bornite lamellae. Covellite and chalcocite were not observed.

The largest amount of haezlewoodite was found in Profile 8. It is mostly present as small (3 μm), rounded inclusions in pentlandite. At the bottom of the sintered chromitite hydrous silicates form wide (200 μm) veins parallel to the strike of the chromitite which contains large (300 μm) grains of pyrrhotite.

Violarite frequently replaces pentlandite completely or partially (Figure 13c). Semi-quantitative analyses of violarite indicate a more Ni-rich composition than the pentlandite from which it formed. In pentlandite the Fe:Ni ratio is approximately 2:1 compared to 1.25:1 for violarite.

5.2 Pentlandite chemistry

Figure 14 shows the quantitative pentlandite analyses in Profile 1. The analyses were done by the Mineralogy Division at Mintek. (See Appendix 4 for a list of the analyses.) The pentlandites have a relatively large variation in their mineral chemistry. Co varies from 0 wt% to 7,5 wt% with the Co-rich varieties present in the bottom 10cm of the chromitite (1-13,14,16). The Ni:Fe ratio is 1.1:1 on average and ranges from 2.2:1 to 0.3:1. Figure 14 shows a systematic increase in Fe with a decrease in Ni. The Co-content also increases with alteration.

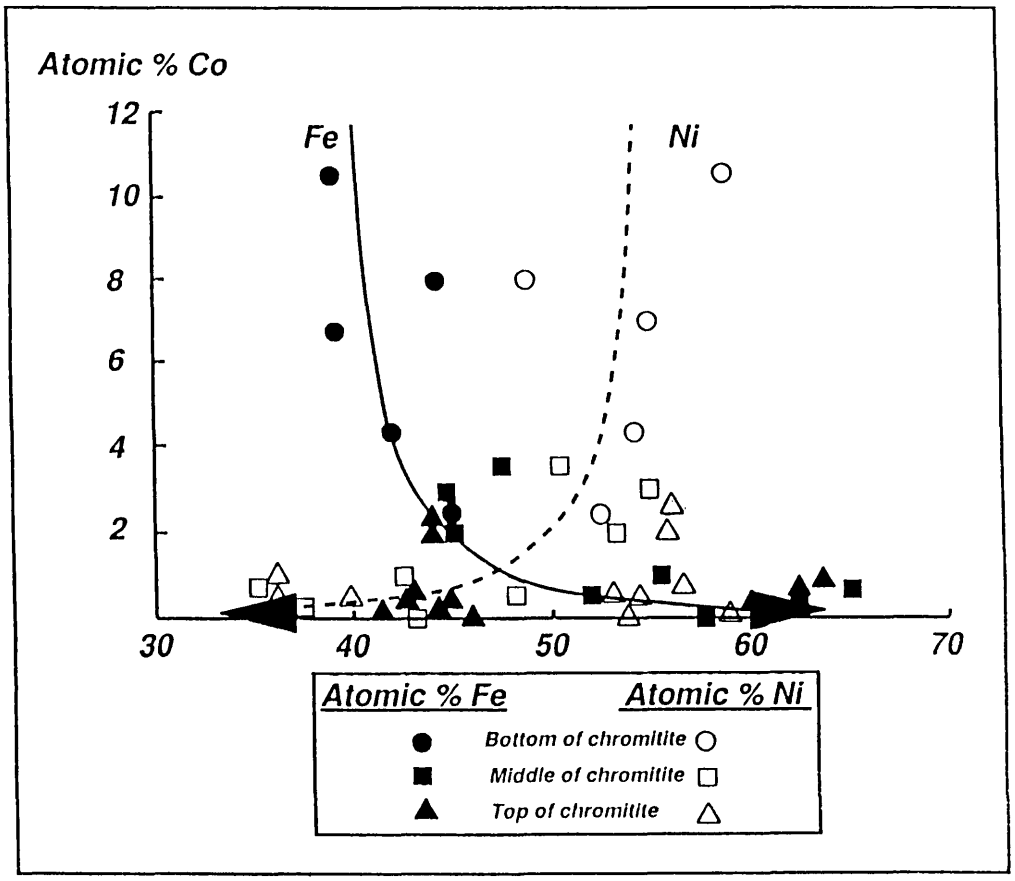

Figure 14. Variation in chemistry of pentlandite of Profile 1.

5.3 Grain size distribution

Quantitative size distribution analyses were performed on chromite and sulphide grains in Profiles 2, 5, 6, 8 and the Reference Profile. The sulphides were measured with a 20X magnification and 200 fields were measured per polished section. The average sulphides measured per field were between 0.02% and 0.08% sulphide area. (Underwood, 1968)

Table 11 and Figures 15a to 15b show the sulphide size distributions.

There is a tendency for the sulphide grains to increase with alteration, although sulphide grains in Profile 8 are relatively small in comparison to the other profiles. This may be due to remobilization of BMS into sulphide veins and the sintering of the chromite in the bottom 10cm of the UG-2 chromitite.

Table 11. Sulphide size distributions

Profile	Maximum size (μm)	Median (μm)
Reference	27	7-17
6	37	5-12
5	78	4-40
2*	55	7-53
8*	23	4-10

(* - Bottom 10 cm of chromitite sintered - not included.)

5.4 Acid soluble Cu, Ni, and Co analyses

The acid soluble Cu-, Ni- and Co- analyses (ACE's) were performed on all the UG-2 chromitite samples and 0-20cm of the footwall directly below the contact. The analyses were done by Atomic Absorption Spectroscopy at the Analytical Division at Mintek after solution in HNO_3 and HCl.

The results of the acid soluble element analyses are shown in Figures 16 to 21.

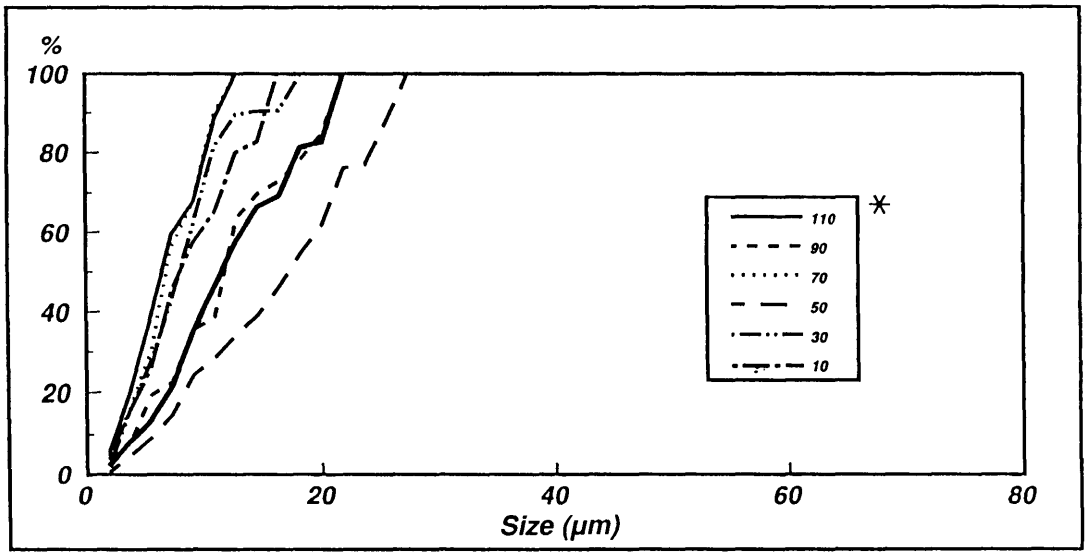

Figure 15a. Cumulative sulphide size distribution of the Reference Profile.

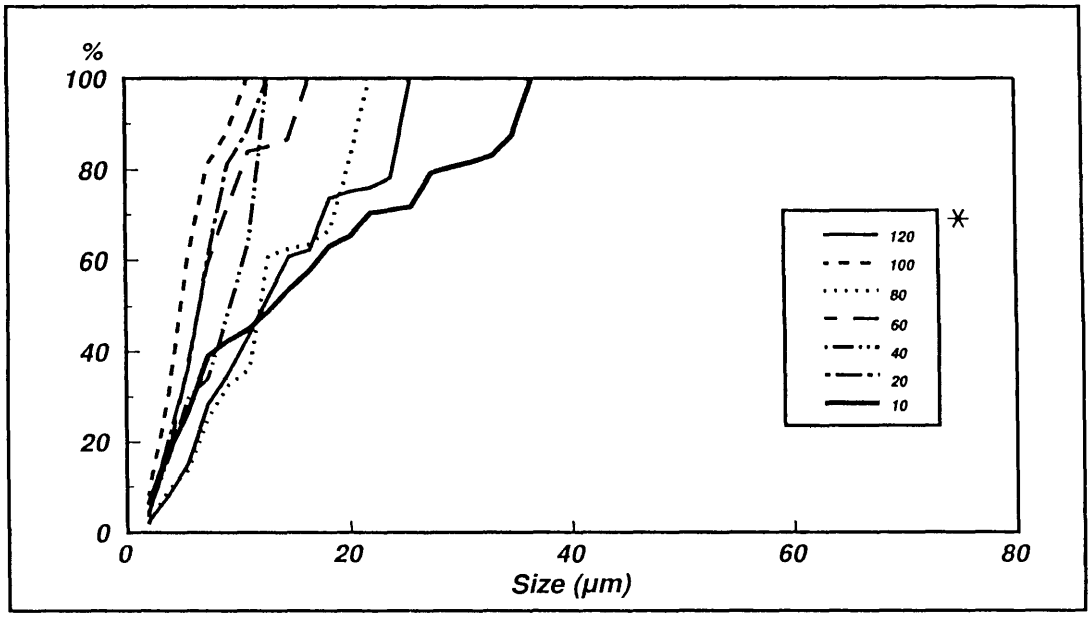

Figure 15b. Cumulative sulphide size distribution of Profile 6.

* *approximate distance from footwall contact (cm)*

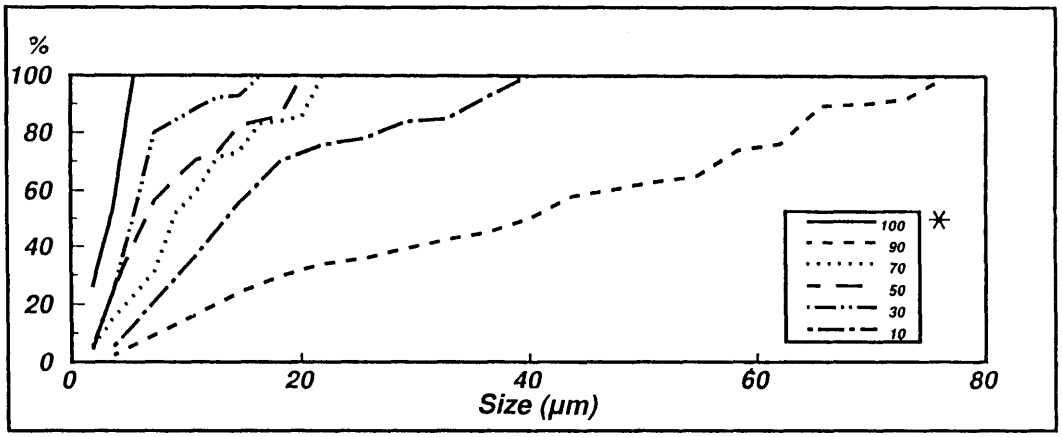

Figure 15c. Cumulative sulphide size distribution of Profile 5.

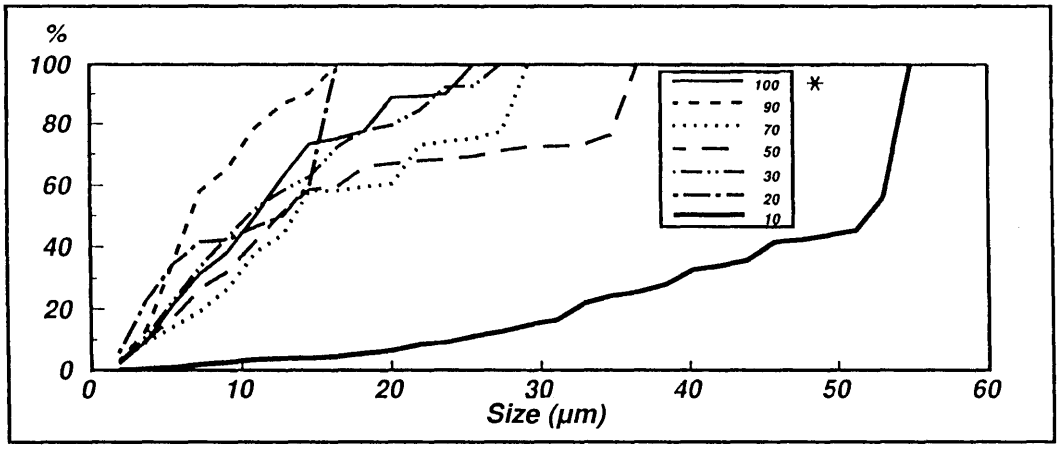

Figure 15d. Cumulative sulphide size distribution of Profile 2.

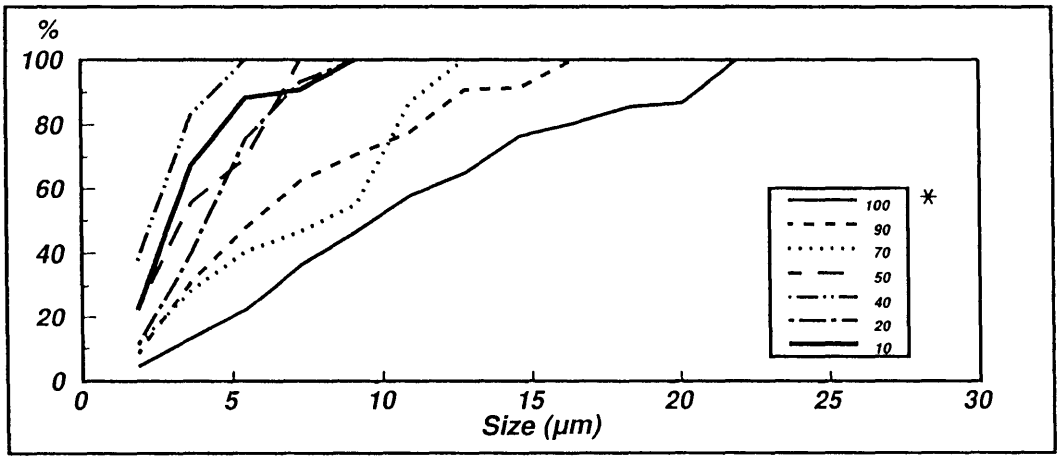

Figure 15e. Cumulative sulphide size distribution of Profile 8.

* *approximate distance from footwall contact (cm)*

Reference Profile - The average values for acid soluble elements (38, 98, and 4 ppm for Cu, Ni, and Co respectively) are low for the Reference Profile, compared to the altered profiles. The bottom 10 cm of the UG-2, which is enriched in platinum group minerals, has a fairly low sulphide concentration with an acid soluble element peak at 40 cm from the bottom contact. As shown in Figure 16, acid soluble Co has a constantly low grade of 4 to 5 ppm. ACE values in the footwall are relatively low.

Profile 6 - Figure 17 shows the ACE distribution in Profile 6. There is a slight increase in the values at the bottom of the UG-2, but the highest values for Cu, Ni and Co are found at approximately 30 to 40 cm from the bottom contact. Profile 6 contains the highest average Cu and Ni values of all the profiles, i.e., 167 and 325 ppm respectively. From the data in Figure 17 it is clear that the footwall of Profile 6 is enriched in sulphide minerals directly below the bottom contact and has one of the highest acid soluble element contents with 1920, 1930, and 210 ppm for Cu, Ni and Co respectively.

Profile 3 - For Profile 3, Figure 18 shows that the acid soluble elements show the same vertical distribution as the PGE's. The Ni-peak coincides with the Pt-peak and the Cu-peak with both the Pt-and Pd-peak. The acid soluble element concentration is low compared to that of the other altered profiles.

Profile 1 and Profile 5 - In Profiles 1 and 5 the ACE's all follow the same trend and show a peak in the middle of the chromitite at 30 and 50 cm respectively from the bottom contact. (Figures 19 and 20). Profile 5 contains the highest acid soluble Cu content of 2370 ppm analyzed in the footwall. The Ni and Co content reach values of 1840 and 249 ppm respectively. Profile 1 is also mineralized in the footwall with Ni and Co values ranging 171 to 368 ppm, and 75 to 176 ppm respectively.

Profile 2 - In Profile 2, the ACE's have a peak at 30 cm from the bottom contact with Cu and Ni, reaching values of 133 and 499 ppm respectively (Figure 21). The footwall is enriched in sulphides, and Ni and Co (396 and 225 ppm respectively) 20 cm below the footwall contact.

Profile 8 - In the case of Profile 8 (shown in Figure 22), Cu values reach a peak of 400 ppm at 30 cm from the bottom contact. Ni, however, is notably variable over the thickness of the chromitite and has a peak of 445 ppm at the top of the UG-2. The footwall directly below the bottom contact is also enriched in sulphides with an unusually high Co value of 245 ppm.

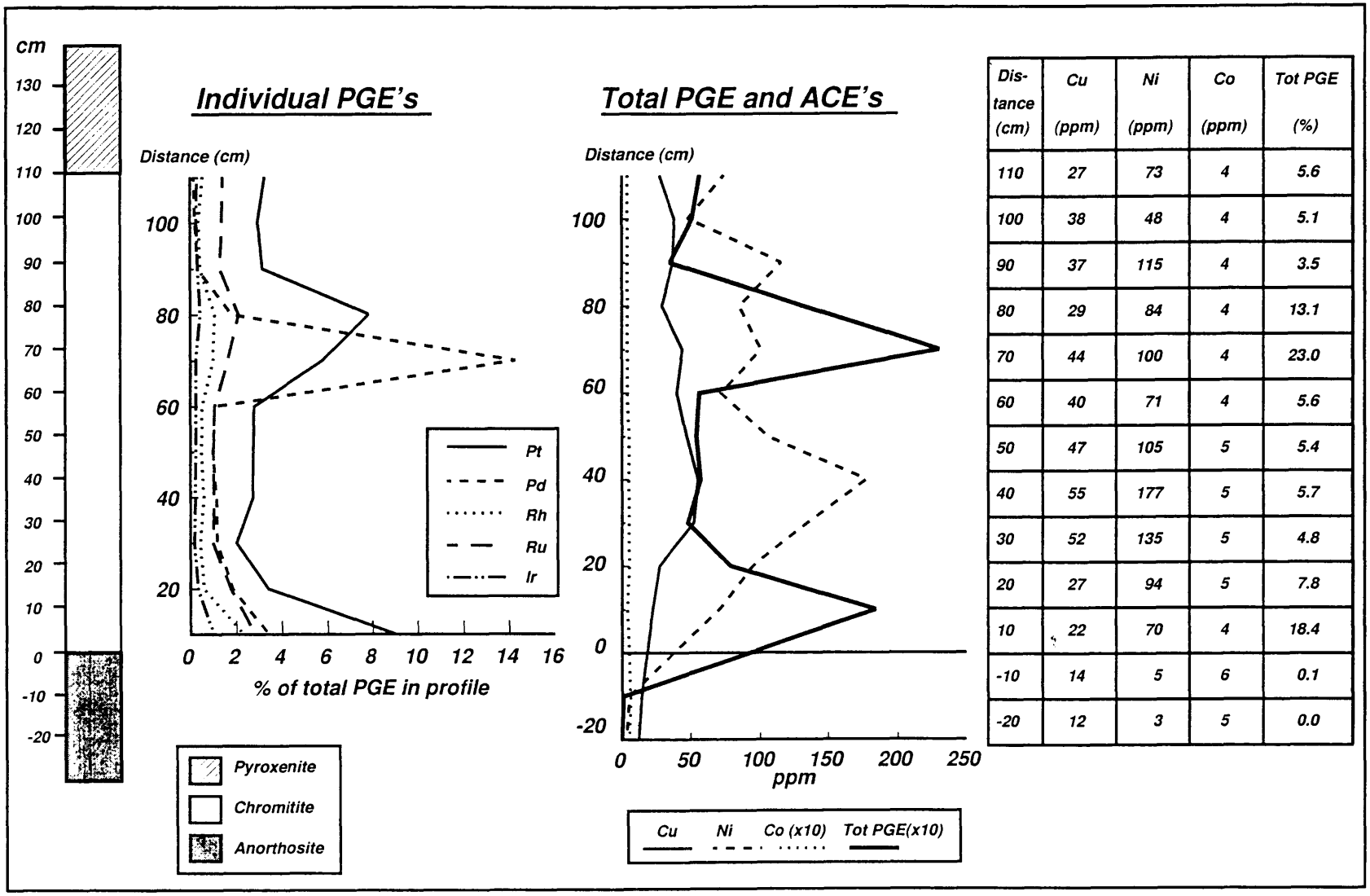

Distance (cm)	Cu (ppm)	Ni (ppm)	Co (ppm)	Tot PGE (%)
110	27	73	4	5.6
100	38	48	4	5.1
90	37	115	4	3.5
80	29	84	4	13.1
70	44	100	4	23.0
60	40	71	4	5.6
50	47	105	5	5.4
40	55	177	5	5.7
30	52	135	5	4.8
20	27	94	5	7.8
10	22	70	4	18.4
-10	14	5	6	0.1
-20	12	3	5	0.0

Figure 16. The PGE and acid soluble element distribution in the Reference Profile.

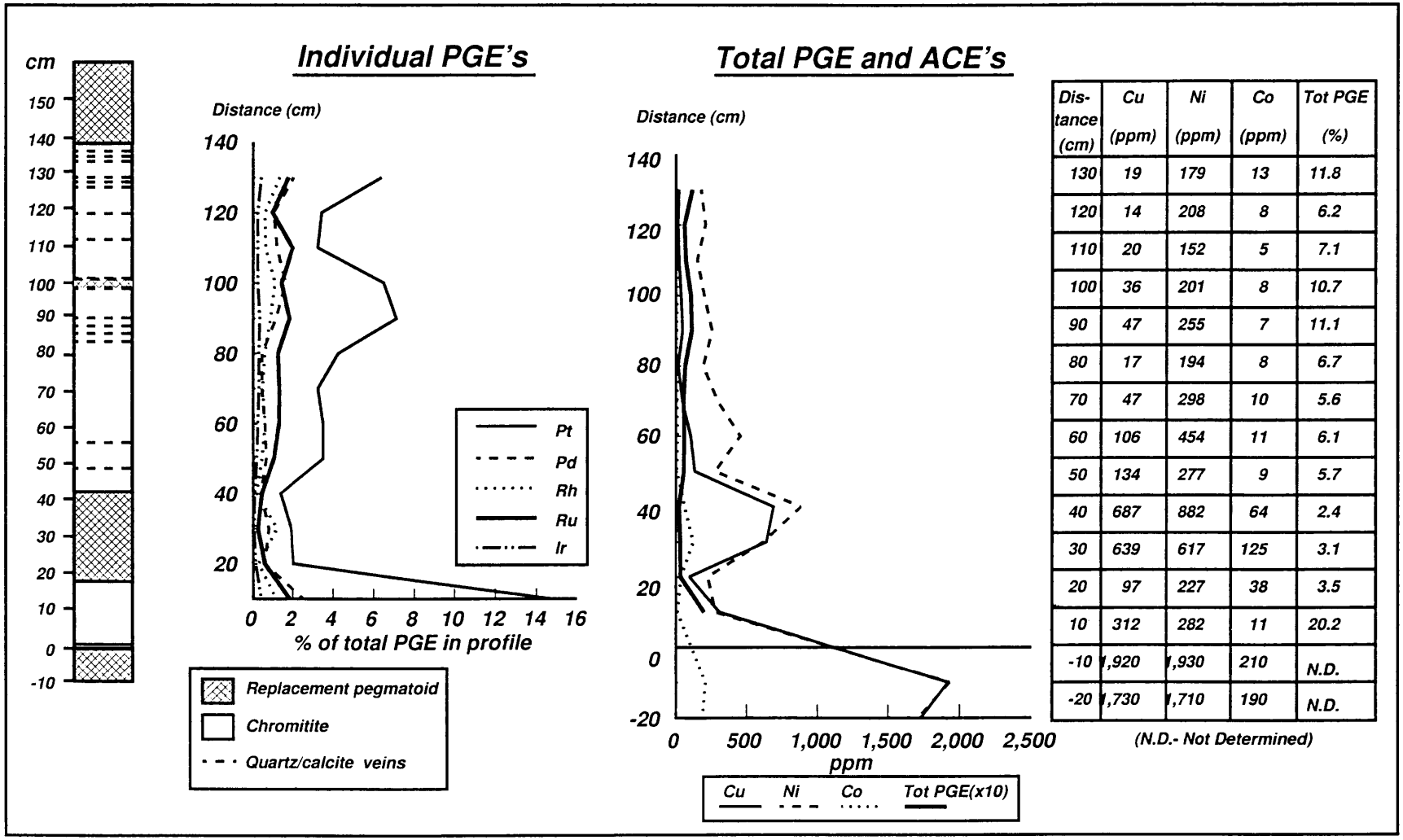

Distance (cm)	Cu (ppm)	Ni (ppm)	Co (ppm)	Tot PGE (%)
130	19	179	13	11.8
120	14	208	8	6.2
110	20	152	5	7.1
100	36	201	8	10.7
90	47	255	7	11.1
80	17	194	8	6.7
70	47	298	10	5.6
60	106	454	11	6.1
50	134	277	9	5.7
40	687	882	64	2.4
30	639	617	125	3.1
20	97	227	38	3.5
10	312	282	11	20.2
-10	1,920	1,930	210	N.D.
-20	1,730	1,710	190	N.D.

(N.D.- Not Determined)

Figure 17. The PGE and acid soluble element distribution of Profile 6.

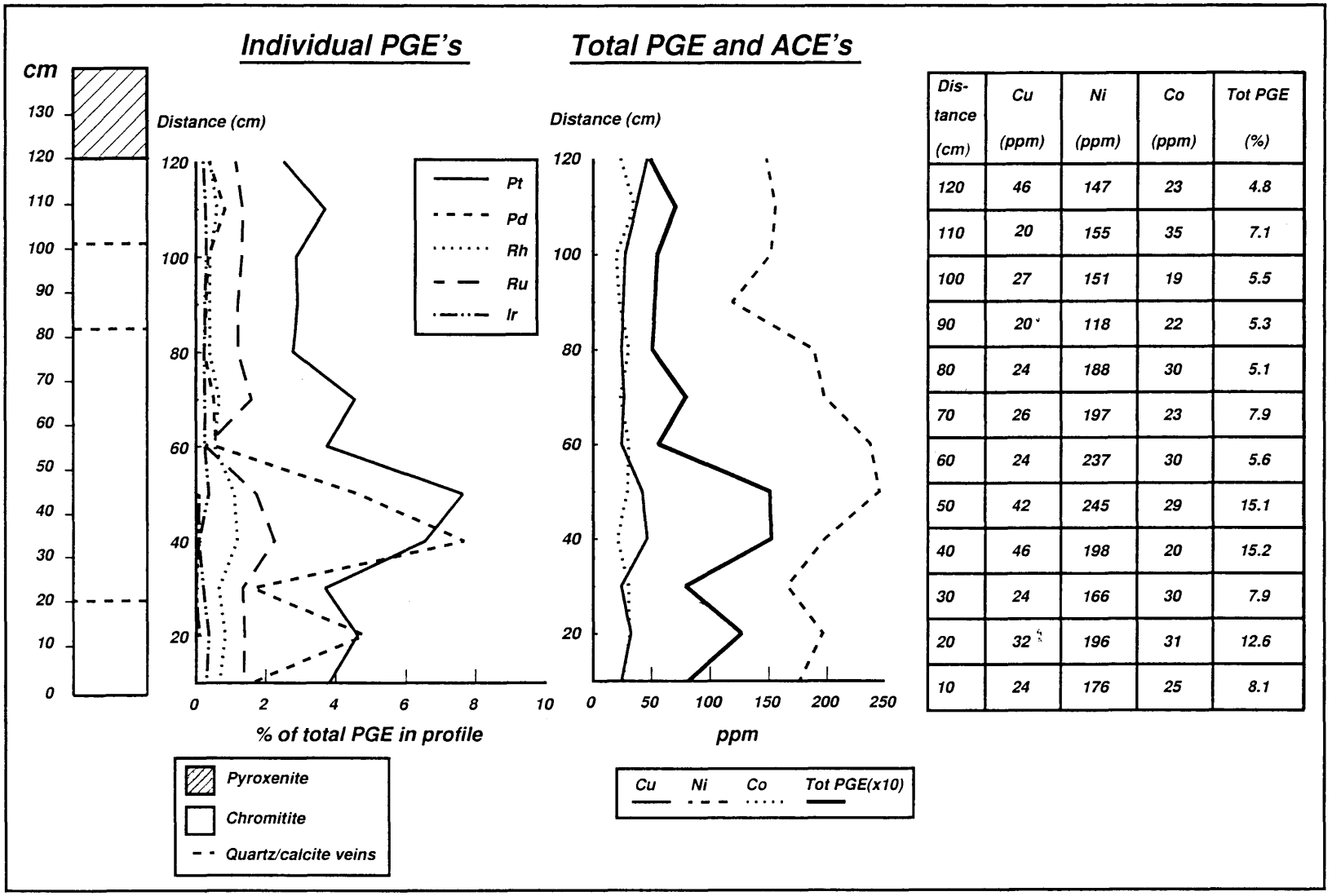

Distance (cm)	Cu (ppm)	Ni (ppm)	Co (ppm)	Tot PGE (%)
120	46	147	23	4.8
110	20	155	35	7.1
100	27	151	19	5.5
90	20	118	22	5.3
80	24	188	30	5.1
70	26	197	23	7.9
60	24	237	30	5.6
50	42	245	29	15.1
40	46	198	20	15.2
30	24	166	30	7.9
20	32	196	31	12.6
10	24	176	25	8.1

Figure 18. The PGE and acid soluble element distribution of Profile 3.

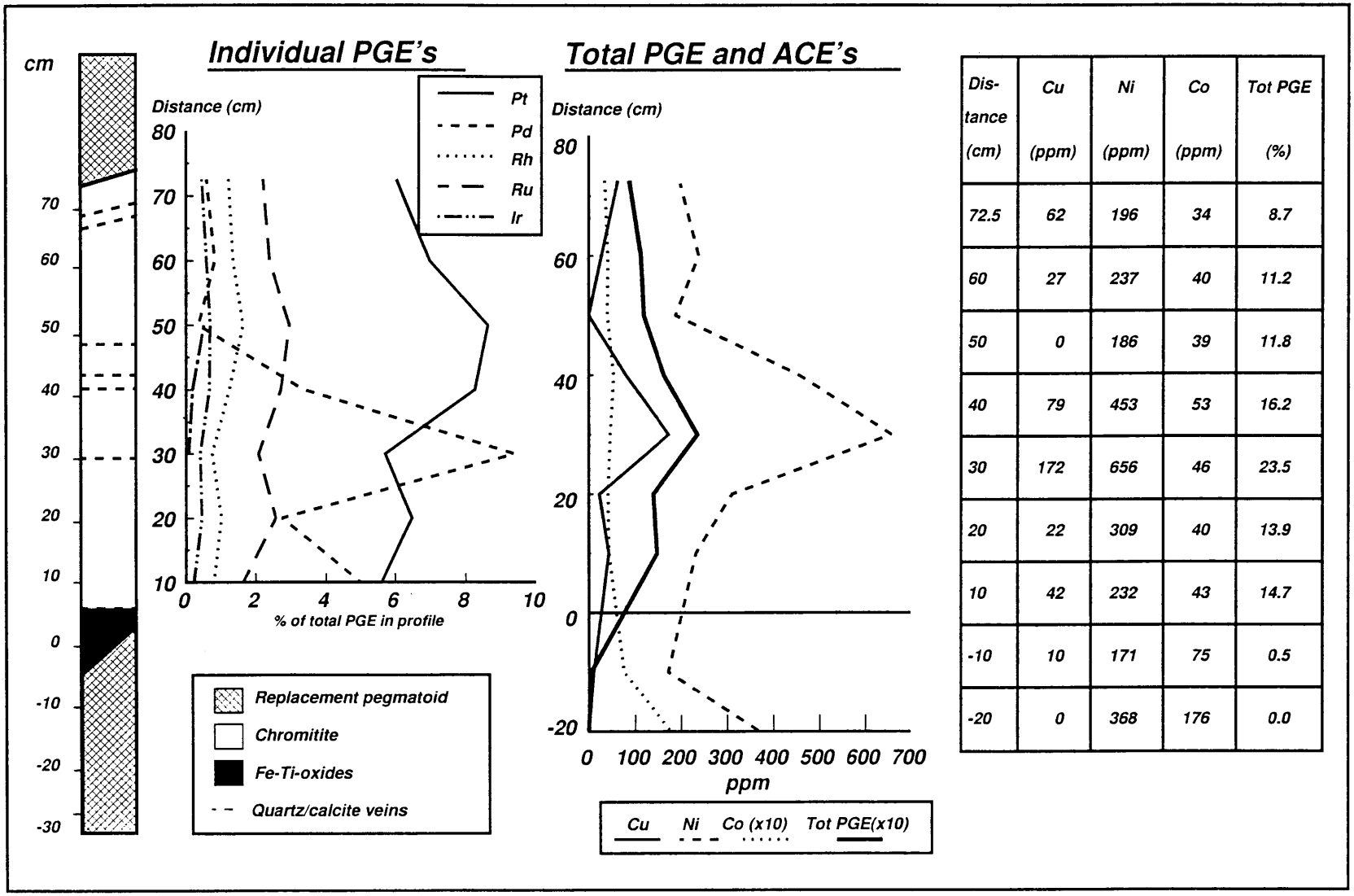

Distance (cm)	Cu (ppm)	Ni (ppm)	Co (ppm)	Tot PGE (%)
72.5	62	196	34	8.7
60	27	237	40	11.2
50	0	186	39	11.8
40	79	453	53	16.2
30	172	656	46	23.5
20	22	309	40	13.9
10	42	232	43	14.7
-10	10	171	75	0.5
-20	0	368	176	0.0

Figure 19. The PGE and acid soluble element distribution of Profile 1.

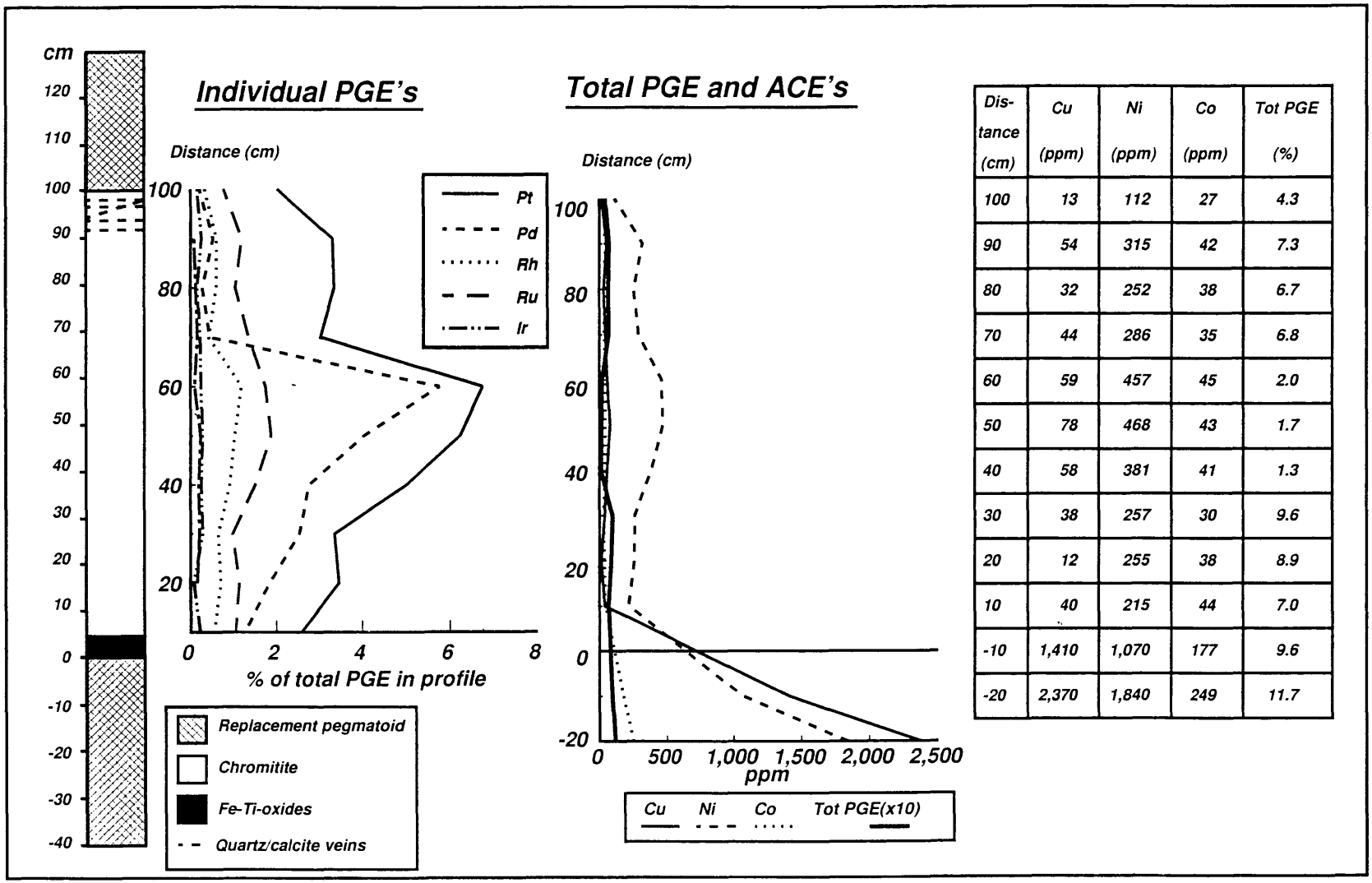

Distance (cm)	Cu (ppm)	Ni (ppm)	Co (ppm)	Tot PGE (%)
100	13	112	27	4.3
90	54	315	42	7.3
80	32	252	38	6.7
70	44	286	35	6.8
60	59	457	45	2.0
50	78	468	43	1.7
40	58	381	41	1.3
30	38	257	30	9.6
20	12	255	38	8.9
10	40	215	44	7.0
-10	1,410	1,070	177	9.6
-20	2,370	1,840	249	11.7

Figure 20. The PGE and acid soluble element distribution of Profile 5.

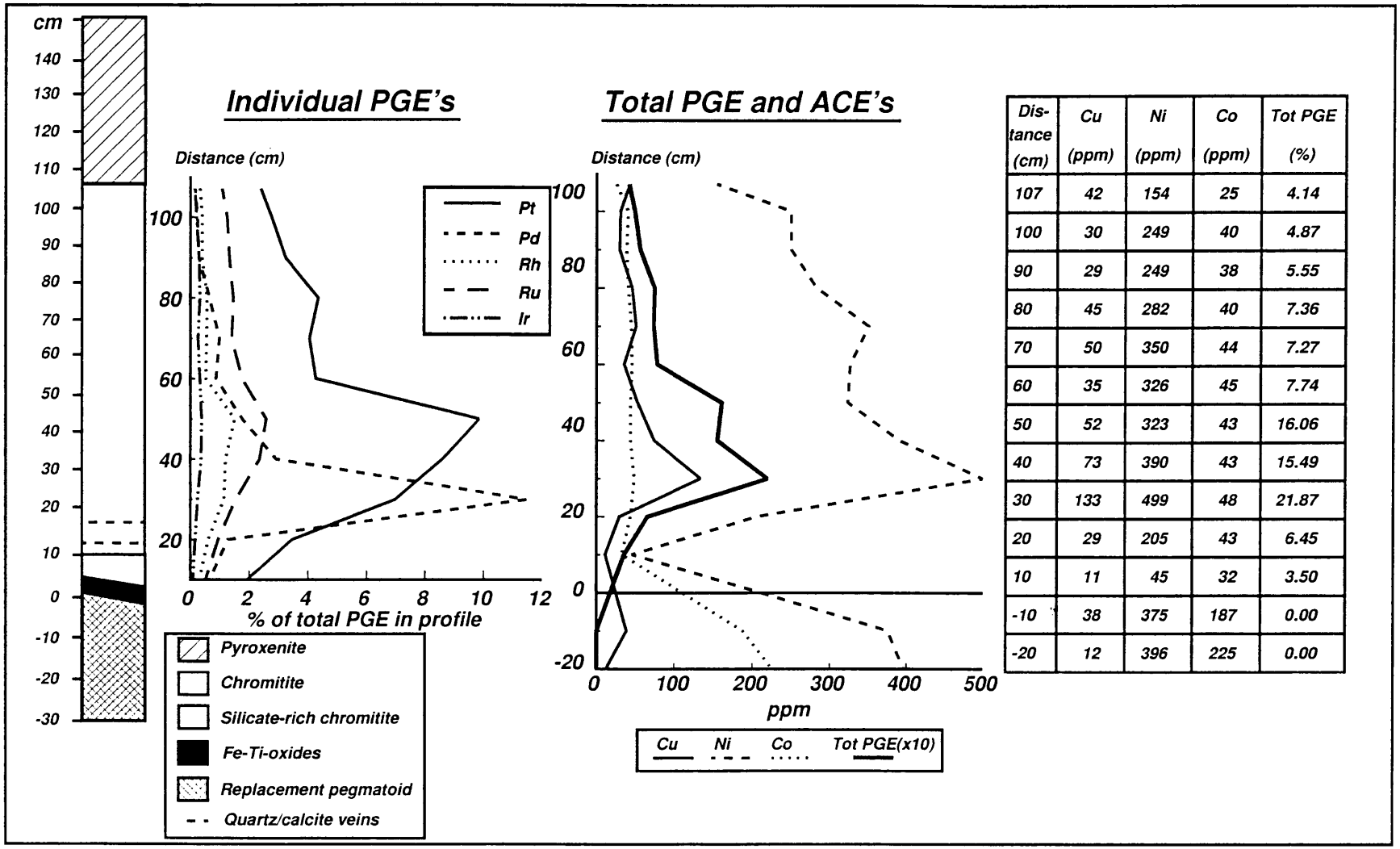

Distance (cm)	Cu (ppm)	Ni (ppm)	Co (ppm)	Tot PGE (%)
107	42	154	25	4.14
100	30	249	40	4.87
90	29	249	38	5.55
80	45	282	40	7.36
70	50	350	44	7.27
60	35	326	45	7.74
50	52	323	43	16.06
40	73	390	43	15.49
30	133	499	48	21.87
20	29	205	43	6.45
10	11	45	32	3.50
-10	38	375	187	0.00
-20	12	396	225	0.00

Figure 21. The PGE and acid soluble element distribution of Profile 2.

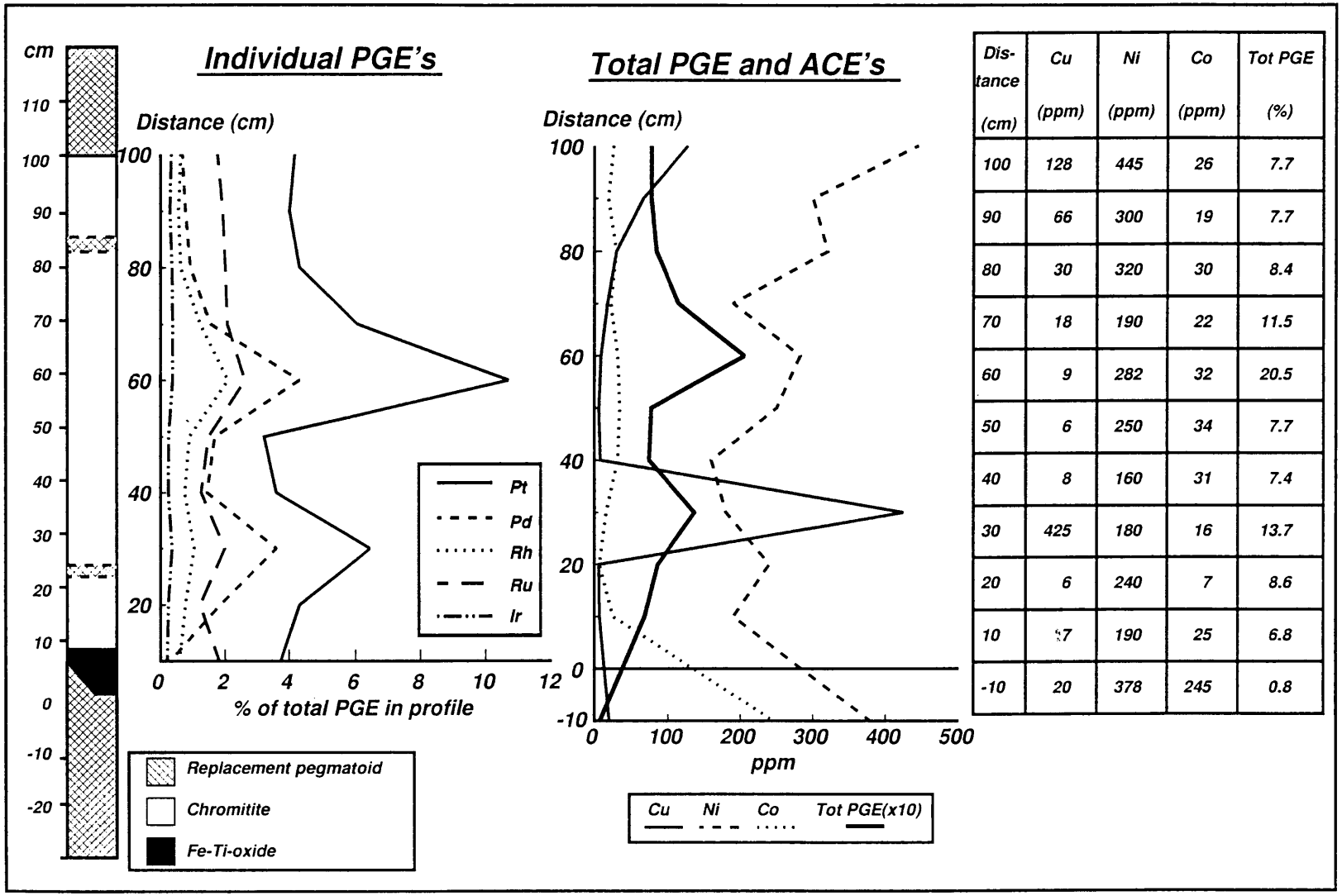

Distance (cm)	Cu (ppm)	Ni (ppm)	Co (ppm)	Tot PGE (%)
100	128	445	26	7.7
90	66	300	19	7.7
80	30	320	30	8.4
70	18	190	22	11.5
60	9	282	32	20.5
50	6	250	34	7.7
40	8	160	31	7.4
30	425	180	16	13.7
20	6	240	7	8.6
10	37	190	25	6.8
-10	20	378	245	0.8

Figure 22. The PGE and acid soluble element distribution of Profile 8

6. PLATINUM GROUP SULPHIDES AND MINERALS

The 150 polished sections were scanned again with a 50x oil immersion objective for the detection of possible platinum group minerals. The positions of possible PGM's were marked with a diamond marker for easier location of the grains. The composition of all the PGM grains were confirmed by qualitative electron microprobe analyses.

The largest diameter and the association of the PGM's with other minerals were documented. For the sake of simplicity the volume of the PGM's were taken as the largest diameter[3].

A total of 784 platinum group minerals were analyzed qualitatively over all six profiles. The PGM's are given as chemical compositions, in which minor or trace elements are ignored. Quantitative data of PGM's could not be obtained (due to the extremely small grain sizes) and the identity of many grains could not be confirmed.

6.1 Mode of occurrence

In the following, the PGM's in the Reference Profile are described, followed by the other profiles in order of increasing degree of alteration.

6.1.1 Reference Profile

Table 12. Mode of occurrence of PGM's in the Reference Profile.

Composition	N	V%	PGM's in association with			
			Sulph (N%)	Sil (N%)	Chr (N%)	Chr g.b. (N%)
Ru-S	20	17	70	5	20	5
Pt-S	14	22	100			
Pt-Pd-Ni-S	8	18	100			
Pt-Rh-Cu-S	2	40	100			
Pt-(Rh)-As-S	1	1	100			
Pt-(Pd)	1	1	100			
Total:	46	Ave:	87%	2%	9%	2%

Abbreviations: N - Number of grains, N% - Number percentage, V% - Volume percentage of PGM's, Sulph - sulphides, Sil - silicates, Chr - chromite, g.b.- grain boundary.

Table 12 gives a summary of the platinum group mineralogy of the Reference Profile. The average diameter of the PGM's measured is 3.7 μm with a range between 1 and 11 μm.

The dominant platinum group mineral is laurite (RuS_2), mostly associated with sulphides, i.e, commonly as inclusions in pentlandite and pyrite. Chalcopyrite contains the remainder of the laurite grains. Thirty-seven percent of the laurite grains contain iridium in detectable amounts. The average diameter of the laurite is 2,8 μm (as shown in Figure 23a). The maximum diameter measured for the laurite is 6 μm. One of the laurite grains is included in a rutile grain, close to two pentlandite grains.

Fifty-eight percent of the platinum group mineral grains are Pt - containing sulphides which are exclusively associated with sulphides. The platinum sulphide (most probably cooperite)[1] was observed usually in pentlandite and pyrite, and in smaller amounts associated with chalcopyrite.

Palladium was found only in one of the phases (most probably braggite). The average diameter of braggite is 3,8 μm with a maximum diameter of 7 μm. The braggite forms inclusions mostly in pentlandite and, in minor amounts, in pyrite and chalcopyrite. Figure 23b shows an elongated PGM resembling braggite with inclusions of cooperite and a Pt-Rh-(Cu)-S phase. The Rh-containing platinum sulphide forms relatively large grains with an average diameter of 6.2 μm and a maximum diameter of 11 μm. These PGM's are mostly associated with pentlandite.

Minor amounts of As are present as compounds with platinum group elements and form a Pt-Rh-As-sulphide (probably platarsite), mostly associated with pentlandite.

Figure 24 shows the distribution of the various PGM's over the chromitite layer in the Reference Profile.

---

1 Ru-S is most likely laurite, as no Ru-monosulphide has been observed to date, but without quantitative analyses the distinction of cooperite from a very Pd-poor braggite is virtually impossible. Similarly complicated is the distinction between sulpharsenides without quantitative analyses, or the distinctions between the different Pt-Rh-Cu-sulphides which are probable to exist. - pers comm.: R.K.W. Merkle.

Figure 23

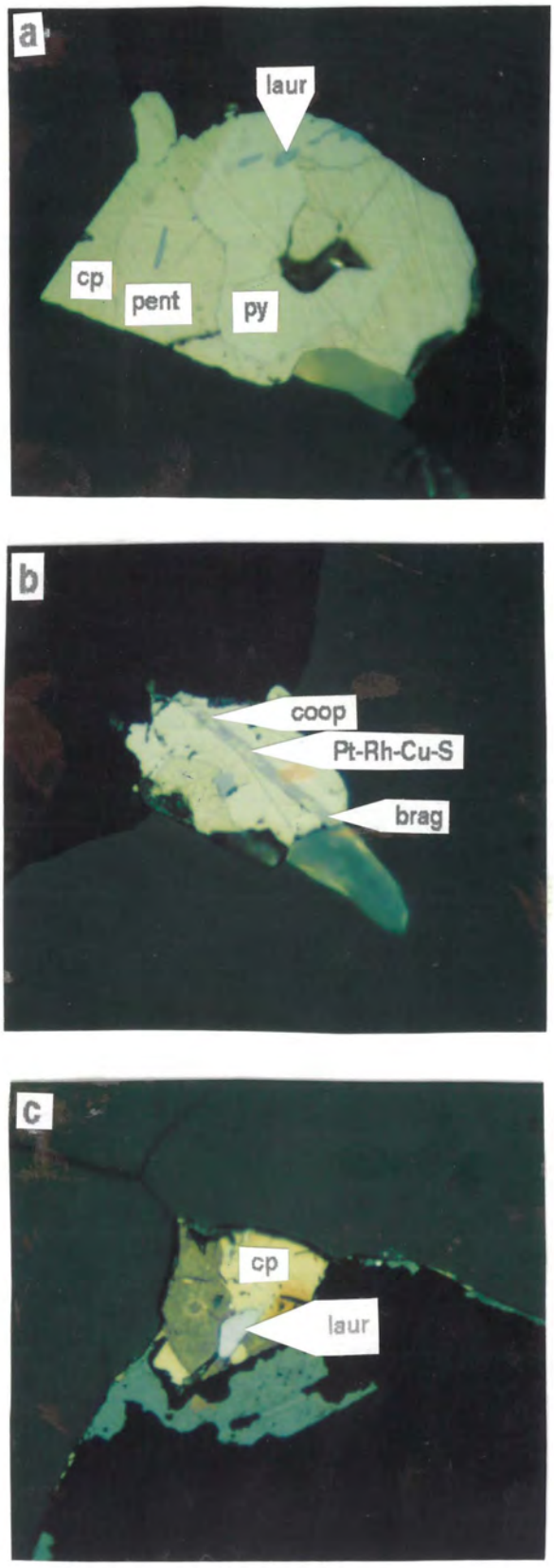

Figure 23

a. A composite sulphide grain consisting of blue laurite (laur) - containing pyrite (py) and pentlandite (pent), and chalcopyrite (chalc). The diameters of the PGM's range from 1 to 4 μm. Uncrossed nicols; oil immersion; width of photomicrographs 36 μm.

b. Elongated blue braggite (brag), with cooperite (coop) and yellowish Pt-Rh-Cu-S inclusions, in pentlandite. A blue laurite grain occurs on the pentlandite/chalcopyrite (cp) contact. Uncrossed nicols; oil immersion; width of photomicrograph 36 μm.

c. A blue laurite (laur) grain on the contact between chalcopyrite (cp) and bornite. Uncrossed nicols; oil immersion; width of photomicrograph 36 μm.

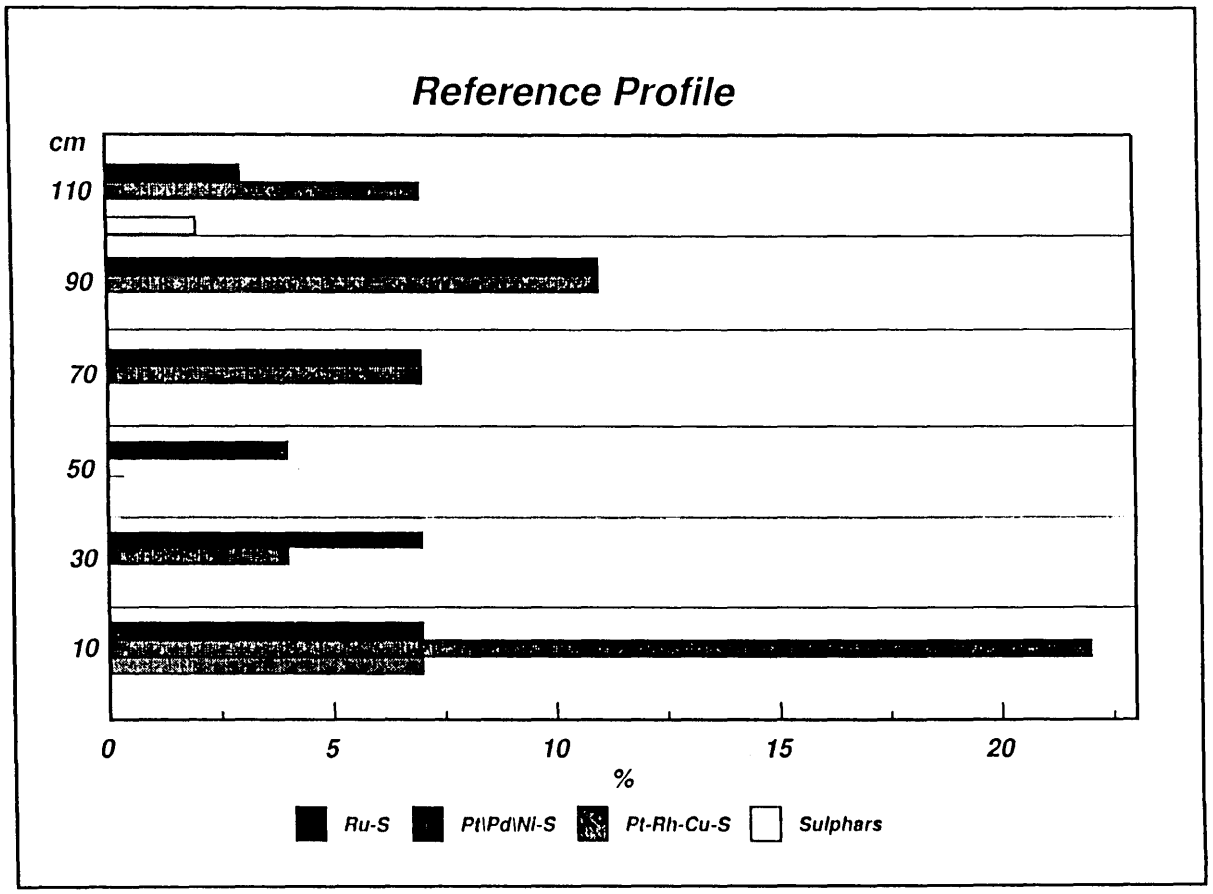

Figure 24. The mode of occurrence of PGM's in the Reference Profile, expressed as a percentage of the total PGM's in the Profile.

(sulphars = sulpharsenides)

6.1.2 Profile 3

The amount of PGM's associated with sulphide grains is much smaller than in the Reference Profile. Table 11 shows that twenty-five percent of the PGM grains in Profile 3 are present in silicate minerals. The PGM's have an average diameter of 2.8 μm and a range of 0.5 to 8 μm.

Laurite (RuS_2) is the most common platinum group mineral in Profile 3 and constitutes a third of the volume of PGM's present. The laurite occurs mostly as inclusions in pentlandite. In almost all the cases some BMS are present close to laurite when the PGM's occur in silicate. Laurite which contains detectable amounts of Os occurs mostly in the bottom third of the chromitite.

The Pt-and Pd-sulphides commonly form inclusions in pentlandite, and occasionally in chalcopyrite. The average diameter measured for these PGE-sulphides is 3.1 μm with a maximum diameter of 8 μm. Palladium-sulphide was detected mostly in the bottom third of the chromitite (Figure 25).

Seventy percent of the platinum-iron alloys are associated with pentlandite. They have an average diameter of 2.2 μm and a range of 1 to 4.5 μm. The Pt-Fe alloy grains occur also within silicate grains or at chromite grain boundaries and have an average diameter of 4.1 μm with a largest observed diameter of 5.5 μm. In all cases the Pt-Fe-alloys, occasionally with detectable Cu contents, are associated with silicates located on chromite grain boundaries. Sulphide grains are always present in the near vicinity. Pt-Fe alloy occurs over the whole thickness of the chromitite layer, but Pt-Fe-Cu alloys were detected mostly in the lowermost third.

Platinum also forms compounds with As or Sb, or both. These minerals have an average diameter of 3,4 μm which is larger than the overall average of PGM's for the Profile. Pt-As phases were observed over the whole width of the chromitite.

The PGM-sulpharsenides constitute a relatively large proportion of the PGM's in Profile 3 and are present over the whole thickness of the chromitite. The average diameter of the sulpharsenides is 3,4 μm with a Ru-As-S phase forming the largest grain of approximately 8 μm in diameter. All the Ru-As-S phases are associated with pentlandite. The Pt-As-S constitutes the largest percentage of sulpharsenides in Profile 3 and contains Rh, Ru and Pd in minor amounts. The platinum-sulpharsenides occur mostly as inclusions in pentlandite or in silicate in the vicinity of pentlandite.

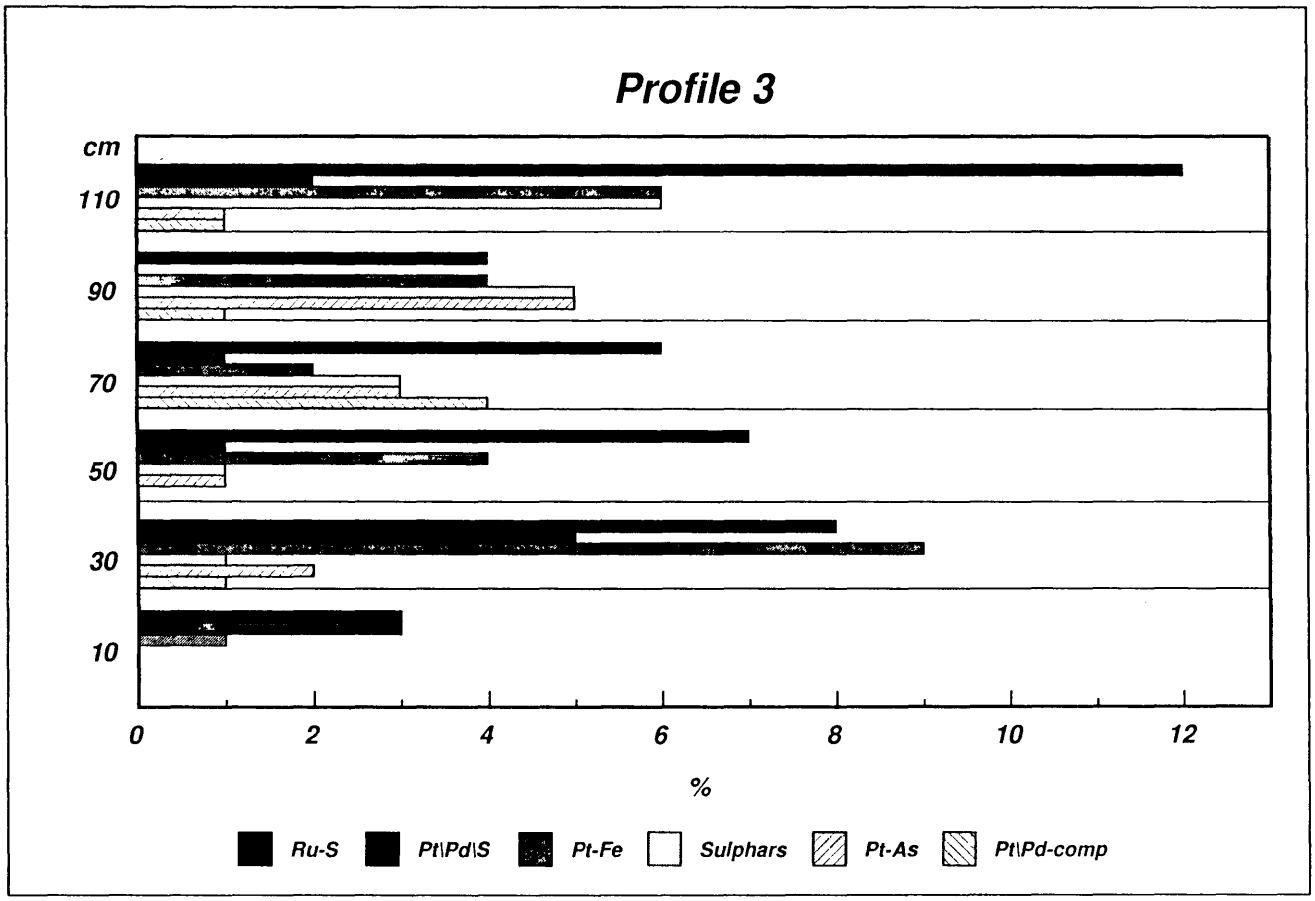

Figure 25. The distribution of PGM's in Profile 3, expressed as a percentage of the total PGM's in the Profile.

(sulphars = sulpharsenides, Pt-Fe includes Pt-Fe-Cu, Pt\Pd-comp = all remaining Pt and\or Pd compounds)

Table 11. The mode of occurrence of PGM's in Profile 3.

Composition	N	V%	PGM's in association with			
			Sulph (N%)	Sil (N%)	Chr (N%)	Chr g.b (N%)
Ru-S	50	33	50	30	10	10
Pt-S	4	9	100			
Pd-S	10	3	100			
Pt-Pd-S	1		100			
Pt-Rh-S	1	2	100			
Pt-Fe	21	9	70	20		10
Pt-Fe-Cu	10	2	70	30		
Pt-As	11	14	46	46	8	
Pt-As-Sb	6	3	50	50		
Pt-Sb	1	1	100			
Pt,Ru,Rh,Ir,Pd sulpharsenides	22	24	74	26		
Total:	137	Ave:	67%	25%	4%	4%

Abbreviations: N - Number of grains, N% - Number percentage of PGM's, V% - Volume percentage, Sulph - sulphides, Sil - silicates, Chr - chromite, g.b.- grain boundary.

6.1.3 Profile 1

Table 12 shows the diversity of the platinum group minerals in Profile 1. The average diameter measured is 2.8 μm ranging from 0.5 to 7 μm.

It is evident from Table 12 that laurite constitutes about a fifth of the overall number of PGM's in Profile 1. This is considerably less than in the Reference Profile. The average laurite grain size is 3.2 μm and the diameter ranges between 1,5 and 6 μm. The majority of laurite grains is present as inclusions in pentlandite, with a minor amount associated with pyrrhotite and chalcopyrite.

Table 12. The mode of occurrence of PGM's in Profile 1.

Composition	N	V%	PGM's in association with			
			Sulph (N%)	Sil (N%)	Chr (N%)	Chr g.b (N%)
Ru-S	14	18	70		15	15
Pd-S	3	2	100			
Pt-Pd-S	1	0.5	100			
Rh-S	2	11	100			
Pt-(Fe)-S	2	0.5	100			
Pt-Fe	19	27.5	64	6	10	20
Pt-As	13	17	15	8	15	62
Pd-Sb-Bi Pt-Sb Pt-Pd-Te-S	3	7	33	66		
Ru,Rh,Pt-sulpharsenides	7	16.5	57	43		
Total:	64	Ave:	60%	9%	22%	9%

Abbreviations: N - Number of grains, N% - Number percentage of PGM's, V% - Volume percentage, Sulph - sulphides, Sil - silicates, Chr - chromite, g.b.- grain boundary.

The Pd-S, Pt-(Fe)-S and Pt-Pd-S minerals are also relatively small and form inclusions of 1.5 to 3 μm in pentlandite and chalcopyrite. Only 3 grains of a Rh-S phase were observed, but the maximum diameter of 7 μm causes a high volume proportion compared to the other PGM's.

Seventy percent of the sulpharsenides contain Rh as a major or minor component. The remainder are Ru- or Pt-bearing sulpharsenides. Pentlandite hosts most of the sulpharsenide inclusions which have an average diameter of 3 μm and a maximum diameter of 6 μm.

The majority of PGM's are Pt-Fe-alloys, sometimes with Cu in minor amounts. These alloys mostly form inclusions with diameters ranging between 0.5 and 7μm in pentlandite.

Pt-As grains constitute approximately twenty percent of the N% of PGM's. Table 12 shows that only a very small amount of Pt-As grains are associated with sulphides - mainly pyrrhotite.

The remainder of the PGM's of Profile 1 are compounds with Te, Sb, and Bi and form relatively small grains with an average diameter of 3 μm and a maximum diameter of 5,5 μm.

PGM's in silicate or at chromite boundaries are virtually always accompanied by a BMS grain within a distance of 40μm at most.

6.1.4 Profile 5

The average PGM diameter size for Profile 5 is 2.9 μm. The diameters range from 0.3 to 10 μm (Table 13).

The most common PGM is laurite with an average diameter of 3 μm and a range of 0,5 to 9 μm. Almost sixty percent of laurite grains are present in BMS, usually pentlandite. Only a small amount, approximately four percent, occur as inclusions in Cu-containing sulphides. Figure 23c shows a laurite grain of 3,5 μm in contact with chalcopyrite and bornite. Thirty-eight percent of the laurite grains contain Ir in detectable amounts. These Ir - containing laurites can be found as inclusions in silicate, chromite or pentlandite. Os is also frequently present in small amounts, together with Ir, mostly in the grains enclosed by chromite. Figure 26a shows a laurite grain in pentlandite and a RuS - "vein" at the contact between two touching chromite particles.

The PtS, PdS, and Pt-Pd-S phases constitute 10% by number of the total PGM's in Profile 5. However, the average size of these PGM-sulphides of 2 μm is relatively small and they contribute only 3.5 percent by volume to the total PGM's. They are commonly present as inclusions in pentlandite.

Table 13. The mode of occurrence of PGM's in Profile 5.

Composition	N	V%	PGM's in association with			
			Sulph (N%)	Sil (N%)	Chr (N%)	Chr g.b (N%)
Ru-S	68	33	59	17	18	6
Os-Ru-S	1	0.5			100	
Pd-S	14	2	75	8		17
Pt-S	2	1	100			
Pt-Pd-S	4	0.5	100			
Pt-Fe	23	13	48	26	9	17
Pt-Fe-Cu	8	3	88			
Pt-As	12	18	33	50		17
Pt-Te-Bi	1	0.5	100			
Pd-Pb	17	11	94			
Pd-Pb-As	2	1	100	6		
Pd-Te-As	1	2				
Pd-Hg-As	1	0.5		100		
Pd-Bi-Sb	1	3	100	100		
Pd-Cu-Au	1	1.5	100			
Pd-Hg	1	1		100		
Ru,Rh,Ir,Pt,Pd sulpharsenides	29	8.5	64	19	7	10
Total:	186	Ave:	67%	16%	8%	9%

Abbreviations: N - Number of grains, N% - Number percentage of PGM's, V% - Volume percentage, Sulph - sulphides, Sil - silicates, Chr - chromite, g.b.- grain boundary.

Figure 26.

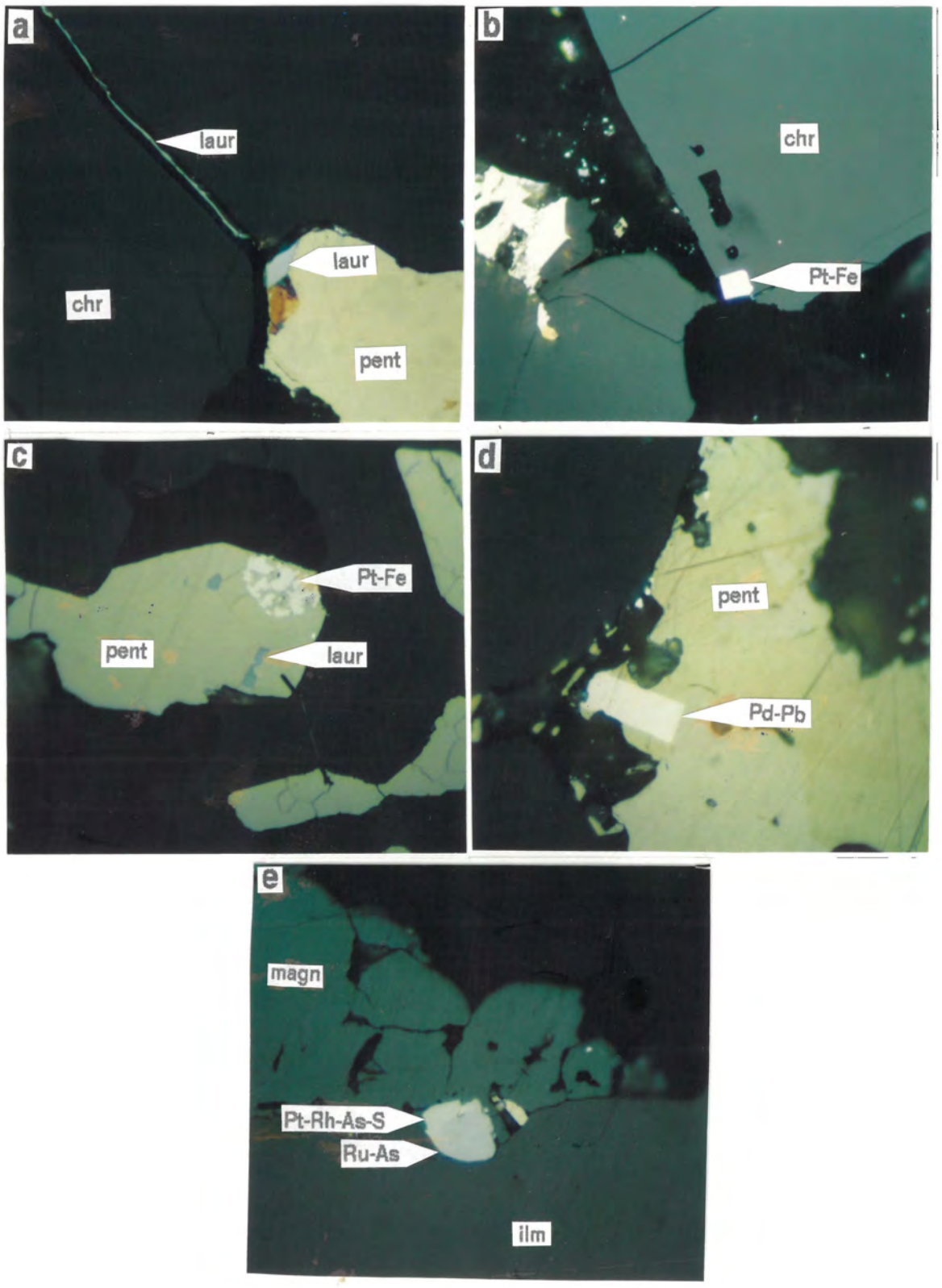

Figure 26.

a. A blue laurite (laur) "vein" occurs at the contact between two touching chromite (chr) grains. The adjacent pentlandite (pent) grain also contains a blue laurite particle on the grain edge. Uncrossed nicols; oil immersion; width of photomicrograph 36 μm.

b. A white, euhedral Pt-Fe grain of 25 μm in diameter on a chromite (chr) grain edge. Uncrossed nicols; oil immersion; width of photomicrograph 420 μm.

c. Pt-Fe forms an intergrowth with pentlandite (pent). The pentlandite also contains two blue laurite (laur) grains. Uncrossed nicols; oil immersion; width of photomicrograph equals 36 μm.

d. An euhedral white Pd-Pb inclusion in pentlandite (pent). Uncrossed nicols; oil immersion; width of photomicrograph equals 36 μm.

e. A composite PGM consisting of Ru-As and Pt-Rh-As-S on the contact between magnetite (magn) and ilmenite (ilm). Uncrossed nicols; oil immersion; width of photomicrograph equals 36 μm.

In other PGM's, Pt forms alloys with Fe or Fe+Cu, and compounds with As, Te, and Bi. Pt-Fe-(Cu)-alloys contribute sixteen percent by volume to the total platinum group minerals. The average diameters of Pt-Fe and Pt-Fe-Cu alloys are 3,2 μm, with a maximum diameter of 8 μm. The Pt-Fe alloy tends to crystallize in euhedral grains (Figure 26b). In Figure 26c the Pt-Fe alloy is intergrown with pentlandite, although an euhedral outline of the PGM is noticeable. Only a small number (9%) of Pt-Fe alloys form intergrowths with pentlandite. The Pt-As phase forms relatively large grains with an average of 4,2 μm (range: 2-10 μm) which causes the volume percentage to be high despite the small number of observed grains. The majority of Pt-As minerals are present in silicate and in 63% of the cases in the near vicinity of sulphides.

Pd forms alloys with a variety of metals. These alloys are only present in the bottom half of the chromitite (Figure 27). Pd-Pb constitutes 9% by number of the total PGM's in the Profile. These alloys with an average diameter of 2,8 μm (maximum diameter - 10 μm) are mostly present as inclusions in pentlandite and chalcopyrite (Figure 26d). The remainder of Pd-rich PGM grains, which include Pd-Te-As, Pd-Hg-As, Pd-Bi-Sb, Pd-Cu-Au, and Pd-Hg, form 5% by number of the total PGM's in Profile 5. All these phases have an average diameter of 3,7 μm with a maximum diameter of 7 μm and occur mostly as inclusions in pentlandite, chalcopyrite and chalcocite.

Amongst the sulpharsenides in Profile 5, Pt-As-S is the most common, 47% by grain numbers, followed by Pd-As-S with 25%. Most of the Rh seems to be present in the sulpharsenides, usually in association with Pt or Ir. The volume percentage of sulpharsenides is relatively low in Profile 5 due to a small average grain size of 2 μm and a range of 1 to 4 μm. When associated with silicates, these PGM's are always in close proximity to a BMS grain.

PGM's in the replacement pegmatoid footwall of Profile 5 consist of Ru-S and Pt-As with minor Pt-S, Pt-Fe, Pd-Bi, and a Rh-Pt-sulpharsenide. The average diameter is 5.2 μm with a range between 1 and 15.4 μm. The laurite is associated with sulphides such as pentlandite and chalcopyrite, and the Pt-As phase occurs mostly as inclusions in chromite grains, as well as in magnetite rims.

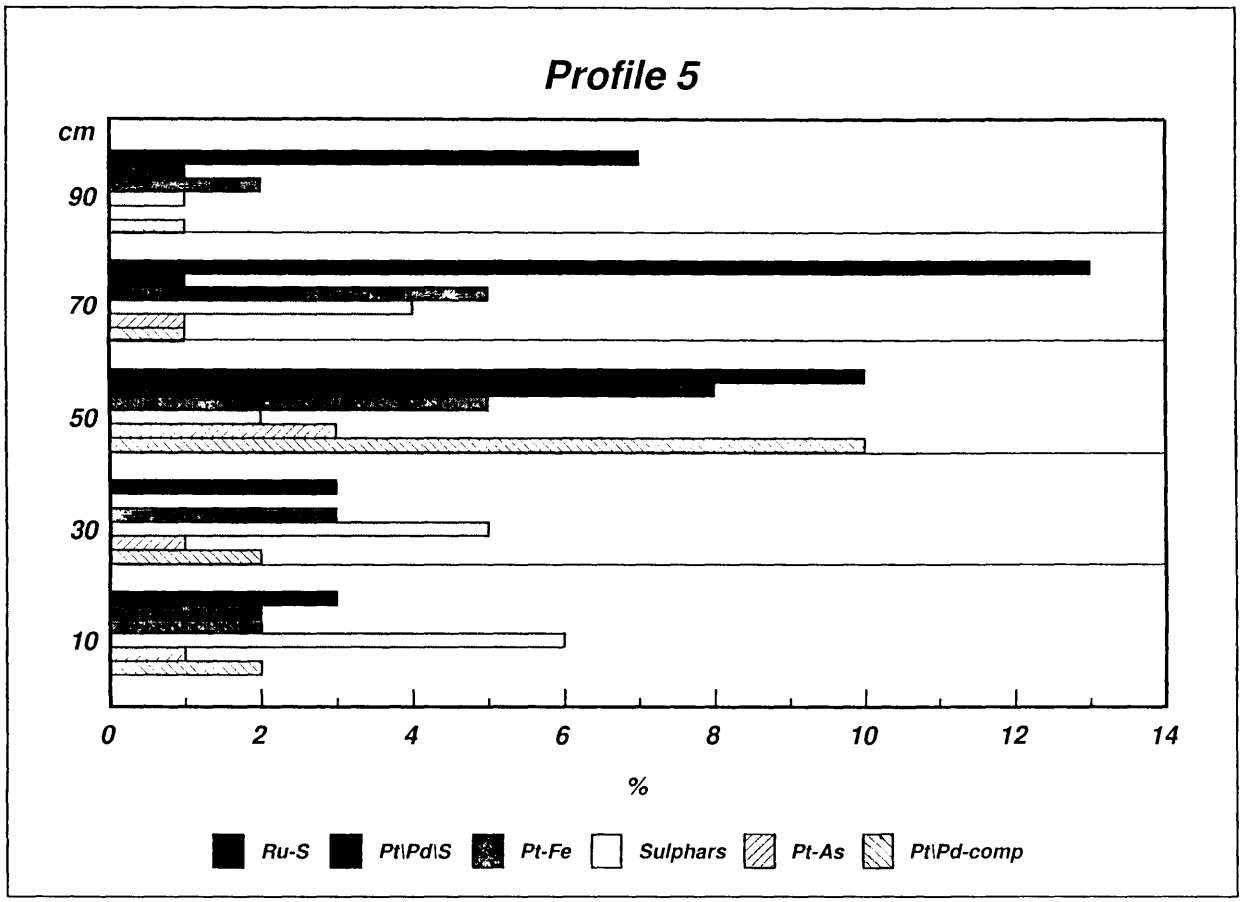

Figure 27. The distribution of PGM's in Profile 5, expressed as a percentage of the total PGM's in the Profile.

(sulphars = sulpharsenides, Pt-Fe includes Pt-Fe-Cu, Pt\Pd-comp = all remaining Pt and\or Pd)

6.1.5 Profile 2

The average diameter of the PGM's in Profile 2 is 2.5 μm with a range from 0.5 to 20 μm. It is clear from Table 14 that more than half of the PGM's are associated with silicate and/or chromite grains. Most of the PGM-sulphides are associated with base metal sulphides and the alloys are mostly associated with silicates, chromite or are situated at chromite grain boundaries.

Laurite is again the most common PGM in Profile 2. The average diameter is 2.9 μm and the maximum diameter 10 μm. Laurite grains forming inclusions in chromite or sulphide grains have diameters slightly larger than the overall average, with 3.4 μm and 3.3 μm respectively. The laurite-hosting BMS are mostly pentlandite (78%) with the remainder divided equally between haezlewoodite, chalcopyrite, bornite, and chalcocite-group minerals. The Ru-S grains in silicate or at chromite/silicate boundaries have relatively small sizes with diameters in the range of 0.5 to 3 μm and an average of 1.8 μm. All the laurite grains in silicate have sulphides in the near vicinity. Twenty-eight percent of the laurite grains contain detectable Ir.

The grain shape of laurite grains varies from euhedral to round, which in fact consist of minute grain faces (Gräser et al., 1993, Merkle and Horsch, 1988), irrespective of their mode of occurrence. The laurite grains which contain Ir or Os are more likely to be visibly subhedral to euhedral. (My observation)

The Pt-and Pd-sulphides are present as anhedral to subhedral grains and constitute 16.6% by number of the PGM's in Profile 2. A few large grains of up to 20 μm causes the volume percentage of these PGM's to be relatively high with 60.7%. Pentlandite constitutes 72% of BMS which contain Pt/Pd-sulphides. Smaller amounts of Pt/Pd-sulphides are associated with bornite, chalcopyrite, and the chalcocite-group minerals.

Pt forms alloys with Fe and Cu, but Cu is commonly present in much smaller amounts than Fe. The low V% in Table 14 is caused by small grain sizes of 0.5 to 6 μm in diameter with an average of 2.4 μm. Almost 90% of the Pt-alloys are hosted by pentlandite, while the remaining 10% occur in chalcopyrite and bornite.

Pt-As grains occur only in the bottom 20cm of the chromitite as small (1-4 μm), subhedral to anhedral grains. In the bottom 2 cm the PGM's are present as inclusions in sintered Fe-Ti-oxides. Within 2-5 cm from the bottom contact, the arsenides are present mostly between sintered chromite grains or at triple points of sintered chromites.

The Pt and Pd phases grouped together in Table 14 form small grains (0.5-4 μm) in silicate and in chromite and occur in the bottom 20 cm of the chromitite (Figure 28).

Three Ru-As grains were found in chromite and Cr-Ti-oxide in the bottom 10 cm of the chromitite. Two of the grains are isolated, rounded inclusions in chromite. The remaining grain is part of a composite PGM with a Pt-Ru-arsenide (Figure 26e). The grain size of these arsenides is approximately 2 μm.

The sulpharsenides form the second-most common group of compounds in Profile 2. Seventy-four percent of the sulpharsenides have Pt, Rh, and Ru as the major PGE. Ir/Rh-sulpharsenides form 14% and the remainder are Ru-, Rh- and Pd-sulpharsenides. The average diameter is 2 μm with a range between 0.5 and 5 μm. The grains are subhedral to anhedral with a light-blue colour.

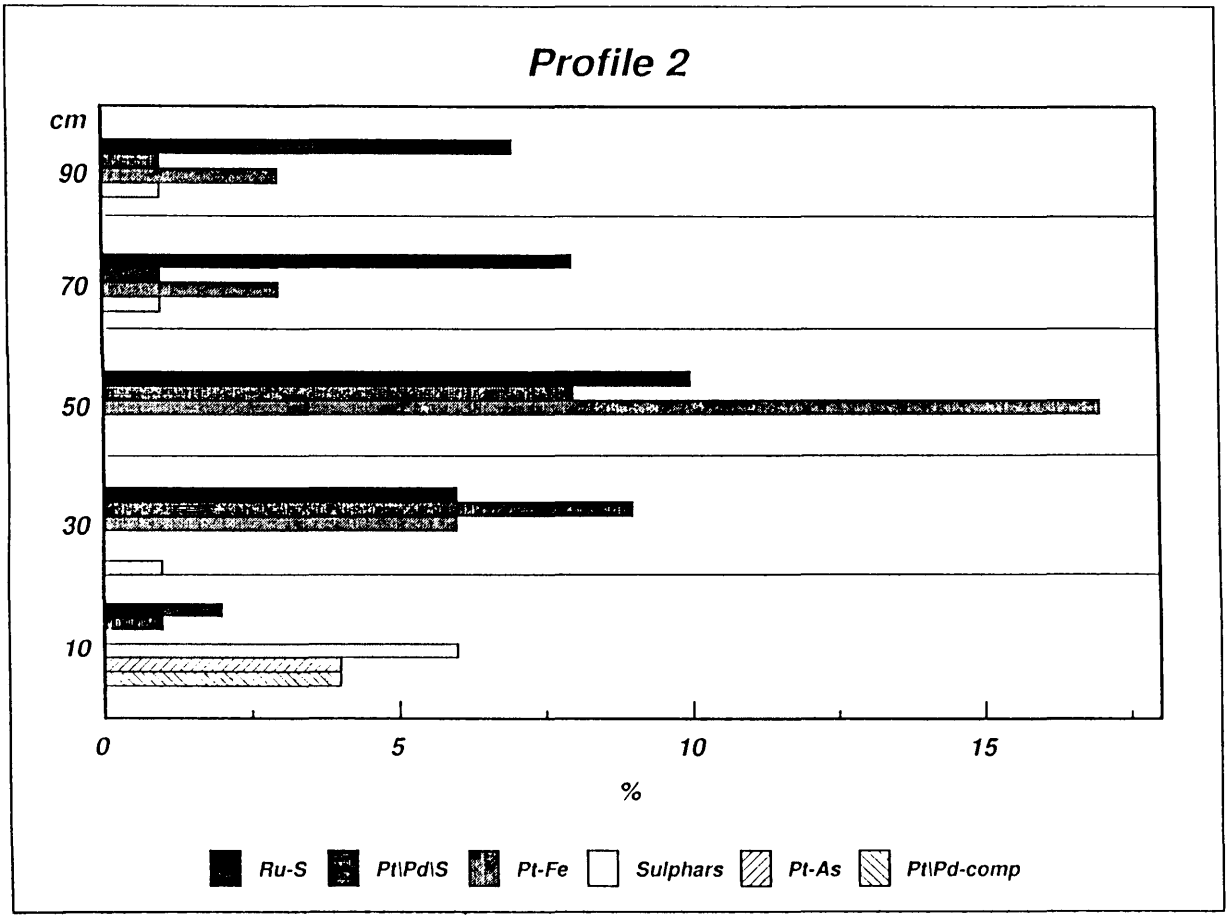

Figure 28. The distribution of PGM's in Profile 2, expressed as a percentage of the total PGM's in the Profile.

(% - % of total PGM's in profile, Pt-Fe includes Pt-Fe-Cu, sulphars - sulpharsenides, Pt\Pd-comp includes all remaining Pt and/or Pd compounds)

Table 14. The mode of occurrence of PGM's in Profile 2.

Composition	N	V%	PGM's in association with			
			Sulph (N%)	Sil (N%)	Chr (N%)	Chr g.b. (N%)
RuS	46	17	53	22	22	3
PtS	10	7.5	78	11		11
PdS	19	52.1	85	15		
Pt-Pd-S	2	1.1	100			
Rh-Ir-S	1			100		
Pt-Fe	31	4.3	50	50		
Pt-Fe-Cu	15	4.3	52	23	19	6
Pt-As	15	1			64	36
Pt-Sb Pt-Ru Pt-Pd-Cu	5	0.5		33	67	
Pd-As-Te Pd-Sb-Bi Pd-Sb-As Pd-Sb Pd-Sb-Cu-As Pd-Ru-As	7	7		17	50	33
Ru-As	2	0.3			100	
Ir,Ru,Pt,Rh-sulpharsenides	33	4.9	13	5	45	37
Total:	186	Ave:	43%	15%	31%	12%

Abbreviations: N - Number of grains, N% - Number percentage of PGM's, V% - Volume percentage, Sulph - sulphides, Sil - silicates, Chr - chromite, g.b.- grain boundary.

6.1.6 Profile 8

The average diameter of the PGM's measured for Profile 8 is 2.1 μm with a range between 0.3 and 9 μm, which is the smallest of all the profiles. The majority of PGM's are sulpharsenides and 80% of the PGM's are associated with chromite or silicates.

Ru-S grains are mostly associated with the oxide minerals and occur as small grains (2.3 μm) with a diameter ranging between 1 and 4μm. Fifty percent of laurite grains contain Os and/or Ir in detectable quantities. In cases where laurite is associated with sulphides, it occurs as inclusions in pentlandite, in the top third of the chromitite layer (Figure 29).

The Ru- and Rh-As phases are completely enclosed in sintered Fe-Ti-oxides in the bottom 10 cm of the chromitite. The sulphides with which the arsenides are associated are mostly pentlandite and minor chalcopyrite, and chalcocite - group minerals.

The PGE in sulpharsenides are mostly Pt with Rh and minor Pd and Ru. Rh- and Ru- sulpharsenides are the second most common sulpharsenides with Pt, Ir as minor components. The sulpharsenides often form composite PGM grains with other sulpharsenide phases, and with Ru-arsenide as shown in Figure 26e.

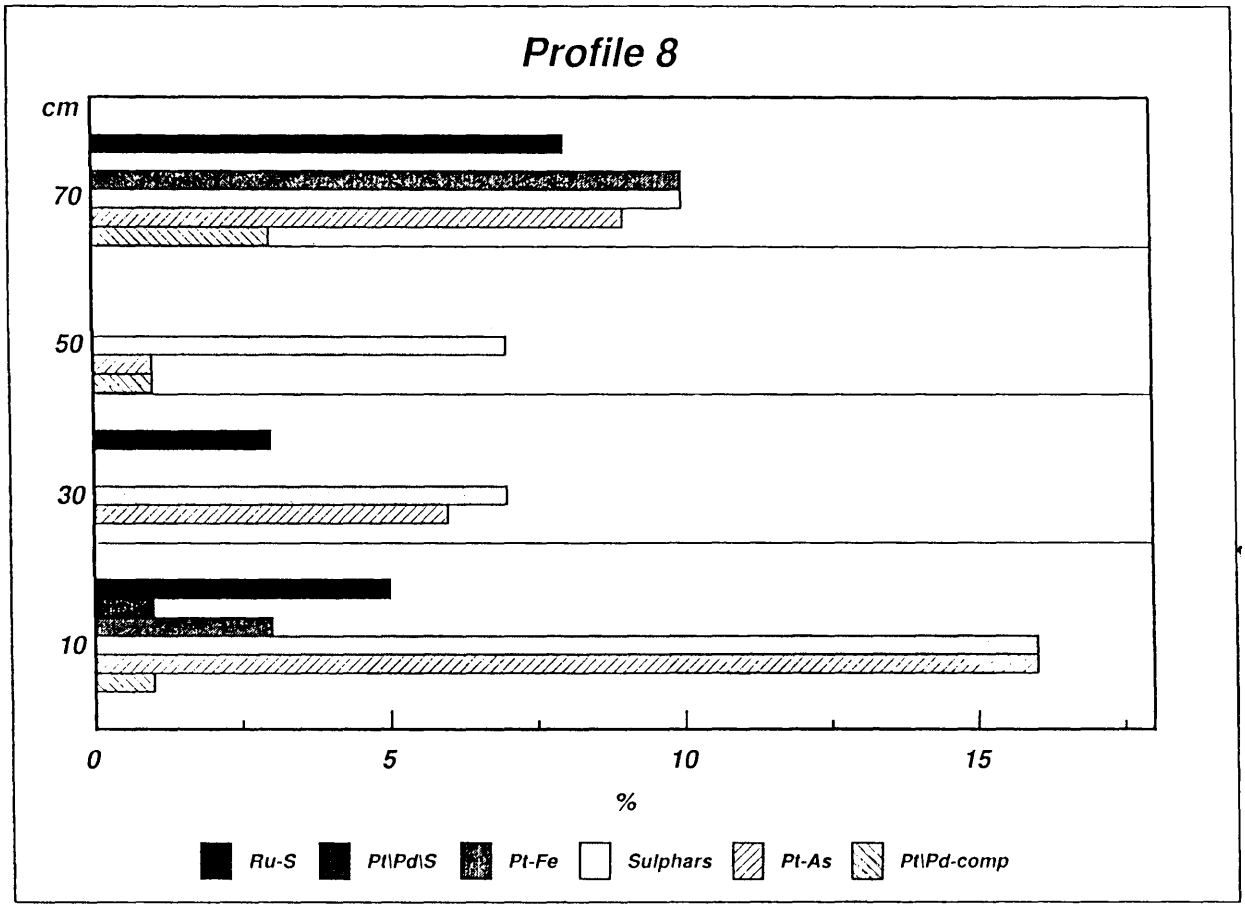

Figure 29. The distribution of PGM's in Profile 8, as a percentage of the total PGM's in the Profile.
(sulphars = sulpharsenides, Pt-Fe includes Pt-Fe-Cu, Pt\Pd-comp includes all remaining Pt and/or Pd compounds)

Table 15. The mode of occurrence of PGM's in Profile 8.

Composition	N	V%	PGM's in association with			
			Sulph (N%)	Sil (N%)	Chr (N%)	Chr g.b. (N%)
Ru-S Pt/Pd-S	24 3	6 0.5	22 100	4	65	9
Pt-Fe-(Cu)	21	12.6	50	10	10	30
Pt-As Rh/Ru-As	28 3	30 2.9	26	13	16 100	45
Pd-(Pt,Sb,As)	6	9			50	50
Pt,Rh,Pd,Ir-sulpharsenides	64	39	11	10	29	50
Total	149	Ave:	20%	9%	28%	43%

Abbreviations: N - Number of grains, N% - Number percentage of PGM's, V% - Volume percentage, Sulph - sulphides, Sil - silicates, Chr - chromite, g.b.- grain boundary.

6.1.7 Summary

Figure 30 gives an overview of the proportions of the various PGM's. The profiles are arranged in order of increasing macroscopic alteration. It is clear from this Figure that the proportion of platinum group sulphides decreases from 96% to 18% with increasing alteration. Profiles 1, 3, 5, and 8 also have a much larger amount (36%-73%) of alloys, Bi-containing, As-containing, Sb-containing, and Te-containing PGM's. It is also important to note that the amount of arsenides and sulpharsenides increases with increasing alteration and is 2%, 28%, and 64% for the Reference Profile, (Profiles 1,3,5,2), and Profile 8 respectively.

6.2 Platinum group element analyses

Individual Pt, Pd, Ru, Rh, and Ir-analyses were carried out on all the UG-2 chromitite profiles. This was done at the Analytical Division at Mintek by atomic absorption spectroscopy after concentrating and isolating the PGE's with fire assay using nickel sulphide as a collector.

Total PGE analyses were determined on the 0-10 and 10-20 cm sections of the footwall, where possible.

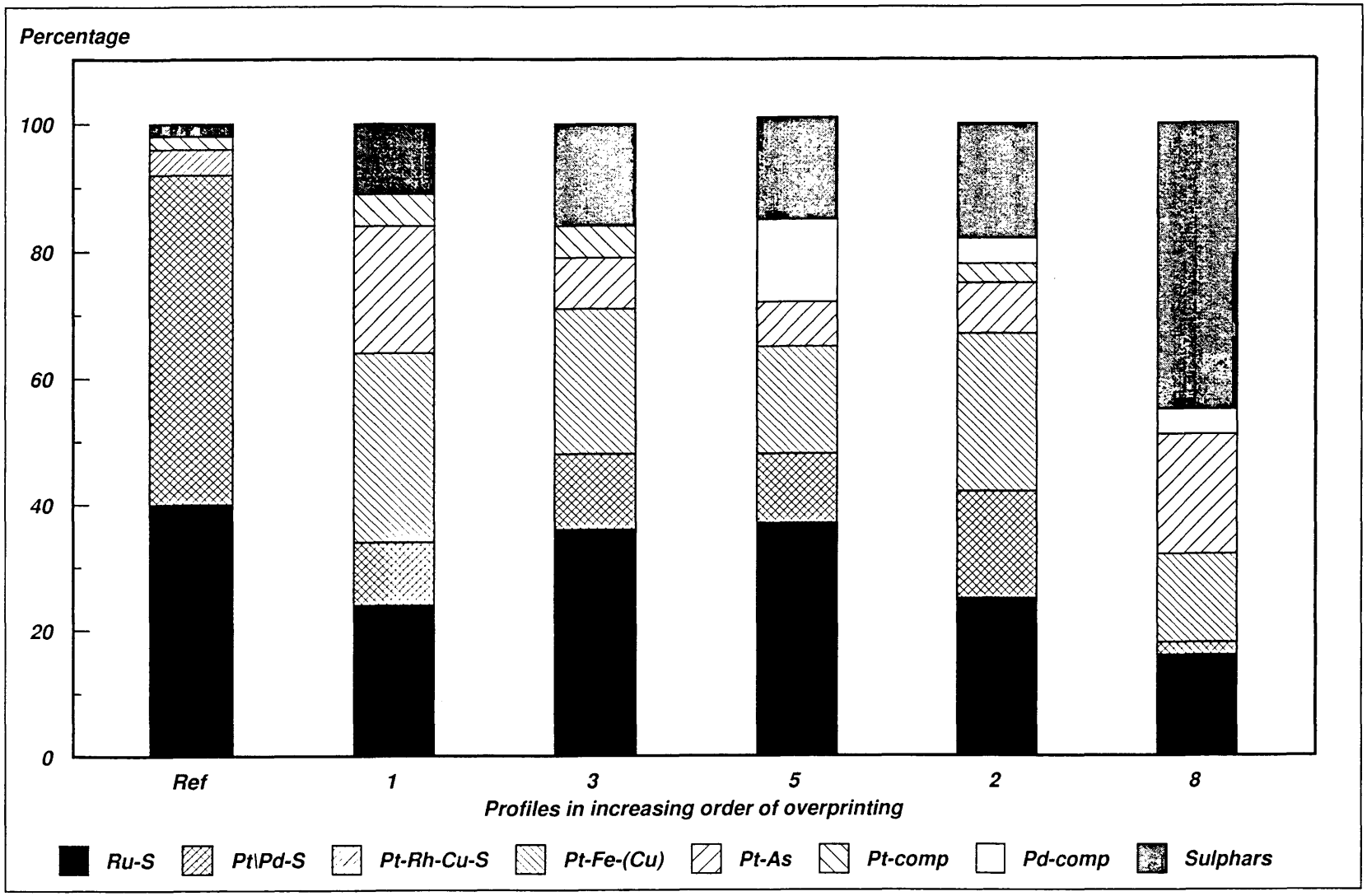

Figure 30. The proportions of the PGM's in the various profiles.

(Pt-comp = Pt-compounds, Pt-comp = Pd-compounds, Sulphars = sulpharsenides)

The average values for the individual PGE's and the total PGE's and Au for the complete UG-2 chromitite were determined by weighting the individual PGE value for every sample (i.e. multiplying the proportion of the length of the sample by the analysed PGE value). By adding the representative PGE values calculated for every sample an average PGE value for the chromitite is obtained. Values lower than the detection limit were taken as zero in calculating the average value.

The PGE values shown in the tables are percentages of the cumulative PGE content in every profile. Figures 16 to 22 (Chapter 5) show the distribution of the individual PGE's over the profiles.

Reference Profile - The Reference Profile shows a distribution which can be described as typical for Western Platinum Mine with a peak at the bottom and in the middle of the UG-2 chromitite (see also McLaren, 1982). The individual platinum group elements all have a peak at the bottom of the UG-2, but the peak at the middle is mainly caused by palladium. The remaining PGE's all have a second peak at a point approximately 10 cm above the palladium peak. Figure 16 shows that the value of the PGE's in the footwall is relatively low.

The altered profiles will be discussed in order of increasing macroscopic alteration.

Profile 6 - In Profile 6 (Figure 17), which shows only slight macroscopic alteration, the PGE have three peaks over the length of the chromitite (Figure 22). The peak at the bottom is the highest and is caused mainly by platinum with the middle and top peaks slightly lower. This profile contains the highest value analyzed for platinum.

Profile 3 - Profile 3 (Figure 18), which also shows slight macroscopic alteration, has two PGE peaks in the bottom half of the chromitite. The peaks are mainly caused by Pt. The remainder top half of the chromitite has a relatively low average PGE value.

Profile 1 - Profile 1 (Figure 19) has a low average PGE-content compared to the other profiles. One peak, approximately 30cm from the bottom contact, is present and is mainly caused by Pt and Pd. The topmost 10 cm of footwall has a very low PGE-content of 0.5% relative to the average of the chromitite.

Profile 5 - This profile (Figure 20), which is sintered at the bottom of the chromitite layer, has only one peak, approximately 60cm from the bottom contact caused by a peak in the Pt, Pd, and Ru values. PGE's show the highest values in the footwall of the profiles with 9.6 and 11.7%

Profile 2 - Profile 2 (Figure 21) has a PGE peak 30cm from the bottom contact which is caused by Pd and Pt. Pt, Rh, and Ru all peak 20cm higher than Pd.

Profile 8 - In Profile 8 (Figure 22), which shows the most intense macroscropic alteration, the distribution pattern is close to the distribution of the Reference Profile, except for the peak at the bottom, which is shifted approximately 30 cm to the top of the chromitite footwall contact. In both cases the peaks are formed by all the individual PGE's, although the Pt values are the highest. The footwall has a relatively high value of 6.8% directly below the contact.

7. DISCUSSION

The sporadic and transgressive nature of the replacement pegmatoids in the Vaalkop area indicates that alteration in the area occurred in a localized manner. Viljoen and Scoon (1985) show a schematic strike section of iron-rich ultramafic pegmatite in the upper critical zone rocks at Amandelbult (Figure 31) which shows selective replacement by the pegmatite. The replacement in the Vaalkop area shows the same selective distribution pattern and may have a similar kind of shape as shown in Figure 31, but limited exposure does not permit the investigation of the entire area.

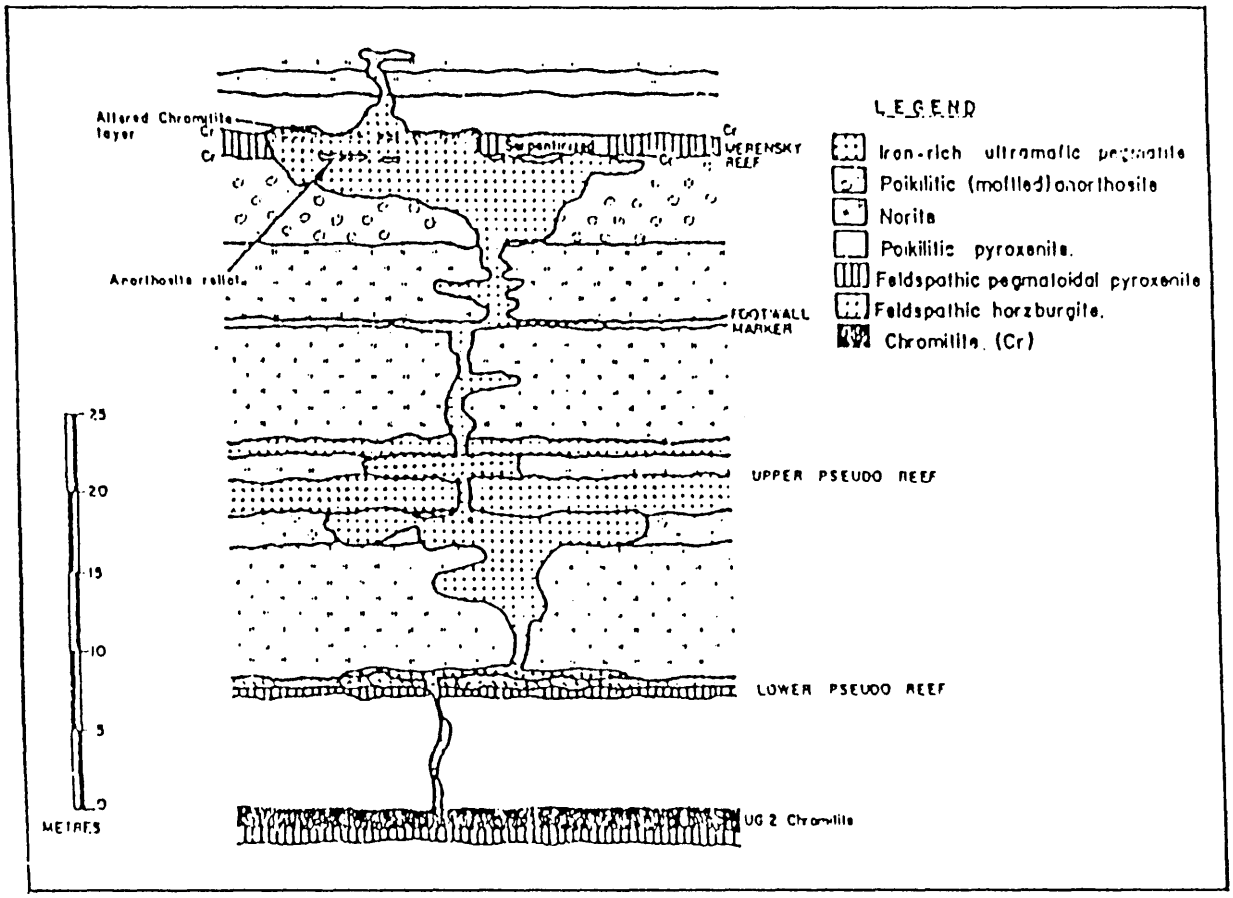

Figure 31. Schematic strike section illustrating the vertical distribution of iron-rich pegmatite at Amandelbult. (Viljoen and Scoon, 1985).

7.1 Silicates and Oxides

The silicate mineral assemblage of the altered profiles is vastly different compared to the Reference Profile. In the Reference Profile, silicate minerals in the chromitite and adjacent hanging-wall are mainly pyroxene and plagioclase with minor biotite, which indicates only low degrees of postmagmatic overprinting.

The silicate mineral assemblage in the altered profiles, which consists mainly of amphibole, pyroxene, chlorite, talc, serpentine, clay-minerals (and sometimes olivine), gives a strong indication of deuteric and hydrothermal alteration (Best, 1982; Schiffries et al., 1987; Ballhaus and Stumpfl, 1986; Barnes, 1979; Deer et al., 1966). Chlorite, talc, serpentine, and clay-minerals indicate reactions between magmatic silicate minerals and fluids, producing low-temperature hydrous silicates. Orthopyroxenes break down to serpentine with admixed talc or may be replaced by amphiboles. Clinopyroxenes tend to be replaced by serpentine or may also be replaced by amphiboles or chlorite. Feldspar is completely altered to clay minerals in the profiles of altered UG-2.

The Reference Profile contains mainly chromite with minor rutile as inclusions.

A wide spectrum of spinel phases are present in the altered profiles. Chromite is present in veins, and as rims around chromite grains. In the bottom sintered area, Fe-Ti-rich phases are predominant as ilmenite with ulvospinel exsolutions. Chromite has occasionally been changed to a low reflectance, Al-rich phase.

The amount of graphite increases with alteration in the profiles of altered UG-2 which also gives an indication of the presence of volatiles during the alteration process. Graphite is an important constituent of some potholes and of pyroxenitic pegmatoids (Kinloch and Peyerl, 1990) and in dunite pipes (Stumpfl and Rucklidge, 1982).

7.2 Base Metal Sulphides

The sulphides in the chromitite of the Reference Profile form mainly composite sulphide grains, consisting of pentlandite with minor chalcopyrite, pyrrhotite, and pyrite. (See also Vermaak, 1985). McLaren (1980) found the main base metal sulphides associated with the PGM's in the UG-2 chromitite to be pentlandite, chalcopyrite, pyrrhotite, Co-pentlandite (well represented in the Marikana-Brits area), millerite, and pyrite.

The profiles of altered UG-2 have more complex sulphide assemblages and contain chalcocite-group minerals, violarite, cubanite, mackinawite, haezlewoodite and millerite. Gersdorffite, cobaltite, maucherite and niccolite occur in the altered footwall of Profile 5. In Profile 8, which represents the most intense macroscopic alteration, chalcocite-group minerals are relatively rare with only minor chalcopyrite containing bornite inclusions.

The mineral assemblage of the altered profiles shows some resemblance to the Townlands iron-rich ultramafic pegmatite body as described by Viljoen and Scoon (1985). The sulphide assemblage of the Townlands pipe includes pyrrhotite, cubanite, chalcopyrite, mooihoekite, and haycockite as major phases. Minor phases are chalcocite, digenite, bornite, native copper, pentlandite, mackinawite, ilvaite, graphite, and various unspecified nickel arsenides. The copper sulphides are more abundant than in other pegmatite bodies (e.g. platiniferous ultramafic pipes), allthough the low proportion of nickel sulphide is characteristic. The diversity in the base metal sulphide assemblage is attributed to the upward streaming of volatile-charged pegmatitic or deuteric fluids. Most of the sulphides occur in serpentine- or chlorite-filled fractures and have been remobilized and overprinted.

The sulphide mineral assemblage of the profiles of altered UG-2 at Vaalkop resembles the assemblage at the Townlands pegmatite body and therefore a similar alteration process can be assumed for the Vaalkop replacement area.

The pentlandite in Profile 1 has a highly variable Co-content (0 - 7.49%) with the highest Co-values in the bottom, sintered chromitite. The pentlandites are also higher in Ni with an average Ni/Fe at% ratio of 1.1:1. This relatively high Co-content in the pentlandites can be a indication of hydrothermal action. Pentlandite from the Mooihoek and Onverwacht dunite pipes also has relatively high Co-values between 5.1 at% and 7.3 at% (Rudashevsky et al., 1992). The latter pentlandite is a late-stage pentlandite containing streaky separations along grain boundaries of olivine and occurs in magnetite-amphibole aggregates. The late-stage pentlandite is also rich in nickel with an at% Fe/Ni ratio of 1.18. In the titanomagnetite area of the hortonolite dunite, the Co-content of the pentlandite is 6.0 at% and the atomic Fe/Ni ratio is 2.85.

Magmatic Co-rich pentlandite from the upper zone of the Western Bushveld Complex has been described by Merkle and Von Gruenewaldt (1986). The surrounding silicate minerals have been subjected to hydrothermal alteration, but the pentlandite is not affected. The Co-rich pentlandite, in which cobalt ranges from 12 to 44 at% is therefore thought to be of magmatic origin. Pentlandite from the main magnetite layer in the eastern Bushveld Complex has large variations in the Fe-, Ni-, and Co-contents of 8.9 to 26.7 at%, 11.7 to 34.1 at%, and 0.3 to 30.4 at% respectively (Harney and Merkle 1992). Cobalt mostly replaces Ni in the pentlandite

crystal lattice. Above the main magnetite layer, Co also substitutes for Fe. The pentlandite in these rocks is associated with 18 different minerals, of which bornite, millerite and secondary magnetite is believed to be of post-magmatic origin.

The pentlandite from the Vaalkop replacement area has large variations in the Co, Ni, and Fe content of 0.27 to 7.49 at%, 43.04 to 27.05 at%, and 23.95 to 32.16 at% respectively. Ni-rich pentlandite occurs at the top of the UG-2 chromitite, whereas the Co-rich pentlandite is found in the sintered, bottom area of the chromitite. Co-rich pentlandite is relatively Fe-rich compared to the pentlandite at the top of the chromitite. The relative location of the Co-rich pentlandite and its surrounding minerals (such as Fe-Ti-oxides, hydrous silicates, bornite, violarite, ccgm and cubanite) suggest that the increased Co-content of the pentlandites is caused by hydrothermal overprinting.

During serpentinization of the Hayachine ultramafic rocks in northeastern Japan (Shiga, 1987), the sulphide assemblages vary, with the degree of serpentinization, from a pyrrhotite - pentlandite assemblage, to a pentlandite - haezlewoodite - godlevskite assemblage, and then to pentlandite - violarite, pentlandite - violarite - millerite, or violarite - millerite assemblages. Fe-contents decrease and Ni- and Co-contents increase with degree of serpentinization. Iron, Ni, and Co became mobile and moved distances of up to about 10 cm at the Hayachine ultramafic rocks during the most active stage of serpentinization. The profiles of intensely altered UG-2 at the Vaalkop show a different mineral assemblage from the Reference Profile with the decrease of Cu-rich phases and increase of minerals such as violarite and haezlewoodite. In the profiles of altered UG-2, veins filled with sulphides are a common occurrence and are an indication of the mobility of the sulphides during hydrothermal overprinting.

In some hydrothermal areas such as the Shetland ophiolite complex, the Quebec Appalachians and dunite-affected Merensky Reef there is an increase in As (Lord et al., 1994; Auclair, 1993; Kinloch and Peyerl, 1990). The profiles of altered UG-2 also have an increase in the As-content in both the BMS and PGM component of the chromitite.

7.3 Platinum group minerals

Chapter 6 gives a description of the mode of occurrence of the PGM's in the Reference Profile and the profiles of altered UG-2. The Reference Profile contains mainly platinum group sulphides which constitute 96 per cent by number of grains (N%) of all the PGM's in the profile. Most of the PGM's (87%) are associated with BMS and occur as inclusions in pentlandite. The mode of occurrence of the PGM's in the Reference Profile is in agreement with observations by McLaren (1982) for the UG-2. The most abundant PGM's in the UG-2 are laurite

[(Ru,Os,Ir)S_2], cooperite (PtS), Pt-Ir-Ru-Cu sulphide, braggite [(Pt,Pd,Ni)S], Pt-Pb-Cu sulphide, vysotskite (PdS), and a Pt-Fe alloy. The PGM's in the borehole cores investigated by McLaren are predominantly associated with BMS (33-85%), and a lesser amount at grain boundaries (6-57%), in silicates (2-29%), or in chromite (2-12%). Ru was not found anywhere by McLaren in its metallic form, which means that for the UG-2, the lower f_S-T boundary is defined by the RuS_2-Ru equilibrium. (Figure 32).

The PGM assemblages of the profiles of altered UG-2 are diverse and the PGM's are mostly associated with silicates and chromite (as inclusions or at grain boundaries). The association of PGM's with BMS decreases from 96 N% in unaltered UG-2 with increasing alteration to 67 N%, 60 N%, 67 N%, 43 N%, and 20 N% in Profiles 3, 1, 5, 2, and 8 respectively. The altered profiles show a systematic variation in the PGM assemblage with an increase in alteration (See chapter 6). In Profiles 3 and 1, less platinum group sulphides were noted and PGE-Fe-(Cu) alloys occur (11% and 27.5% by volume for Profiles 3 and 1 respectively). The PGM assemblage of these two profiles are similar to one of the boreholes investigated by McLaren (1982), which were drilled close to a discordant ultramafic pegmatoid at Maandagshoek. There, the PGM-assemblage is characterized by the presence of Pt-Fe, Pd-Cu, Pd-Pb, and Pd-Te phases. McLaren found Pt-Fe at Maandagshoek to be intergrown with BMS in contrast to the other UG-2 borehole cores he investigated, where the Pt-Fe alloy occurs as wedge-shaped or short, prismatic crystals. Other PGM's occurring at Maandagshoek include sperrylite, arsenides, sulpharsenides, and tellurides. At this locality the PG-mineralogy was influenced by the pegmatoid, and the f_S-T conditions were located between the Pt-PtS and Ru-RuS_2 equilibria. (Figure 32).

Merkle (1982) investigated UG-1 chromitite in the vicinity of a magnetite-pipe. The UG-1 was influenced by later-stage fluids and the PGM assemblage consists predominantly of laurite enclosed by chromite, Pt-Fe-, Pt-Rh-Fe-, and Pt-Pd-Fe alloys i.e., en assemblage similar to the one observed in the profiles of altered UG-2 at Vaalkop. However, the unmetasomatized UG-1 described by Merkle consists mainly of laurite, native Ru, native Os, or Pt-Pd-Rh sulphides and resembles the PGM assemblage at the Reference Profile at Vaalkop which consists of laurite, cooperite and PGM-sulphides.

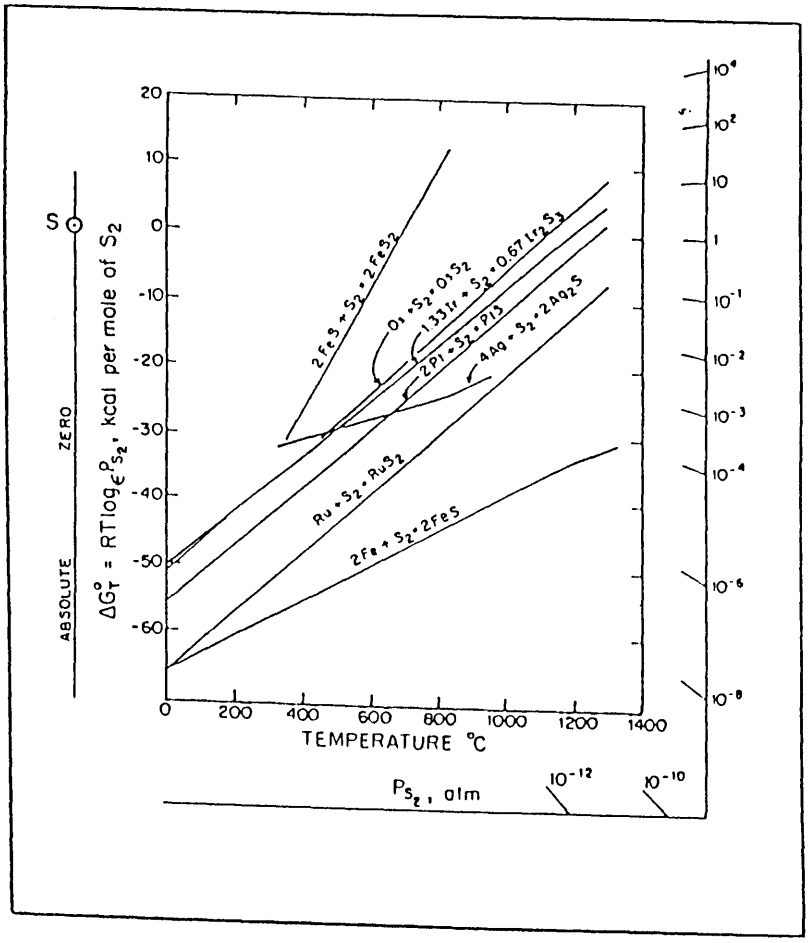

Figure 32. Stability relationships of some selected PGM, FeS_2 and Ag_2S as a function of temperature and free energy of formation/partial pressure of S_2. (After Toma et. al (1977))

In Profile 5, which shows major macroscopic alteration, laurite constitutes one third of the PGM assemblage and the PGM sulphides only 37 vol-% of the total PGM's. An increased amount of PGM's form compounds with "volatile" elements such as Pb, As, Te, Hg, and Bi (20% by volume of all the PGM's in Profile 5). Alloys of PGE's and volatile elements also occur in pegmatoid and dunite-affected Merensky reef (Kinloch and Peyerl, 1990). Palladium forms alloys with Hg, Pb, Sn, As, and Sb, which suggests the presence of significant amounts of "volatiles" during formation of the Merensky reef pegmatoid. The PGM assemblage of the pegmatoid and dunite-affected Merensky reef as described by Kinloch and Peyerl also includes Pt-Fe alloy, various Pd-alloys, laurite, sperrylite, and PGE tellurides.

Other localities where the PGM assemblage are also rich in volatile elements are the Mooihoek and Onverwacht pipes. The minerals include: (Pt,Fe) alloy, tetraferroplatinum, laurite, hollingworthite (RhAsS), unnamed (Rh,Ru)AsS, sperrylite ($PtAs_2$), geversite ($PtSb_2$), platarsite (PtAsS), cabriite (Pd_2SnCu), rustenburgite ($(Pt,Pd)_3Sn$), unnamed $(Pd,Pt)_4(Cu,Fe)_2(Sn,Sb)_3$, $(Pt,Ir)_3Sb$, (Rh,Ir,Pt)SbS, Rh(Sb,Bi)S, and Pt(Bi,Sb) (Rudashevsky 1992, Peyerl, 1982). Arsenic-containing and alloy-type PGM's are common in the UG-2 chromitite in the vicinity of the Driekop dunite pipe as described by Peyerl (1982). The PGM assemblage shows a progressive change from a Pt-Fe and Pt-Pd-Sb-As type to a normal Rustenburg Pt-Pd-sulphide type away from the pipe.

At the Shetland ophiolite complex, PGM's form compounds with As and Sb, as well as Cu and Fe (Prichard et al., 1988). The As- and Sb containing PGM's in the complex occur in the serpentine or chlorite matrix, or at the rims of grains. Prichard et al. suggest that the PGM's have a primary magmatic origin with lower-temperature processes of alteration superimposed on the igneous processes, which may have modified and redistributed the PGM's. They also proposed that As and Sb could have been introduced with late magmatic fluids, or by a later, lower-temperature process.

The increase in As- containing PGM's and PGM-alloys with alteration in the Vaalkop area is therefore consistent with the commonly held view that late-stage low-temperature fluids modified the primary PGM assemblage. PGE's could be remobilized and redistributed in areas influenced by volatiles. Transport of Pt and Pd can occur through complexing by either OH^-, HS^-, or Cl^- in hydrothermal solutions (Gammons et al., 1993; Gammons et al., 1992; Mountain and Wood, 1988; Schiffries, 1982; Wood, 1991; Wood et al., 1989). Chloride complexing will be important under highly oxidising and acidic conditions. The predominant chloride complexes of Pt and Pd are $PtCl_4^{-2}$ from 25° to 300°C and $PdCl_3^-$ at 300°C respectively.

7.4 Chemical analyses

Metasomatic processes can have large variations in their effects on a small scale. Therefore it is difficult to decipher generally valid trends from microscopic work. Analytical results may allow more generalized deductions and Spearman correlations are therefore calculated. Still, many relationships cannot be interpreted due to a limited number of analyses, averaging of chemical analyses over 10 cm, primary heterogeneity, existence of magmatic trends (e.g. PGE-peaks) and variable effects of the pegmatoid. Some confirmation of microscopic observations are possible, for instance the extreme alteration from the Reference Profile to Profile 8.

Element concentrations obtained for the chromitite were tested for systematic relationships in Spearman correlation matrices (Conover,1980) for the matrices (Appendix 5). Values below the lower limits of detection were omitted in the calculations. Missing values were treated pairwise.

In the Reference Profile, TiO_2 is negatively correlated with Pt (r=–0.76) and Ru (r=–0.70), although Ti occurs in chromite and also as rutile in composite sulphide grains. Pb, which occurs as a sulphide, is positively correlated (r=0.76) with TiO_2. Pd is predominantly present as a sulphide and is negatively correlated (r=–0.73) with Cr_2O_3. Sr is a trace element in feldspar and a negative correlation (r=–0.71) exists between Sr and Cr_2O_3. A positive correlation (r=0.65 and 0.85) exists between Fe_2O_3, Zn, and V in the chromite of the Reference Profile. Fe_2O_3 is also a major component of pyroxene and is negatively correlated (r=–0.6, –0.82, –0.65) with the BMS elements Cu, Ni and S. Zn and V, which are predominantly present in chromite in the Reference Profile, are negatively correlated (r=–0.67, –0.71 and –0.73) with Cu, Ni and S.

In Profile 3, TiO_2 is strongly correlated with Fe_2O_3 and Cr_2O_3 (r = 0.91 to 0.87). This is an indication of the increase in Ti in the chromites due to overprinting. Fe_2O_3, Cr_2O_3 and TiO_2 correlate with Zn, V, Ni, and Co which occur as trace elements in chromite. The PGE's, except for Ir, are correlated with one another and also with Ni which is the main constituent of the BMS. Pd and Rh are positively correlated (r=0.85 and 0.68) with TiO_2 and are concentrated in alteration zones. Pd and Rh also correlate (R= 0.69, 0.71, 0.84 and 0.65) with Zn, Co, V and Pb.

In Profiles 1 and 8, Al_2O_3, which is a major constituent of feldspar and chromite is negatively correlated with TiO_2, MnO, Fe_2O_3 and V, which are increasing in chromite grains due to

overprinting. Al_2O_3, Cr_2O_3 and Ni are positively correlated with one another and decrease in chromite due to overprinting. The PGE's, Cu, Ni and S are all positively correlated and are bound to sulphides or concentrated as sulphides in silicates.

In Profiles 1, 5 and 2, the PGE's are positively correlated with each other and also with Ni, and sometimes Cu. In Profile 2, the PGE's, Cu, Ni and S were removed from the sintered zone and are negatively correlated with Ti and V which are abundant in the bottom, sintered area. The positive correlation between the PGE's indicate a similarity in the behaviour of Pt, Pd, Rh, Ru and Ir.

In Profile 8, the oxides are sintered and virtually no silicates occur in the sintered areas. This is shown in the negative correlation of Al_2O_3 with TiO_2, MnO_2, and Fe_2O_3. The positive correlation between TiO_2 with MnO_2 and Fe_2O_3 is indicative of metasomatic addition of the former. The negative correlation of Pd and Rh with TiO_2 and MnO_2 reflects the mobilization of the PGE's during metasomatism. Ru and Ir are positively correlated with Cr_2O_3 which is manifested by the presence of laurite inclusions in chromite grains. The positive correlation of S with Cu and Fe is also an indication of the mobilization of the sulphides which is shown in the occurrence of sulphide veins. Pb is introduced as PbS and is positively correlated with TiO_2, Fe_2O_3 and S.

8. SUMMARY AND CONCLUSIONS

The "normal" UG-2 chromitite in the Reference Profile consists of a "leopard-skin" chromitite with an anorthositic footwall. Chromite, pyroxene, and feldspar are the main constituents of the UG-2 chromitite with interstitial pentlandite, chalcopyrite, and pyrrhotite. Platinum group minerals occur as inclusions in the BMS and chromite and are mainly laurite and Pt/Pd-sulphides.

Late-stage hydrothermal fluids sporadically altered the chemistry and mineral assemblage of the UG-2 chromitite. The hydrothermal fluids contained a relatively large amount of volatiles, which is shown in the presence of graphite and hydrous silicates such as amphibole, chlorite, talc, clay-minerals and serpentine in the profiles of altered UG-2 chromitite.

The hydrothermal fluids were initially Fe-and Ti-rich and during ascent the chromitite acted as a physical barrier which caused the fluid to react with the chromite at the bottom of the UG-2 chromitite. Ilmenite and magnetite were formed with a simultaneous increase in the grain size of the oxide phase due to sintering. Interstitial silicate were altered to low-grade metamorphic minerals and were mobilized in veins parallel to the strike of the UG-2 chromitite in the chromitite and footwall.

The BMS which now came into contact with the relatively Fe-poor hydrothermal fluids were deprived of Fe and Fe-poor BMS such as chalcocite-group minerals, bornite, violarite, haezlewoodite, and millerite were formed. Pyrrhotite was the first BMS to react with the fluid and was removed from the BMS assemblage, but reappeared again in Profile 8. Chalcopyrite was altered to covellite, chalcocite-group minerals and bornite. Cu-sulphide phases are relatively rare in the strongly altered Profile 8. Pentlandite was the last BMS to react with the hydrothermal fluids to form violarite as a rim or as a replacement, and mackinawite exsolutions in pentlandite. Haezlewoodite is most common in Profile 8 and occurs as inclusions in pentlandite. A temperature range for hydrothermal alteration reactions of the BMS of approximately 200-300°C can be deduced according to the relative thermal stabilities of the BMS (Barnes, 1979).

In the Reference Profile, platinum group sulphides are the dominant PGM species. Laurite crystallized before the nucleation of chromite and therefore occurs as inclusions in chromite (Merkle, 1992). Platinum and Pd were collected by the immiscible sulphide melt and exsolved from the BMS on cooling.

In the altered Profiles 1, 3, 5, 2, and 8 a relatively large proportion (35-50%) of the PGM's occurs as alloys with Cu and Fe, as sulpharsenides, and as Pt and Pd compounds with Sb, Bi, Te, Hg, and Pb.

The amount of Pt-Fe and\or Pt-Fe-Cu alloys increase with increasing alteration of the UG-2 chromitite, but also occur in the Reference Profile. The presence of the volatiles also caused the formation of Pt-Fe alloy-BMS eutectic intergrowths (Kinloch and Peyerl, 1990).

During physical contact of earlier-formed PGE-enriched phases with hydrothermal fluids, the PGE phases (mainly PGE-sulphides) were dissolved and redistributed as Pd- and/or Pt-compounds and as sulpharsenides. Palladium is the most common PGE that formed compounds with the elements Sb, Bi, Te, Hg and Pb, possibly due to its mobility and solubility in the hydrothermal fluids.

The differences in the mineral assemblages between the various profiles indicate that the "normal" UG-2 mineral assemblage was altered by postmagmatic hydrothermal fluids, but by varying degrees and compositions of postmagmatic alteration.

9. ACKNOWLEDGEMENTS.

I would like to express my deepest gratitude to Dr. R.K.W. Merkle and Prof. C.P. Snyman for their assistance in the form of guidance, discussions and criticism.

I would like to thank Western Platinum Mine for providing the sample material and for their financial support.

A special thanks to Mintek for initiating the study, for the chemical analyses and the use of their equipment.

Furthermore, I would like to thank my family and friends for their moral support and assistance.

10. REFERENCES

Auclair, M., Gauthier, M., Trottier, J., Jebrak, M., and Chartrand, F. (1993) Mineralogy, geochemistry, and paragenesis of the Eastern Metals serpentenite-associated Ni-Cu deposit, Quebec Appalachians. Economic Geology 88:123-138.

Ballhaus, G.C. and Stumpfl, E.F. (1986) Sulfide and platinum mineralization in the Merensky reef: evidence from hydrous silicates and fluid inclusions. Contribution to Mineralogy and Petrology 94:193-204.

Barnes, H.L., (Ed.) (1979) Geochemistry of Hydrothermal Ore Deposits, 2nd Edition. John Wiley and Sons, 798 pages.

Beeson, M.H. and Jackson, E.D. (1969) Chemical composition of altered chromites from Stillwater Complex, Montana. American Mineralogist 54:1084-1100.

Best, M.G. (1982) Igneous and Metamorphic Petrology. W.H.Freeman and Company, pages.

Bliss, N.W. and MacLean, W.H. (1969) The paragenesis of zoned chromite from central Manitoba. Geochimica et Cosmochimica Acta 39:973-990.

Béziat, D. and Monchoux, P. (1991) Les spinelles chromozinciféres du district aurifére de Salsigne (Montagne Noire, France). European Journal of Mineralogy 3:957-969.

Cabri, L.J. (1972) The mineralogy of the platinum-group elements. Minerals Science and Engineering 4:3-29.

Conover W.J. (1980) Practical nonparametric statistics. John Wiley and Sons. 493 pages.

Davey S.R. (1992) Lateral variations within the upper critical zone of the Bushveld Complex on the farm Rooikoppies 297 JQ, Marikana, South Africa. South African Journal of Geology 95(3/4), 141-149.

Deer, W.A., Howie, R.A. and Zussman, J. (1977) An Introduction to rock forming minerals. Longman Group Limited, London, 528 pages.

Fleet, M.E., Angeli, N. and Yuanming Pan (1993) Oriented chlorite lamellae in chromite from the Pedra Branca mafic- ultramafic complex, Ceara, Brazil. American Mineralogist 78:68-74.

Gammons, C.H., Bloom, M.S. and Yu, Y. (1992) Experimental investigation of hydrothermal geochemistry of platinum and palladium: I. Solubility of platinum and palladium sulphide minerals in $NaCl/H_2SO_4$ solutions at 300°C. Geochimica et Cosmochimica Acta 56:3881-3894.

Gammons, C.H. and Bloom, M.S. (1993) Experimental investigation of the hydrothermal geochemistry of platinum and palladium: II. The solubility of PtS and PdS in aqueous sulphide solutions to 300°C. Geochimica et Cosmochimica Acta 57:2451-2467.

Goble, R.J. (1980) Copper sulfides from Alberta: Yarrowite Cu_9S_8 and spionkopite $Cu_{39}S_{28}$. Canadian Mineralogist 18:511-518.

Gräser, P.P.H., Botha, A.J. and Merkle, R.K.W. (1993) Quantification of the shape difference between laurite grains of different chemical compositions. Electronmicroscopy Society of South Africa 1993, Abstracts.

Harney, M.W. and Merkle, R.K.W. (1992) Sulfide mineralogy at the main magnetite layer, upper zone, eastern Bushveld Complex, and the effect of hydrothermal processes on pentlandite composition. European Journal of Mineralogy 4:557-569.

Kaiser, H. and Specker, H. (1956) Bewertung und Vergleich von Analysenverfahren. Zeitschrift für Analytische Chemie 149:46-66.

King, R.P. (1978) Determination of particle size distribution from measurements on sections. Powder Technology 21:147-150.

Kinloch, E.D. (1982) Regional trends in the platinum-group mineralogy of the critical zone of the Bushveld Complex, South Africa. Economic Geology 77, 1328-1347.

Kinloch, E.D. and Peyerl, W. (1990) Platinum-group minerals in various rock types of the Merensky Reef: Genetic Implications. Economic Geology 85, 537-555.

Liebenberg L. (1970) The sulphides in the layered sequence of the Bushveld Complex. The Geological Society of South Africa, Special Publication 1:108-207.

Lorand, J.P. and Pinet, M. (1984) L'orcelite des peridotites de Beni Bousera (Maroc), Ronda (Espagne), Table Mountain et Blow-Me-Down Mountain (Terre-Neuve) et du Pinde Septentrional. Canadian Mineralogist 22:553-560.

Lord, R.A., Prichard, H.M., and Neary, C.R. (1994) Magmatic platinum group element concentrations and hydrothermal upgrading in Shetland Ophiolite Complex. Transactions of the Institute of Mining and Metallurgy Section B-Applications 103:B87-B106.

McLaren, C.H., (1980) 'n Mineralogiese ondersoek van die platinumgroepminerale in die boonste chromitietlaag (UG2) van die Bosveldkompleks : Unpublished Ph.D. thesis, Rand Afrikaans University, 360 pages.

McLaren C.H. and De Villiers, J.P.R. (1982) The Platinum-group chemistry and mineralogy of the UG-2 layer of the Bushveld Complex. Economic Geology 77:1348-1366.

Merkle, R.K.W. (1987) The effects of metasomatizing fluids on the PGE-content of the UG-1 chromitite layer. In Geo-Platinum '87. Ed. H.M. Prichard, P.J. Potts, J.F.W. Bowles and S.J. Cribb, pp:359-360.

Merkle, R.K.W. (1992) Platinum-group minerals in the middle group of chromitite layers at Marikana, western Bushveld Complex: indications for collection mechanisms and postmagmatic modification. Canadian Journal of Earth Sciences 29:209-221.

Merkle, R.K.W. and Horsch, H.E. (1988) The relationship between composition and habit of laurite inclusions in chromite from the Bushveld Complex. Institute for Geological Research on the Bushveld Complex, Research Report 69, 27 pages.

Merkle, R.K.W. and Von Gruenewaldt, G. (1986) Compositional variation of Co-rich pentlandite : Relation to the evolution of the upper zone of the Western Bushveld Complex, South Africa. Canadian Mineralogist 24:529-546.

Moorhouse, W.W. (1959) The study of Rocks in Thin Section. Harper and Row, Publishers, New York and Evanston, 514 pages.

Mountain B.W. and Wood, S.A. (1988) Chemical controls on the solubility, transport, and deposition of platinum and palladium in hydrothermal solutions : A thermodynamic approach. Economic Geology 83:492-510.

Mumme, W.G., Sparrow, G.J., and Walker, G.S. (1988) Roxbyite, a new copper sulphide mineral from the Olympic Dam deposit, Roxby Downs, South Australia. Mineralogical Magazine 52:323-330.

Peyerl, W. (1982) The Influence of the Driekop dunite pipe on the platinum-group mineralogy of the UG-2 chromitite in its vicinity. Economic Geology 77: 1432-1438.

Prichard, H.M. and Tarkian, M. (1988) Platinum and palladium minerals from two PGE-rich localities in the Shetland ophiolite complex. Canadian Mineralogist 26:979-990.

Ramdohr, P. (1980) The ore minerals and their intergrowths. 2nd ed., Volume 1 and 2. Pergamon Press, 1207 pages.

Rudashevsky, N.S., Avdontsev, S.N. and Dneprovskaya, M.B. (1992) Evolution of PGE mineralization in hortonolitic dunites of the Mooihoek and Onverwacht pipes, Bushveld Complex. Mineralogy and Petrology 47:37-54.

Schiffries, C.M. (1982) The petrogenesis of a platiniferous dunite pipe in the Bushveld Complex : Infiltration metasomatism by a chloride solution. Economic Geology 77:1439-1453.

Shiga, Y. (1987) Behaviour of iron, nickel, cobalt and sulfur during serpentinization, with reference to the Hayachine ultramafic rocks of the Kamaishi mining district, northeastern Japan. Canadian Mineralogist 25:611-624.

Stumpfl, E.F. and Rucklidge, J.C. (1982) The platiniferous dunite pipes of the Eastern Bushveld. Economic Geology 77:1419-1431.

Toma, S.A. and Murphy, S. (1977) The composition and properties of some native platinum concentrates from different localities. Canadian Mineralogist 15:59-69.

Underwood, E.E. (1968) Particle-size distribution. Quantitative Microscopy, Dehoff, R.T., and Rhines, F.N. New York, McGraw-Hill Book Company, 151-181.

Vermaak, C.F. (1985) The UG-2 layer - South Africa's slumbering chromitite giant. Chromium Review 5:9-22.

Vermaak, C.F. and Hendriks, L.P. (1976) A review of the mineralogy of the Merensky Reef, with specific reference to new data on the precious metal mineralogy. Economic Geology 71:1244-1269.

Viljoen, M.J. and Scoon, R.N. (1985) The distribution and main geologic features of discordant bodies of iron-rich ultramafic pegmatite in the Bushveld Complex. Economic Geology 80:1109-1128.

Von Gruenewaldt, G., Sharpe, M.R., and Hatton, C.J. (1985) The Bushveld Complex: introduction and review: Econonomic Geology 80: 803-812.

Winkels Herding, S., Merkle, R.K.W. and Von Gruenewaldt, G. (1991) Pegmatoidal pockets in the UG-2 chromitite, Western Bushveld Complex. ICAM '91 Proceedings 2, Paper 65, 14 pages.

Wood S.A. (1991) Experimental determination of the hydrolysis constants of Pt^{2+} and Pd^{2+} at 25°C from the solubility of Pt and Pd in aqueous hydroxide solutions. Geochimica et Cosmochimica Acta 55:1759-1767.

Wood S.A., Mountain, B.W. and Fenlon, B.J. (1989) Thermodynamic constraints on the solubility of platinum and palladium in hydrothermal solutions: reassessment of hydroxide, bisulfide, and ammonia complexing. Economic Geology 84:2020-2028.

11. APPENDICES

APPENDIX 1

Element	Reproducibility # (wt%)
SiO_2	1.13
TiO_2	0.22
Al_2O_3	1.29
Fe_2O_3	1.02
MnO	<0.01
MgO	0.40
CaO	0.13
Na_2O	<0.01
K_2O	<0.01
P_2O_5	<0.01
Cr_2O_3	1.05
Element	**Reproducibility # (ppm)**
Zn	6.42
Cu	7.34
ac Cu *	1.83 wt%
Ni	145.20
ac Ni *	7.32 wt%
Co	15.29
ac Co *	2.71 wt%
Ga	5.69
Mo	0.82
Nb	0.82
Zr	2.08
Y	0.58
Sr	2.77
Pb	5.85
V	75.23
Ba	21.97
Sc	0.58
S	53.38

Lower limit of detection.

TiO_2	0.1%
Cr_2O_3	0.3%
MnO	0.2%
NiO	0.2%
P_2O_5	0.01%

- estimated according to Kaiser and Specker - based on duplicate analyses of six samples.

* - based on duplicate analyses of 14 samples.

APPENDIX 2

Major element analyses of the Profiles

a. Major element analyses of the Reference Profile.

Sample nr.	MgO (%)	Al_2O_3 (%)	SiO_2 (%)	CaO (%)	TiO_2 (%)	Cr_2O_3 (%)
BOTTOM						
R-1R	10.10	19.30	17.30	3.13	0.57	27.60
R-2R	10.50	19.90	15.50	2.56	0.59	29.30
R-3R	9.84	19.95	16.80	2.64	0.62	29.15
R-4R	9.72	19.85	17.40	2.69	0.66	29.48
R-5R	9.35	19.96	16.70	2.72	0.60	29.63
R-6R	9.68	19.20	16.60	2.72	0.54	28.55
R-7R	9.96	19.28	17.50	2.71	0.52	28.74
R-8R	9.81	18.67	16.00	2.66	0.53	29.61
R-9R	9.27	18.84	16.00	2.59	0.60	30.78
R-10R	9.23	18.46	15.40	2.46	0.59	30.89
TOP						
Ave.	9.75	19.34	16.54	2.69	0.58	29.37
TOP						
R-1FW	1.25	33.02	47.70	15.20	<lld	<lld
R-2FW	1.54	32.07	47.10	15.10	<lld	<lld
R-3FW	2.22	31.03	47.30	15.00	<lld	<lld
R-4FW	0.93	32.78	47.40	15.50	<lld	<lld
R-5FW	1.36	34.38	50.10	15.80	<lld	<lld
BOTTOM						

Sample nr.	MnO (%)	Fe_2O_3 (%)	NiO (%)	P_2O_5 (%)	L.O.I. (%)	Total
BOTTOM						
R-1R	<lld	21.00	0.12	0.02	1.30	100.50
R-2R	<lld	21.20	0.13	0.01	1.31	99.70
R-3R	<lld	21.20	0.13	0.03	1.22	99.70
R-4R	<lld	20.40	0.13	0.10	<lld	102.10
R-5R	<lld	20.70	0.13	0.03	1.45	99.80
R-6R	<lld	20.30	0.13	0.02	1.24	97.80
R-7R	<lld	20.50	0.13	0.03	1.25	99.40
R-8R	<lld	21.00	0.13	0.06	1.19	98.40
R-9R	<lld	21.60	0.13	0.06	1.22	99.90
R-10R	<lld	22.00	0.12	0.02	1.32	99.20
TOP						
	<lld	21.00	0.13	0.04	1.15	
TOP						
R-1FW	<lld	0.52	<lld	n.a.	0.20	97.79
R-2FW	<lld	0.81	<lld	n.a.	0.18	96.76
R-3FW	<lld	0.92	<lld	n.a.	0.17	96.60
R-4FW	<lld	0.38	<lld	n.a.	0.17	97.16
R-5FW	<lld	0.47	<lld	n.a.	0.17	102.30
BOTTOM						

b. Major element analyses of Profile 3.

Sample nr.	MgO (%)	Al_2O_3 (%)	SiO_2 (%)	CaO (%)	TiO_2 (%)	Cr_2O_3 (%)
BOTTOM						
3-1R	10.67	18.05	10.84	1.83	1.05	33.88
3-2R	10.33	17.21	9.31	1.85	1.24	34.11
3-3R	9.94	17.64	8.53	1.22	1.17	34.60
3-4R	10.32	17.42	10.80	1.58	1.09	32.23
3-5R	10.31	18.01	10.80	1.82	1.12	34.24
3-6R	10.49	17.48	10.23	1.72	1.06	33.88
3-7R	10.36	17.39	13.60	2.51	0.94	30.43
3-8R	10.18	17.65	13.23	2.38	0.92	30.85
3-9R	9.80	16.97	12.90	2.26	0.95	30.22
3-10R	10.07	17.34	12.39	2.17	1.02	31.12
3-11R	10.15	16.69	11.84	2.05	0.97	30.90
3-12R	9.79	17.69	14.39	2.87	0.96	31.49
TOP						
Ave.	10.20	17.48	11.57	2.02	1.04	32.33

Sample nr.	MnO (%)	Fe_2O_3 (%)	NiO (%)	P_2O_5 (%)	Total
BOTTOM					
3-1R	0.23	23.12	0.40	<lld	101.10
3-2R	0.26	24.86	0.45	0.20	100.70
3-3R	0.33	24.55	0.75	<lld	99.00
3-4R	0.28	22.86	0.40	<lld	97.60
3-5R	0.28	23.16	0.65	0.30	101.90
3-6R	0.29	23.56	0.40	0.20	100.20
3-7R	0.27	21.84	0.40	<lld	98.80
3-8R	0.29	22.11	0.30	0.20	98.30
3-9R	0.29	21.66	0.30	<lld	95.40
3-10R	0.29	21.86	0.30	<lld	96.50
3-11R	0.31	22.62	0.46	<lld	96.00
3-12R	0.29	22.83	0.32	<lld	101.10
TOP					
Ave.	0.28	22.92	0.45	0.10	

c. Major element analyses of Profile 1.

Sample nr.	MgO (%)	Al_2O_3 (%)	SiO_2 (%)	CaO (%)	TiO_2 (%)	Cr_2O_3 (%)
BOTTOM						
1-1R	6.29	13.35	4.19	0.81	2.57	32.05
1-2R	9.63	16.97	7.01	4.58	0.81	35.30
1-3R	10.0	16.47	7.87	1.99	0.80	34.69
1-4R	9.21	16.47	6.15	1.31	0.87	35.25
1-5R	9.43	15.53	8.61	1.49	0.87	32.89
1-6R	9.89	15.90	8.96	2.10	0.92	33.48
1-7R	8.70	15.19	7.93	2.69	1.22	34.23
TOP						
Ave.	9.03	15.70	7.25	1.71	1.15	33.98
TOP						
1-1FW	19.68	1.50	46.59	10.05	0.66	0.47
1-2FW	21.10	1.69	45.19	9.87	0.22	0.18
1-3FW	20.28	1.53	46.44	12.77	0.29	0.18
1-4FW	21.13	1.78	45.56	10.99	0.22	0.22
1-5FW	18.22	1.00	39.66	7.25	0.19	0.12
BOTTOM						

Sample nr.	MnO (%)	Fe_2O_3 (%)	NiO (%)	P_2O_5 (%)	L.O.I. (%)	Total
BOTTOM						
1-1R	0.40	36.63	0.62	0.02	<lld	97.00
1-2R	0.32	25.21	0.67	0.01	<lld	97.50
1-3R	0.33	25.84	0.86	0.00	0.13	98.90
1-4R	0.35	27.51	0.82	0.00	0.35	97.90
1-5R	0.36	27.05	0.38	0.02	0.99	96.60
1-6R	0.33	25.88	0.42	0.05	<lld	98.00
1-7R	0.36	27.72	0.48	0.01	<lld	98.50
TOP						
Ave.	0.35	27.98	0.61	0.02	0.21	
TOP						
1-1FW	0.30	17.36	0.06	0.14	5.12	101.90
1-2FW	0.30	23.24	0.08	0.03	-0.07	101.80
1-3FW	0.30	19.93	0.07	0.01	-0.89	101.10
1-4FW	0.29	20.26	0.08	0.05	-0.98	101.60
1-5FW	0.44	31.34	0.06	<lld	-0.07	98.20
BOTTOM						

d. Major element analyses of Profile 5.

Sample nr.	MgO (%)	Al_2O_3 (%)	SiO_2 (%)	CaO (%)	TiO_2 (%)	Cr_2O_3 (%)
BOTTOM						
5-1R	7.67	15.50	2.51	0.37	2.30	35.01
5-2R	9.95	17.23	5.81	0.78	1.10	34.74
5-3R	9.72	17.46	7.13	1.27	1.00	33.20
5-4R	10.72	17.76	9.51	1.87	1.01	32.95
5-5R	10.47	17.23	10.00	2.30	1.03	32.31
5-6R	10.19	17.57	10.20	2.39	0.95	31.55
5-7R	10.16	17.27	9.42	2.00	1.01	32.51
5-8R	10.11	17.52	12.09	2.71	0.87	30.30
5-9R	10.01	17.42	11.21	2.66	0.91	31.87
5-10R	10.42	16.80	13.27	2.49	0.90	29.68
TOP						
Ave.	9.94	17.18	9.17	1.88	1.11	32.41
TOP						
5-1FW	17.91	1.14	36.53	7.61	2.09	0.45
5-2FW	23.97	1.25	44.29	10.01	0.20	0.21
5-3FW	24.25	1.22	43.91	9.54	0.16	0.24
5-4FW	23.07	1.07	43.54	9.96	0.20	0.22
BOTTOM						

Sample nr.	MnO (%)	Fe_2O_3 (%)	NiO (%)	P_2O_5 (%)	L.O.I. (%)	Total
BOTTOM						
5-1R	0.31	32.75	0.31	<lld	<lld	96.70
5-2R	0.26	27.61	0.53	<lld	<lld	98.00
5-3R	0.20	24.60	0.50	0.19	<lld	95.40
5-4R	0.23	24.35	0.76	<lld	<lld	99.20
5-5R	0.23	24.43	0.65	<lld	<lld	98.70
5-6R	0.23	23.08	0.59	<lld	<lld	97.70
5-7R	0.23	24.48	0.42	<lld	<lld	97.50
5-8R	0.22	23.89	0.34	<lld	<lld	98.00
5-9R	0.23	24.30	0.48	<lld	<lld	99.10
5-10R	0.26	24.40	0.26	<lld	<lld	98.50
TOP						
Ave.	0.24	25.49	0.482	0.02		
TOP						
5-1FW	0.32	29.96	0.18	0.10	3.35	99.82
5-2FW	0.31	21.54	0.24	0.05	-1.00	101.10
5-3FW	0.33	21.27	0.16	0.01	-0.78	100.30
5-4FW	0.28	21.71	0.24	0.03	-0.33	99.99
BOTTOM						

e. Major element analyses of Profile 2.

Sample nr.	MgO (%)	Al_2O_3 (%)	SiO_2 (%)	CaO (%)	TiO_2 (%)	Cr_2O_3 (%)
BOTTOM						
2-1R	2.61	5.73	2.11	0.75	11.15	20.11
2-2R	7.25	15.34	4.72	1.07	1.26	34.16
2-3R	10.84	17.88	8.59	1.54	0.83	32.76
2-4R	11.03	18.72	7.95	1.68	0.92	33.89
2-5R	10.34	18.10	7.45	1.48	0.88	34.86
2-6R	10.80	18.49	8.15	1.74	0.88	34.17
2-7R	10.83	19.35	8.61	1.81	0.91	34.06
2-8R	10.59	18.40	8.87	1.81	0.99	34.06
2-9R	10.45	18.30	8.14	1.76	0.98	33.86
2-10R	10.67	18.73	8.77	1.97	0.97	34.82
2-11R	9.12	18.68	12.50	3.23	1.04	32.36
TOP						
Ave.	9.50	16.97	7.81	1.71	1.891	32.64
TOP						
2-1FW	19.29	0.89	39.40	8.44	0.32	0.25
2-2FW	22.86	1.66	47.22	11.93	0.23	0.24
2-3FW	19.16	1.15	43.05	9.55	0.29	0.17
2-4FW	18.96	1.08	41.27	10.69	0.25	0.13
BOTTOM						

Sample nr.	MnO (%)	Fe_2O_3 (%)	NiO (%)	P_2O_5 (%)	L.O.I. (%)	Total
BOTTOM						
2-1R	0.58	53.18	0.44	0.00	<lld	96.70
2-2R	0.37	32.42	0.39	0.00	<lld	96.90
2-3R	0.32	23.73	0.83	0.00	0.20	97.30
2-4R	0.23	24.01	0.53	0.20	0.95	99.20
2-5R	0.22	24.28	0.52	<lld	<lld	98.10
2-6R	0.23	23.92	0.40	<lld	0.17	98.80
2-7R	0.22	23.77	0.46	<lld	0.65	99.00
2-8R	0.23	23.82	0.40	<lld	0.86	99.20
2-9R	0.23	24.34	0.37	<lld	0.96	98.40
2-10R	0.22	23.84	0.39	<lld	0.97	100.40
2-11R	0.22	22.99	0.63	<lld	1.49	100.90
TOP						
Ave.	0.28	27.30	0.49	0.02	0.57	
TOP						
2-1FW	0.45	28.53	0.08	<lld	2.93	100.60
2-2FW	0.31	20.59	0.08	0.01	-2.73	102.40
2-3FW	0.37	28.03	0.07	0.08	-0.70	101.20
2-4FW	0.27	22.99	0.07	0.07	6.22	102.00
BOTTOM						

f. Major element analyses of Profile 8.

Sample nr.	MgO (%)	Al_2O_3 (%)	SiO_2 (%)	CaO (%)	TiO_2 (%)	Cr_2O_3 (%)
BOTTOM						
8-1R	6.62	10.49	3.19	1.80	11.88	22.63
8-2R	9.49	17.29	5.45	1.51	0.87	35.46
8-3R	8.72	17.07	4.56	0.67	0.87	35.96
8-4R	9.31	17.21	9.46	2.09	0.74	33.72
8-5R	9.57	16.86	9.88	1.99	0.74	33.34
8-6R	9.03	16.45	2.42	0.75	0.92	39.21
8-7R	8.92	17.66	6.82	1.98	0.85	37.30
8-8R	9.26	16.50	8.53	2.28	0.93	34.41
8-9R	8.50	15.20	5.82	1.65	1.30	37.11
8-10R	8.81	14.81	5.74	1.34	1.38	35.61
TOP						
Ave.	8.82	15.95	6.20	1.61	2.05	34.48
TOP						
8-1FW	13.52	<lld	26.51	2.22	5.91	<lld
8-2FW	15.52	<lld	39.89	8.31	0.75	<lld
8-3FW	16.51	2.96	41.17	7.13	0.74	<lld
8-4FW	18.15	11.66	57.85	6.09	0.11	<lld
8-5FW	16.77	5.85	45.41	7.78	0.60	<lld
8-6FW	16.75	<lld	36.76	5.49	0.67	<lld
8-7FW	15.98	0.39	39.50	8.18	1.20	<lld
8-8FW	16.87	<lld	36.47	5.23	0.63	<lld
BOTTOM						

APPENDIX 3

a. Trace element analyses of the Reference profile (ppm).

Sample nr.	Zn	Cu	Ni	Co	Ga	Mo	Nb	Zr	Y	Sr
BOTTOM										
R-1R	519	51	1103	331	50	<lld	<lld	8	13	105
R-2R	514	61	1141	284	47	<lld	5	26	<lld	105
R-3R	502	82	1123	274	47	<lld	5	10	8	108
R-4R	502	92	1148	309	45	<lld	5	19	5	100
R-5R	519	78	1170	316	45	<lld	5	12	7	101
R-6R	503	133	1350	286	48	<lld	<lld	16	5	102
R-7R	466	273	1890	263	47	<lld	5	10	5	107
R-8R	508	93	1189	300	47	<lld	4	26	9	100
R-9R	522	83	1102	298	47	<lld	<lld	21	10	100
R-10R	577	61	1052	300	43	<lld	4	15	6	83
TOP										

Sample nr.	Rb	U	Th	Pb	V	Ba	Sc	As	S
BOTTOM									
R-1R	<lld	<lld	<lld	<lld	1274	79	12	<lld	156
R-2R	7	<lld	<lld	<lld	1312	06	10	<lld	209
R-3R	<lld	6	<lld	14	1270	90	11	<lld	255
R-4R	<lld	<lld	5	8	1209	95	10	<lld	303
R-5R	<lld	5	<lld	9	1161	90	12	<lld	227
R-6R	<lld	<lld	<lld	<lld	1093	105	13	<lld	474
R-7R	4	<lld	<lld	<lld	1030	145	13	<lld	1327
R-8R	4	<lld	<lld	6	1156	130	10	<lld	297
R-9R	8	<lld	<lld	6	1324	93	9	<lld	264
R-10R	<lld	<lld	<lld	8	1699		8	<lld	177
TOP									

Lower limit of detection (ppm).

Mo	4
Nb	4
Y	4
Rb	4
U	5
Pb	5
As	7
Zr	4
Th	5

b. Trace element analyses of Profile 3 (ppm).

Sample nr.	Zn	Cu	Ni	Co	Ga	Mo	Nb	Zr	Y	Sr
BOTTOM										
3-1R	599	68	1450	236	49	<lld	4	4	5	76
3-2R	746	82	1515	255	38	<lld	6	6	<lld	48
3-3R	766	52	1389	252	62	4	4	4	<lld	53
3-4R	553	125	1438	218	50	<lld	<lld	<lld	<lld	77
3-5R	611	101	1471	243	56	<lld	5	<lld	<lld	84
3-6R	585	82	1502	246	50	<lld	4	4	4	80
3-7R	535	91	1415	207	44	<lld	<lld	5	5	105
3-8R	494	75	1384	200	43	<lld	4	5	5	99
3-9R	549	51	1302	182	48	<lld	<lld	5	5	104
3-10R	579	97	1265	221	51	<lld	6	6	6	100
3-11R	679	57	1336	225	49	<lld	4	5	7	73
3-12R	572	121	1088	201	48	4	<lld	<lld	<lld	130
TOP										

Sample nr.	Rb	U	Th	Pb	V	Ba	Sc	As	S
BOTTOM									
3-1R	<lld	<lld	<lld	6	1639	83	9	<lld	213
3-2R	<lld	18	<lld	15	1744	96	10	<lld	323
3-3R	<lld	41	<lld	11	1757	105	9	<lld	232
3-4R	<lld	<lld	6	16	1563	77	9	<lld	354
3-5R	<lld	<lld	<lld	14	1605	76	13	<lld	409
3-6R	<lld	<lld	<lld	15	1497	64	9	<lld	402
3-7R	<lld	<lld	<lld	10	1334	64	12	<lld	349
3-8R	13	<lld	<lld	<lld	1098	86	9	<lld	202
3-9R	<lld	<lld	<lld	13	1067	87	10	<lld	141
3-10R	<lld	<lld	<lld	<lld	1266	87	13	<lld	325
3-11R	8	<lld	<lld	7	1392	79	11	<lld	238
3-12R	<lld	7	<lld	9	1551	79	10	<lld	328
TOP									

c. Trace element analyses of Profile 1 (ppm).

Sample nr.	Zn	Cu	Ni	Co	Ga	Mo	Nb	Zr	Y	Sr
BOTTOM										
1-1R	975	107	1390	375	50	<lld	<lld	5	<lld	21
1-2R	659	67	1842	261	48	<lld	4	<lld	<lld	47
1-3R	665	334	2384	270	43	<lld	4	4	4	34
1-4R	736	166	2012	297	46	<lld	4	5	4	23
1-5R	923	43	1630	254	40	<lld	5	<lld	<lld	14
1-6R	583	94	1457	233	43	<lld	<lld	6	7	42
1-7R	733	141	1281	287	49	<lld	<lld	5	6	33
TOP										

Sample nr.	Rb	U	Th	Pb	V	Ba	Sc	As	S
BOTTOM									
1-1R	<lld	<lld	<lld	6	2212	164	11	<lld	505
1-2R	<lld	<lld	<lld	13	1446	68	7	<lld	422
1-3R	<lld	<lld	<lld	11	1521	42	9	<lld	1301
1-4R	4	7	<lld	16	1648	59	10	7	853
1-5R	4	<lld	<lld	19	1647	42	11	29	145
1-6R	<lld	9	<lld	18	1896	54	11	<lld	344
1-7R	<lld	6	<lld	7	2073	51	14	<lld	518
TOP									

d. Trace element analyses of Profile 5. (ppm)

Sample nr.	Zn	Cu	Ni	Co	Ga	Mo	Nb	Zr	Y	Sr
BOTTOM										
5-1R	980	99	1236	330	58	<lld	7	<lld	<lld	13
5-2R	810	58	1496	261	59	6	5	<lld	4	32
5-3R	622	119	1590	236	61	<lld	4	<lld	5	48
5-4R	551	133	1624	273	51	<lld	<lld	<lld	<lld	69
5-5R	560	161	1802	222	49	<lld	<lld	<lld	10	75
5-6R	584	143	1877	223	44	<lld	4	5	4	81
5-7R	517	107	1506	240	48	<lld	4	<lld	4	73
5-8R	549	105	1378	203	47	<lld	5	<lld	<lld	115
5-9R	580	138	1478	222	49	<lld	<lld	<lld	<lld	103
5-10R	686	72	1300	200	38	<lld	4	<lld	4	79
TOP										

Sample nr.	Rb	U	Th	Pb	V	Ba	Sc	As	S
BOTTOM									
5-1R	<lld	6	6	9	2025	128	10	<lld	479
5-2R	<lld	<lld	<lld	5	1659	51	7	<lld	329
5-3R	<lld	<lld	<lld	8	1578	51	7	<lld	356
5-4R	<lld	48	<lld	<lld	1588	56	9	<lld	524
5-5R	<lld	<lld	<lld	10	1480	45	12	<lld	694
5-6R	<lld	5	6	8	1619	56	11	<lld	644
5-7R	<lld	<lld	<lld	10	1741	57	10	<lld	381
5-8R	<lld	<lld	<lld	7	1553	38	12	<lld	310
5-9R	<lld	<lld	<lld	<lld	1671	57	11	<lld	572
5-10R	<lld	5	<lld	16	1498	45	14	<lld	187
TOP									

e. Trace element analyses of Profile 2 (ppm).

Sample nr.	Zn	Cu	Ni	Co	Ga	Mo	Nb	Zr	Y	Sr
BOTTOM										
2-1R	945	64	836	370	45	<lld	8	13	5	5
2-2R	1016	97	1366	323	49	<lld	5	4	<lld	26
2-3R	572	260	2020	256	46	<lld	<lld	<lld	<lld	73
2-4R	580	174	1865	238	51	<lld	5	<lld	<lld	81
2-5R	644	108	1563	276	51	<lld	<lld	<lld	<lld	60
2-6R	594	103	1615	234	55	<lld	<lld	<lld	5	76
2-7R	609	128	1689	267	55	<lld	<lld	<lld	<lld	84
2-8R	576	121	1543	230	53	<lld	4	5	<lld	94
2-9R	583	100	1455	217	51	<lld	<lld	<lld	<lld	78
2-10R	591	85	1402	231	48	<lld	4	<lld	4	84
2-11R	630	90	1015	220	55	<lld	6	<lld	<lld	118
TOP										

Sample nr.	Rb	U	Th	Pb	V	Ba	Sc	As	S
BOTTOM									
2-1R	<lld	5	<lld	<lld	7245	707	19	<lld	111
2-2R	<lld	5	<lld	<lld	1726	66	8	<lld	332
2-3R	<lld	13	<lld	14	1536	50	9	<lld	788
2-4R	<lld	<lld	<lld	16	1422	61	10	<lld	490
2-5R	<lld	<lld	<lld	9	1607	50	8	<lld	401
2-6R	<lld	<lld	<lld	<lld	1469	45	12	<lld	332
2-7R	<lld	5	<lld	13	1461	46	11	<lld	400
2-8R	<lld	<lld	<lld	6	1404	48	11	<lld	350
2-9R	<lld	<lld	<lld	<lld	1580	46	9	<lld	264
2-10R	<lld	<lld	<lld	8	1868	53	12	<lld	323
2-11R	<lld	<lld	<lld	<lld	1985	81	11	<lld	355
TOP									

f. Trace element analyses of Profile 8 (ppm).

Sample nr.	Zn	Cu	Ni	Co	Ga	Mo	Nb	Zr	Y	Sr
BOTTOM										
8-1R	709	46	1064	258	40	6	13	23	4	24
8-2R	759	32	1459	293	51	4	5	<lld	7	55
8-3R	1630	725	1291	323	55	<lld	5	4	<lld	5
8-4R	734	44	1292	259	49	<lld	5	<lld	6	66
8-5R	777	36	1338	238	51	<lld	<lld	<lld	<lld	65
8-6R	861	51	1514	307	60	<lld	<lld	<lld	<lld	13
8-7R	780	45	1268	295	59	<lld	5	<lld	5	61
8-8R	749	70	1375	271	54	<lld	<lld	<lld	<lld	51
8-9R	814	122	1284	298	56	<lld	7	<lld	<lld	14
8-10R	898	228	1480	314	59	4	<lld	5	6	21
TOP										

Sample nr.	Rb	U	Th	Pb	V	Ba	Sc	As	S
BOTTOM									
8-1R	<lld	<lld	<lld	11	5067	777	23	<lld	365
8-2R	<lld	<lld	6	6	2332	41	12	<lld	265
8-3R	<lld	<lld	<lld	6	2178	38	7	<lld	1633
8-4R	9	<lld	<lld	<lld	1905	126	11	<lld	211
8-5R	4	<lld	<lld	<lld	1943	139	10	20	266
8-6R	<lld	<lld	<lld	5	2565	40	6	<lld	330
8-7R	<lld	<lld	<lld	5	2396	47	8	<lld	189
8-8R	4	<lld	<lld	18	2338	48	13	<lld	441
8-9R	<lld	<lld	<lld	8	2562	64	11	<lld	522
8-10R	<lld	<lld	9	14	2311	71	11	<lld	1055
TOP									

APPENDIX 4

Quantitative pentlandite analyses.

Pol. sec. nr.	Co (%)	Ni (%)	Cu (%)	Zn (%)	Sb (%)	As (%)	Fe (%)	S (%)	Total
BOTTOM									
1-16	1.65	30.04	0.50	0.01	0.00	0.00	33.77	32.87	98.84
1-16	7.49	27.05	0.35	0.00	0.23	0.02	32.16	32.88	100.2
1-15	4.75	25.95	0.00	0.00	0.39	0.00	35.49	32.62	99.20
1-15	3.11	30.61	0.03	0.06	0.05	0.00	33.14	32.79	99.79
1-14	5.49	29.89	0.15	0.03	0.00	0.07	31.52	31.92	99.05
MIDDLE									
1-13	2.20	27.85	0.00	0.05	0.00	0.00	34.92	34.16	99.16
1-13	2.05	27.75	0.00	0.14	0.38	0.00	34.95	33.41	98.61
1-13	1.50	30.00	0.00	0.03	0.01	0.00	34.00	33.42	98.95
1-12	0.45	34.90	0.00	0.17	0.00	0.00	30.34	34.02	99.88
1-11	0.55	36.58	0.82	0.00	0.00	0.00	26.14	34.46	98.55
1-11	0.00	38.23	0.00	0.13	0.00	0.03	27.00	33.11	98.50
TOP									
1-9	0.21	43.55	0.00	0.10	0.00	0.00	22.72	32.60	99.18
1-9	0.15	40.75	0.00	0.00	0.00	0.00	25.99	31.84	98.72
1-9	0.33	43.29	0.17	0.00	0.00	0.04	23.19	34.21	101.2
1-8	0.00	28.56	0.00	0.12	0.13	0.00	38.83	33.67	101.3
1-8	0.05	30.49	0.00	0.14	0.00	0.00	37.34	33.52	101.5
1-7	1.24	29.91	0.00	0.07	0.33	0.00	36.28	32.85	100.6
1-7	1.62	28.62	0.05	0.06	0.00	0.05	36.35	33.28	100.0
1-4	0.19	40.50	0.73	0.00	0.00	0.00	24.25	32.96	98.63
1-4	0.00	30.30	0.28	0.06	0.16	0.01	35.38	33.99	100.1
1-4	0.27	43.04	0.00	0.00	0.16	0.02	23.95	33.93	101.3
1-2	0.41	28.51	0.20	0.00	0.15	0.00	36.65	34.07	99.97

REFERENCE PROFILE

(correlation coefficient with error probability underneath)

	Al2O3	TiO2	Cr2O3	MnO2	Fe2O3	P2O5	Pt	Pd	Rh	Ru	Ir	Zn	Cu	Ni	Co	V	Ba	S	Sr	Pb
Al2O3	1.00	0.49	−0.30	1.00	−0.26	−0.06	−0.44	0.26	0.01	−0.46	−0.51	−0.32	−0.24	0.15	0.01	−0.14	−0.13	−0.14	0.60	0.29
	1.00	0.13	0.37	0.00	0.44	0.86	0.18	0.43	0.97	0.16	0.13	0.33	0.47	0.65	0.97	0.68	0.69	0.68	0.07	0.39
TiO2		1.00	0.37	1.00	0.22	0.33	−0.76	−0.48	−0.55	−0.70	−0.56	0.12	−0.34	−0.50	0.23	0.48	−0.07	−0.24	−0.16	0.76
		1.00	0.27	0.00	0.51	0.32	0.02	0.15	0.10	0.04	0.09	0.72	0.31	0.13	0.49	0.15	0.83	0.47	0.64	0.02
Cr2O3			1.00	1.00	0.55	0.34	−0.22	−0.73	−0.57	−0.27	−0.02	0.57	−0.15	−0.42	0.21	0.48	0.43	−0.19	−0.77	0.58
			1.00	0.00	0.10	0.30	0.50	0.03	0.09	0.53	0.53	0.09	0.66	0.21	0.54	0.15	0.20	0.57	0.03	0.83
MnO				1.00	1.00	1.00	1.00	1.00	1.00	1.00	1.00	1.00	1.00	1.00	1.00	1.00	1.00	1.00	1.00	1.00
				1.00	0.00	0.00	0.00	0.00	0.00	0.00	0.00	0.00	0.00	0.00	0.00	0.00	0.00	0.00	0.00	0.00
Fe2O3					1.00	−0.19	0.12	−0.31	−0.48	0.17	0.35	0.65	0.60	−0.82	−0.06	0.85	0.45	−0.65	−0.22	0.28
					1.00	0.57	0.72	0.35	0.15	0.62	0.30	0.05	0.07	0.01	0.87	0.01	0.18	0.05	0.52	0.39
P2O5						1.00	−0.24	−0.15	0.04	−0.32	−0.26	−0.28	0.51	0.16	0.15	−0.24	0.28	0.51	−0.34	0.45
						1.00	0.48	0.65	0.91	0.34	0.44	0.41	0.13	0.64	0.66	0.47	0.40	0.13	0.31	0.18
Pt							1.00	0.54	0.71	0.96	0.92	0.21	−0.09	0.06	0.10	−0.02	0.75	−0.76	0.03	−0.75
							1.00	0.11	0.04	0.01	0.01	0.52	0.78	0.87	0.76	0.96	0.05	0.42	0.94	0.25
Pd								1.00	0.80	0.53	0.27	−0.58	0.12	0.44	−0.26	−0.43	0.02	0.14	0.70	−0.58
								1.00	0.02	0.11	0.41	0.08	0.72	0.18	0.43	0.20	0.94	0.68	0.04	0.08
Rh									1.00	0.69	0.52	−0.33	0.16	0.47	0.21	−0.46	0.11	0.16	0.24	−0.67
									1.00	0.04	0.12	0.32	0.64	0.16	0.53	0.17	0.75	0.64	0.47	0.04
Ru										1.00	0.92	0.23	−0.19	−0.03	0.13	0.09	0.01	−0.25	−0.04	−0.75
										1.00	0.01	0.50	0.57	0.93	0.69	0.79	0.80	0.46	0.90	0.03
Ir											1.00	0.50	−0.30	−0.23	0.26	0.28	0.20	−0.38	−0.20	−0.62
											1.00	0.13	0.37	0.49	0.44	0.40	0.56	0.26	0.56	0.06
Zn												1.00	−0.67	−0.71	0.52	0.74	0.02	−0.73	−0.57	0.11
												1.00	0.04	0.03	0.12	0.03	0.96	0.03	0.09	0.73
Cu													1.00	0.76	−0.47	−0.77	0.21	0.99	0.04	−0.16
													1.00	0.02	0.16	0.02	0.52	0.01	0.90	0.62
Ni														1.00	−0.29	0.96	0.04	0.76	0.31	0.32
														1.00	0.38	0.01	0.91	0.02	0.35	0.35
Co															1.00	0.22	−0.46	−0.47	−0.52	0.19
															1.00	0.51	0.17	0.16	0.12	0.58
V																1.00	0.06	−0.76	−0.35	0.25
																1.00	0.86	0.02	0.30	0.45
Ba																	1.00	0.75	−0.03	0.11
																	1.00	0.66	0.93	0.73
S																		1.00	0.08	−0.16
																		1.00	0.81	0.63
Sr																			1.00	−0.25
																			1.00	0.46
Pb																				1.00
																				1.00

N=10

PROFILE 3

(correlation coefficient with error probability underneath)

	Al2O3	TiO2	Cr2O3	MnO	Fe2O3	P2O5	Pt	Pd	Rh	Ru	Ir	Zn	Cu	Ni	Co	V	Ba	S	Sr	Pb
Al2O3	1.00	0.11	0.47	−0.16	0.34	0.26	0.60	0.11	0.13	0.02	−0.11	−0.13	0.28	0.20	0.09	0.41	−0.21	0.18	0.11	−0.14
	1.00	0.73	0.12	0.59	0.26	0.39	0.84	0.73	0.67	0.96	0.72	0.68	0.35	0.52	0.76	0.18	0.49	0.55	0.73	0.65
TiO2		1.00	0.91	−0.25	0.87	0.29	0.60	0.85	0.68	0.41	0.25	0.82	0.13	0.63	0.87	0.85	0.21	0.35	−0.73	0.60
		1.00	0.01	0.41	0.01	0.34	0.05	0.01	0.02	0.17	0.42	0.01	0.68	0.04	0.01	0.01	0.48	0.25	0.02	0.05
Cr2O3			1.00	−0.16	0.94	0.38	0.47	0.74	0.56	0.28	0.17	0.73	0.14	0.60	0.86	0.91	0.14	0.35	−0.64	0.41
			1.00	0.60	0.01	0.21	0.12	0.01	0.06	0.36	0.57	0.02	0.64	0.05	0.01	0.01	0.65	0.25	0.04	0.18
MnO				1.00	−0.13	−0.12	−0.65	−0.46	−0.61	−0.56	−0.45	−0.02	−0.42	−0.57	−0.20	−0.27	0.26	−0.33	0.49	−0.25
				1.00	0.02	0.70	0.03	0.18	0.04	0.06	0.14	0.94	0.17	0.06	0.50	0.37	0.39	0.28	0.87	0.40
Fe2O3					1.00	0.46	0.46	0.74	0.53	0.79	0.11	0.71	0.06	0.70	0.80	0.89	0.12	0.29	−0.73	0.49
					1.00	0.13	0.13	0.02	0.08	0.54	0.73	0.02	0.83	0.02	0.01	0.01	0.70	0.33	0.02	0.10
P2O5						1.00	0.32	0.75	0.73	0.01	0.37	0.14	0.15	0.67	0.37	0.73	−0.18	0.32	−0.18	0.30
						1.00	0.28	0.62	0.68	0.98	0.22	0.66	0.62	0.04	0.23	0.66	0.56	0.28	0.56	0.32
Pt							1.00	0.82	0.94	0.83	0.37	0.46	0.27	0.82	0.52	0.52	−0.37	0.53	−0.44	0.66
							1.00	0.07	0.02	0.01	0.22	0.13	0.36	0.01	0.09	0.08	0.22	0.08	0.15	0.03
Pd								1.00	0.93	0.73	0.15	0.69	0.26	0.68	0.71	0.84	−0.08	0.43	−0.71	0.65
								1.00	0.01	0.02	0.63	0.02	0.40	0.03	0.02	0.01	0.79	0.15	0.02	0.03
Rh									1.00	0.88	0.26	0.52	0.32	0.70	0.54	0.70	−0.25	0.47	−0.51	0.67
									1.00	0.01	0.40	0.08	0.30	0.02	0.07	0.02	0.41	0.12	0.09	0.04
Ru										1.00	0.29	0.33	0.31	0.46	0.26	0.44	−0.15	0.31	−0.34	0.33
										1.00	0.33	0.28	0.30	0.13	0.38	0.14	0.62	0.31	0.26	0.27
Ir											1.00	0.45	−0.12	0.35	0.40	0.10	0.09	0.03	−0.22	−0.11
											1.00	0.13	0.69	0.25	0.19	0.75	0.77	0.93	0.47	0.70
Zn												1.00	−0.32	0.48	0.89	0.71	0.32	0.05	−0.85	0.29
												1.00	0.30	0.12	0.01	0.02	0.29	0.87	0.01	0.33
Cu													1.00	0.08	−0.06	0.11	−0.51	0.79	0.34	0.24
													1.00	0.79	0.83	0.72	0.09	0.01	0.26	0.43
Ni														1.00	0.69	0.57	−0.25	0.39	−0.57	0.61
														1.00	0.02	0.06	0.40	0.20	0.06	0.04
Co															1.00	0.79	0.13	0.30	−0.78	0.37
															1.00	0.01	0.67	0.32	0.01	0.22
V																1.00	0.16	0.24	−0.68	0.40
																1.00	0.61	0.43	0.03	0.19
Ba																	1.00	−0.72	−0.36	−0.25
																	1.00	0.02	0.22	0.41
S																		1.00	0.13	0.50
																		1.00	0.68	0.09
Sr																			1.00	−0.29
																			1.00	0.34

N=12

PROFILE 1

(correlation coefficient with error probability underneath)

	Al2O3	TiO2	Cr2O3	MnO	Fe2O3	P2O5	LOI	Pt	Pd	Rh	Ru	Ir	Zn	Cu	Ni	Co	V	Ba	S	Sr	Pb
Al2O3	1.00	−0.86	0.88	−0.85	−0.85	−0.52	0.18	0.70	0.25	0.67	0.67	0.73	−0.62	0.09	0.81	−0.32	−0.87	−0.03	0.20	0.65	0.36
	1.00	0.03	0.03	0.09	0.04	0.20	0.66	0.06	0.54	0.09	0.10	0.08	0.13	0.83	0.05	0.43	0.03	0.95	0.63	0.11	0.38
TiO2		1.00	−0.69	0.67	0.85	0.57	−0.46	−0.72	−0.25	−0.67	−0.67	−0.69	0.41	−0.13	−0.90	0.36	0.96	0.41	−0.23	−0.40	−0.36
		1.00	0.09	0.13	0.04	0.16	0.26	0.08	0.54	0.13	0.13	0.09	0.31	0.75	0.03	0.38	0.02	0.32	0.57	0.33	0.38
Cr2O3			1.00	−0.75	−0.61	−0.72	0.02	0.61	0.21	0.64	0.46	0.58	−0.54	0.29	0.61	−0.04	−0.68	0.05	0.43	0.64	0.07
			1.00	0.07	0.14	0.08	0.96	0.14	0.60	0.12	0.26	0.16	0.19	0.45	0.14	0.93	0.09	0.90	0.29	0.12	0.84
MnO				1.00	0.86	0.18	0.25	−0.57	−0.11	−0.54	−0.54	−0.49	0.93	0.00	−0.46	0.54	0.64	−0.02	−0.04	−0.93	−0.29
				1.00	0.04	0.65	0.53	0.16	0.79	0.19	0.19	0.23	0.02	1.00	0.26	0.19	0.12	0.97	0.93	0.02	0.48
Fe2O3					1.00	0.17	−0.06	−0.57	−0.71	−0.50	−0.50	−0.50	0.75	0.18	−0.64	0.68	0.89	0.25	0.11	−0.71	−0.43
					1.00	0.69	0.88	0.16	0.86	0.22	0.22	0.22	0.07	0.66	0.12	0.09	0.03	0.54	0.79	0.08	0.29
P2O5						1.00	−0.33	−0.59	−0.50	−0.64	−0.46	−0.62	−0.02	−0.72	−0.64	−0.46	0.42	0.15	−0.84	−0.11	0.26
						1.00	0.41	0.15	0.23	0.12	0.24	0.13	0.96	0.08	0.12	0.26	0.30	0.72	0.04	0.79	0.53
LOI							1.00	0.22	−0.10	−0.10	0.22	0.22	0.39	0.04	0.57	−0.08	−0.37	−0.56	0.04	−0.57	0.57
							1.00	0.60	0.81	0.81	0.60	0.60	0.33	0.92	0.16	0.85	0.36	0.17	0.92	0.16	0.16
Pt								1.00	0.75	0.89	0.96	0.99	−0.36	0.54	0.89	0.04	−0.57	0.05	0.54	0.43	0.07
								1.00	0.06	0.03	0.08	0.02	0.38	0.22	0.03	0.93	0.16	0.90	0.19	0.29	0.86
Pd									1.00	0.86	0.71	0.81	0.04	0.68	0.50	0.54	−0.07	0.32	0.71	0.18	−0.54
									1.00	0.04	0.08	0.05	0.93	0.10	0.22	0.19	0.86	0.43	0.08	0.66	0.19
Rh										1.00	0.79	0.92	−0.32	0.54	0.71	0.25	−0.50	0.25	0.64	0.54	−0.32
										1.00	0.05	0.02	0.43	0.19	0.08	0.54	0.22	0.54	0.12	0.19	0.43
Ru											1.00	0.94	−0.39	0.54	0.82	−0.04	−0.43	−0.02	0.50	0.39	0.14
											1.00	0.02	0.34	0.19	0.04	0.93	0.29	0.97	0.22	0.34	0.73
Ir												1.00	−0.25	0.52	0.88	0.14	−0.54	0.11	0.58	0.36	−0.02
												1.00	0.54	0.20	0.03	0.72	0.19	0.79	0.16	0.38	0.95
Zn													1.00	0.00	−0.21	0.64	0.43	0.13	0.04	−0.93	−0.25
													1.00	1.00	0.60	0.12	0.29	0.76	0.93	0.03	0.54
Cu														1.00	0.32	0.57	0.14	−0.11	0.96	0.07	−0.50
														1.00	0.43	0.16	0.73	0.79	0.02	0.86	0.22
Ni															1.00	−0.11	−0.79	−0.23	0.39	0.21	0.32
															1.00	0.79	0.05	0.57	0.34	0.60	0.43
Co																1.00	0.46	0.47	0.64	−0.39	−0.79
																1.00	0.26	0.25	0.12	0.34	0.07
V																	1.00	0.31	0.00	−0.43	−0.43
																	1.00	0.45	1.00	0.29	0.29
Ba																		1.00	−0.04	0.14	−0.40
																		1.00	0.93	0.72	0.33
S																			1.00	0.11	−0.57
																			1.00	0.79	0.16
Sr																				1.00	−0.04
																				1.00	0.93
Pb																					1.00
																					1.00

N=7

PROFILE 2

(correlation coefficient with error probability underneath)

	Al2O3	TiO2	Cr2O3	MnO	Fe2O3	P2O5	LOI	Pt	Pd	Rh	Ru	Ir	Zn	Cu	Ni	Co	V	Ba	S	Sr	Pb
Al2O3	1.00	−0.26	0.26	−0.66	−0.56	0.30	0.68	0.04	−0.25	−0.06	0.25	0.25	−0.30	0.20	0.31	−0.47	−0.37	−0.32	0.22	0.80	0.37
	1.00	0.41	0.41	0.08	0.08	0.35	0.03	0.89	0.43	0.85	0.44	0.44	0.34	0.53	0.33	0.14	0.24	0.31	0.48	0.01	0.24
TiO2		1.00	−0.40	0.27	0.38	−0.10	0.08	−0.74	−0.58	−0.60	−0.83	−0.63	0.46	−0.71	−0.86	0.00	0.47	0.60	−0.66	0.01	−0.66
		1.00	0.21	0.39	0.23	0.75	0.79	0.02	0.07	0.06	0.01	0.05	0.15	0.03	0.01	1.00	0.14	0.06	0.04	0.98	0.04
Cr2O3			1.00	−0.45	0.11	−0.10	−0.21	0.43	0.16	0.45	0.43	0.53	0.12	0.07	0.21	0.09	−0.21	−0.41	0.06	−0.03	0.16
			1.00	0.16	0.74	0.75	0.51	0.18	0.62	0.15	0.17	0.10	0.70	0.83	0.52	0.78	0.51	0.20	0.85	0.94	0.62
MnO				1.00	0.44	0.20	−0.57	0.02	0.47	0.11	−0.20	−0.22	0.04	0.12	0.02	0.52	−0.07	0.27	−0.07	−0.62	−0.11
				1.00	0.16	0.53	0.07	0.93	0.14	0.74	0.54	0.49	0.90	0.71	0.94	0.10	0.82	0.40	0.82	0.05	0.74
Fe2O3					1.00	0.10	−0.55	0.03	0.47	0.11	−0.19	−0.22	0.04	0.12	0.02	0.52	−0.07	0.27	−0.71	−0.62	−0.11
					1.00	0.75	0.08	0.93	0.14	0.74	0.54	0.49	0.90	0.71	0.94	0.10	0.82	0.40	0.83	0.05	0.74
P2O5						1.00	0.20	0.40	0.40	0.40	0.40	0.40	−0.30	0.40	0.40	0.00	−0.40	0.20	0.40	0.10	0.50
						1.00	0.52	0.21	0.21	0.21	0.21	0.21	0.34	0.21	0.21	1.00	0.20	0.52	0.20	0.75	0.21
LOI							1.00	−0.27	−0.58	−0.35	−0.08	−0.06	−0.50	−0.05	−0.04	−0.85	−0.07	−0.04	0.01	0.86	0.08
							1.00	0.40	0.07	0.28	0.79	0.85	0.12	0.89	0.91	0.01	0.82	0.91	0.98	0.01	0.81
Pt								1.00	0.79	0.94	0.92	0.85	−0.42	0.85	0.82	0.13	−0.71	−0.41	0.76	−0.08	0.69
								1.00	0.01	0.01	0.01	0.01	0.19	0.01	0.01	0.69	0.03	0.19	0.02	0.81	0.03
Pd									1.00	0.85	0.59	0.45	−0.16	0.74	0.72	0.58	−0.45	−0.11	0.69	−0.49	0.64
									1.00	0.01	0.06	0.16	0.62	0.02	0.02	0.07	0.16	0.74	0.03	0.12	0.04
Rh										1.00	0.74	0.69	−0.24	0.76	0.70	0.30	−0.56	−0.20	0.76	−0.19	0.68
										1.00	0.02	0.03	0.45	0.20	0.03	0.35	0.08	0.53	0.02	0.54	0.03
Ru											1.00	0.92	−0.48	0.76	0.83	−0.08	−0.68	−0.55	0.68	0.06	0.63
											1.00	0.01	0.13	0.20	0.01	0.80	0.03	0.08	0.03	0.84	0.05
Ir												1.00	−0.41	0.65	0.67	−0.16	−0.73	−0.61	0.45	0.10	0.47
												1.00	0.20	0.04	0.03	0.60	0.02	0.05	0.15	0.76	0.14
Zn													1.00	−0.68	−0.64	0.56	0.66	0.44	−0.40	−0.44	−0.52
													1.00	0.03	0.04	0.08	0.04	0.16	0.24	0.17	0.10
Cu														1.00	0.94	0.00	−0.84	−0.48	0.83	0.13	0.76
														1.00	0.01	1.00	0.01	0.13	0.01	0.68	0.16
Ni															1.00	0.00	−0.78	−0.58	0.75	0.08	0.78
															1.00	1.00	0.01	0.07	0.02	0.81	0.01
Co																1.00	0.22	0.35	0.10	−0.76	0.16
																1.00	0.49	0.26	0.76	0.02	0.61
V																	1.00	0.66	−0.49	−0.33	−0.52
																	1.00	0.04	0.12	0.30	0.10
Ba																		1.00	−0.09	−0.20	−0.13
																		1.00	0.77	0.53	0.69
S																			1.00	0.18	0.78
																			1.00	0.56	0.01
Sr																				1.00	0.15
																				1.00	0.63
Pb																					1.00
																					1.00

N=11

PROFILE 5 (10)

(correlation coefficient with error probability underneath)

	Al2O3	TiO2	Cr2O3	MnO	Fe2O3	P2O5	LOI	Pt	Pd	Rh	Ru	Ir	Zn	Cu	Ni	Co	V	Ba	S	Sr	Pb
Al2O3	1.00	−0.45	−0.23	−0.62	−0.68	0.18	1.00	0.60	0.04	0.53	0.36	0.33	−0.57	0.50	0.59	−0.02	−0.14	−0.08	0.23	0.40	−0.60
	1.00	0.18	0.50	0.07	0.04	0.60	0.00	0.07	0.26	0.11	0.28	0.32	0.09	0.14	0.08	0.96	0.67	0.81	0.49	0.24	0.07
TiO2		1.00	0.85	0.49	0.78	−0.06	1.00	0.10	0.40	0.18	0.29	0.07	0.33	−0.10	0.10	0.79	0.44	0.45	0.31	−0.24	0.11
		1.00	0.01	0.15	0.02	0.86	0.00	0.76	0.22	0.60	0.38	0.84	0.32	0.76	0.76	0.02	0.18	0.18	0.35	0.01	0.74
Cr2O3			1.00	0.46	−0.81	0.29	1.00	0.01	0.33	0.12	0.01	0.13	0.38	−0.21	−0.01	0.90	0.54	0.50	0.12	−0.92	−0.21
			1.00	0.17	0.02	0.38	0.00	0.96	0.32	0.73	0.99	0.71	0.25	0.53	0.99	0.10	0.11	0.13	0.73	0.01	0.54
MnO				1.00	0.62	0.18	1.00	−0.17	0.16	−0.02	−0.37	−0.18	0.17	−0.43	−0.25	−0.32	0.15	0.14	−0.13	−0.66	0.25
				1.00	0.06	0.60	0.00	0.60	0.62	0.93	0.27	0.59	0.59	0.20	0.46	0.33	0.66	0.67	0.69	0.05	0.46
Fe2O3					1.00	0.29	1.00	−0.37	0.06	−0.29	−0.32	−0.09	0.52	−0.50	−0.31	0.58	0.33	0.26	−0.23	−0.89	0.28
					1.00	0.38	0.00	0.27	0.87	0.38	0.33	0.77	0.12	0.13	0.33	0.08	0.32	0.44	0.50	0.01	0.40
P2O5						1.00	1.00	0.00	0.17	0.06	−0.40	0.47	0.17	0.06	0.17	0.06	−0.17	−0.12	−0.17	−0.29	0.00
						1.00	0.00	1.00	0.60	0.86	0.22	0.16	0.60	0.86	0.60	0.86	0.66	0.73	0.60	0.38	1.00
LOI							1.00	1.00	1.00	1.00	1.00	1.00	1.00	1.00	1.00	1.00	1.00	1.00	1.00	1.00	1.00
							1.00	0.00	0.00	0.00	0.00	0.00	0.00	0.00	0.00	0.00	0.00	0.00	0.00	0.00	0.00
Pt								1.00	0.85	0.73	0.38	0.60	−0.23	0.61	0.85	0.09	−0.30	−0.24	−0.30	0.11	−0.37
								1.00	0.01	0.03	0.25	0.07	0.49	0.07	0.01	0.80	0.36	0.48	0.36	0.74	0.27
Pd									1.00	0.69	0.60	0.07	0.65	0.83	0.12	−0.08	0.12	−0.08	−0.25	−0.22	−0.22
									1.00	0.04	0.07	0.84	0.05	0.01	0.73	0.81	0.73	0.81	0.46	0.51	0.51
Rh										1.00	0.42	−0.50	0.74	0.76	0.20	0.04	0.20	0.04	0.15	−0.16	−0.40
										1.00	0.21	0.17	0.03	0.02	0.56	0.91	0.56	0.91	0.66	0.63	0.24
Ru											1.00	−0.23	0.84	0.60	0.15	−0.21	0.15	−0.22	0.00	−0.08	−0.16
											1.00	0.50	0.01	0.07	0.66	0.54	0.65	0.54	1.00	0.82	0.63
Ir												1.00	−0.46	−0.37	0.23	0.18	0.13	−0.19	−0.53	0.10	−0.08
												1.00	0.17	0.27	0.49	0.60	0.69	0.57	0.11	0.76	0.82
Zn													1.00	0.75	−0.15	−0.21	0.09	0.87	0.38	−0.12	0.10
													1.00	0.03	0.65	0.54	0.79	0.01	0.25	0.71	0.76
Cu														1.00	0.08	−0.26	−0.07	0.63	0.07	−0.12	−0.12
														1.00	0.80	0.43	0.83	0.05	0.84	0.73	0.71
Ni															1.00	0.22	−0.46	0.67	−0.83	−0.27	−0.12
															1.00	0.51	0.17	0.05	0.01	0.42	0.73
Co																1.00	0.90	0.13	−0.38	−0.25	−0.27
																1.00	0.01	0.70	0.25	0.46	0.42
V																	1.00	0.41	−0.37	−0.17	−0.25
																	1.00	0.22	0.26	0.62	0.46
Ba																		1.00	0.07	−0.15	−0.17
																		1.00	0.84	0.66	0.62
S																			1.00	−0.07	−0.15
																			1.00	0.83	0.66
Sr																				1.00	−0.37
																				1.00	0.26
Pb																					1.00
																					1.00

N=10

PROFILE 8

(correlation coefficient with error probability underneath)

	Al2O3	TiO2	Cr2O3	MnO	Fe2O3	P2O5	Pt	Pd	Rh	Ru	Ir	Zn	Cu	Ni	Co	V	Ba	S	Sr	Pb
Al2O3	1.00	−0.84	0.18	−0.79	−0.81	0.23	0.25	0.59	0.61	−0.12	0.18	−0.04	−0.50	−0.40	−0.60	−0.47	−0.43	−0.64	0.50	−0.58
	1.00	0.60	0.60	0.02	0.02	0.50	0.46	0.08	0.07	0.73	0.58	0.90	0.13	0.90	0.87	0.16	0.20	0.06	0.13	0.08
TiO2		1.00	0.02	0.52	0.93	−0.20	0.09	−0.61	−0.63	0.22	−0.07	0.06	0.57	−0.02	0.27	0.67	0.13	0.63	−0.61	0.86
		1.00	0.94	0.12	0.01	0.54	0.80	0.07	0.06	0.51	0.33	0.85	0.09	0.94	0.42	0.04	0.69	0.06	0.07	0.01
Cr2O3			1.00	−0.42	0.10	−0.41	0.78	0.44	0.46	0.65	0.80	0.73	0.39	0.21	0.79	0.31	−0.76	0.09	−0.53	−0.06
			1.00	0.21	0.76	0.23	0.02	0.13	0.17	0.05	0.02	0.03	0.24	0.53	0.01	0.35	0.02	0.79	0.11	0.87
MnO				1.00	0.46	−0.25	−0.71	−0.81	−0.75	−0.14	−0.43	−0.26	0.19	−0.30	−0.33	0.24	0.83	0.27	0.01	0.28
				1.00	0.17	0.46	0.03	0.02	0.03	0.68	0.20	0.43	0.57	0.37	0.32	0.48	0.01	0.41	0.99	0.40
Fe2O3					1.00	−0.38	0.76	−0.46	−0.50	0.24	−0.03	0.29	0.69	−0.12	0.43	0.59	0.03	0.76	−0.77	0.75
					1.00	0.25	0.15	0.16	0.13	0.48	0.93	0.39	0.04	0.73	0.20	0.08	0.93	0.02	0.02	0.03
P2O5						1.00	−0.16	0.14	0.00	−0.25	−0.13	−0.36	−0.41	0.34	−0.47	−0.23	0.02	−0.14	0.38	0.14
						1.00	0.64	0.69	1.00	0.46	0.71	0.28	0.23	0.31	0.16	0.50	0.95	0.69	0.25	0.68
Pt							1.00	0.59	0.60	0.65	0.74	0.56	0.35	0.29	0.73	0.33	−0.93	0.33	−0.59	0.12
							1.00	0.08	0.07	0.05	0.03	0.09	0.30	0.39	0.03	0.32	0.01	0.32	0.08	0.71
Pd								1.00	0.88	0.20	0.43	0.39	−0.20	0.39	0.27	−0.22	−0.73	−0.22	−0.13	−0.59
								1.00	0.01	0.55	0.19	0.24	0.55	0.24	0.41	0.50	0.03	0.50	0.70	0.08
Rh									1.00	0.38	0.59	0.35	−0.22	0.27	0.21	−0.15	−0.67	−0.15	0.02	−0.62
									1.00	0.25	0.08	0.30	0.50	0.41	0.53	0.65	0.07	0.65	0.96	0.06
Ru										1.00	0.84	0.38	0.50	−0.07	0.43	0.56	−0.48	0.56	−0.52	0.17
										1.00	0.01	0.25	0.13	0.84	0.20	0.09	0.15	0.09	0.12	0.62
Ir											1.00	0.65	0.45	0.25	0.62	0.17	−0.67	0.17	−0.40	0.01
											1.00	0.05	0.18	0.45	0.06	0.61	0.04	0.61	0.23	0.98
Zn												1.00	0.64	0.31	0.88	−0.08	−0.60	0.53	−0.67	0.03
												1.00	0.06	0.35	0.01	0.81	0.07	0.11	0.04	0.94
Cu													1.00	−0.01	0.73	0.16	−0.28	0.88	−0.81	0.58
													1.00	0.99	0.03	0.62	0.39	0.01	0.02	0.08
Ni														1.00	0.27	−0.21	−0.32	0.09	−0.12	0.02
														1.00	0.41	0.53	0.22	0.79	0.70	0.94
Co															1.00	0.09	−0.72	0.55	−0.77	0.26
															1.00	0.79	0.03	0.10	0.02	0.44
V																1.00	−0.08	0.08	−0.44	0.42
																1.00	0.81	0.81	0.18	0.21
Ba																	1.00	−0.14	−0.52	0.01
																	1.00	0.68	0.12	0.97
S																		1.00	−0.79	0.66
																		1.00	0.02	0.05
Sr																			1.00	−0.47
																			1.00	0.16
Pb																				1.00
																				1.00

N=10

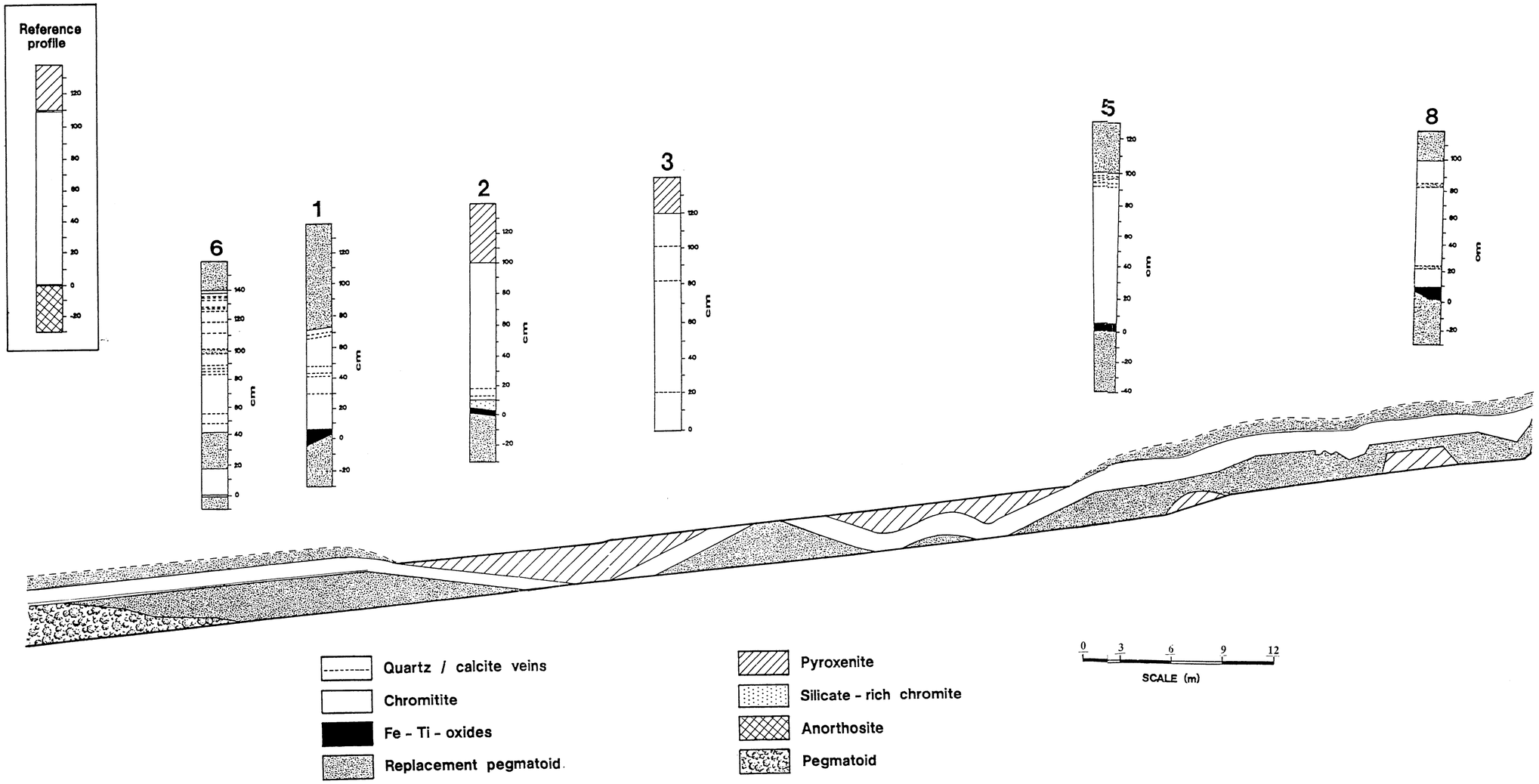
Reference profile
6
1
2
3
5
8
cm
Quartz / calcite veins
Chromitite
Fe - Ti - oxides
Replacement pegmatoid
Pyroxenite
Silicate - rich chromite
Anorthosite
Pegmatoid
0 3 6 9 12
SCALE (m)